

Densification and characterization of magnesium aluminate spinel from commercial grade reactants: Effect of milling and additives

Dissertation submitted to the

National Institute of Technology, Rourkela

in partial fulfillment of the requirements of the degree of

Master of Technology(R)

in

Ceramic Engineering

By

Sanjay Krishna Mohan

(Roll Number: *613CR3004*)

Under the supervision of

Prof. Ritwik Sarkar



July, 2016

Department of Ceramic Engineering
National Institute of Technology, Rourkela
Odisha



Ceramic Engineering Department
National Institute of Technology Rourkela

Date:

Certificate of Examination

Roll Number: **613CR3004**

Name: Sanjay Krishna Mohan

Title of Dissertation: Densification and characterization of magnesium aluminate spinel from commercial grade reactants: Effect of milling and additives.

We the below signed, after checking the dissertation mentioned above and the official record book (s) of the student, hereby state our approval of the dissertation submitted in partial fulfillment of the requirements of the degree of Master of Technology by Research in Ceramic Engineering at National Institute of Technology Rourkela. We are satisfied with the volume, quality, correctness, and originality of the work.

R. Sarkar
Principal Supervisor

S. Bhattacharya
Member (MSC)

S. K. Behera
Member (MSC)

R.K. Patel
Member (MSC)

S. Biswas
Examiner

J. Bera
Chairman (MSC)



Ceramic Engineering Department
National Institute of Technology Rourkela

Prof. Ritwik Sarkar

Associate Professor

Date:

Supervisor's Certificate

This is to certify that the work presented in this dissertation entitled "*Densification and characterization of magnesium aluminate spinel from commercial grade reactants: Effect of milling and additives*" by "*Sanjay Krishna Mohan*", Roll Number *613CR3004*, is a record of original research carried out by him under my supervision and guidance in partial fulfillment of the requirements of the degree of *Master of Technology (by Research)* in *Ceramic Engineering*. Neither this dissertation nor any part of it has been submitted for any degree or diploma to any institute or university in India or abroad.

Prof. Ritwik Sarkar

Dedication

I dedicate this thesis to my parents, sister (Maina) and Anuradha

Declaration of Originality

I, *Sanjay Krishna Mohan*, Roll Number *613CR3004* hereby declare that this dissertation entitled "Densification and characterization of magnesium aluminate spinel from commercial grade reactants: effect of milling and additives" represents my original work carried out as a postgraduate student of NIT Rourkela and, to the best of my knowledge, contains no material previously published or written by another person, nor any material presented for the award of any other degree or diploma of NIT Rourkela or any other institution. Any contribution made to this research by others, with whom I have worked at NIT Rourkela or elsewhere, is explicitly acknowledged in the dissertation. Works of other authors cited in this dissertation have been duly acknowledged under the section "Bibliography". I have also submitted my original research records to the scrutiny committee for evaluation of my dissertation.

I am fully aware that in case of any non-compliance detected in future, the Senate of NIT Rourkela may withdraw the degree awarded to me on the basis of the present dissertation.

Date:

NIT Rourkela

Sanjay Krishna Mohan

Acknowledgement

With deep respect, I avail this opportunity to express my gratitude to Dr. Ritwik Sarkar, Associate Professor, National Institute of Technology, Rourkela for his inspiration and guidance and valuable suggestions throughout this research work. His vast knowledge in the field of Science and Technology has helped a lot to enlighten me. It would have been impossible on my part to come out with this project report without him.

I would like to express my gratitude to Dr. Bibhuti Bhusan Nayak, HOD, Ceramic Engineering and all other faculties for constant support and valuable suggestions during my project. I would also express my sincere thanks to the laboratory technicians of Department of Ceramic Engineering, N.I.T., Rourkela, especially P. K. Mohanty, A. Kumar and S. Garai for constant practical assistance and help whenever required.

I am indebted to my senior research colleagues Akhilesh Singh, Satyananda Behera, Kanchan Majhi, Ashley Thomas, Rupita Ghosh, Abhishek Badolia, Vinay Kumar, Jayarao Gorinta, Abhisek Choudhary, Ezhil Venus, Raju Mula, for their unconditional support whenever needed. I am very much grateful to my friend Biswajit Baruah for his constant support and motivation. I am grateful to all other research scholars Venkatesh, Sarath, Abhinay, Pranati, Aishwarya, Pinky, Ipsita, Pallavi, Anantha, Shubham, for all their support during my project.

I am thankful to my parents, my sister Maina, my friend Anuradha, cousins, relatives who encouraged and constantly supported me during the total period of time and without whose support my project would not have been complete.

I thank Lord Krishna for giving me this blessed life and make me work together with all affiliated people who made me capable for accomplishment of this thesis.

Abstract

Among different refractory materials, magnesium aluminate spinel is of great importance from the industrial point of view, mainly due to its excellent corrosion and thermal shock resistances. Magnesium aluminate spinel (MgAl_2O_4), the only compound forms in the $\text{MgO-Al}_2\text{O}_3$ system, has the most desirable characteristics for refractory application, along with the environmental friendliness. Other than refractory there are studies for its applications as humidity sensors, transparent ceramic, anode material in aluminum cell, etc. In combination with alumina, spinel is of great importance as the refractory lining material for the steel ladles essential for iron & steel industries due to excellent corrosion and thermal shock resistances. Again in association with magnesia it is important for the burning zones and transition zones of cement rotary kilns. The major reason for this application is its better resistance to thermal shock and alkali materials, which indicates two or three times longer service lives than other basic bricks such as conventional MgO-chrome . Magnesium aluminate spinel has always an environment friendly advantage, so it has received favor from researchers, scientists and industrialists all over world.

Despite all these properties and application, the magnesium aluminate spinel is not commercially successful at per due to its high cost of production. The formation of magnesium aluminate spinel from its reactant is associated with a volume expansion which hinders to obtain dense magnesium aluminate spinel in a single step firing process. The commercial synthesis process involves two stage firing process which increases the cost of production

The present work focused on synthesis of magnesium aluminate spinel from commercial grade oxide using a single step sintering process. The effect of planetary milling, effect of additives like zinc Oxide, zirconium dioxide was studied. The effect of insitu generated magnesia and alumina from nitrate precursor was also studied. The sintering study was done in the temperature range $1200-1600^\circ\text{C}$. The phase and microstructure was studied with varying milling time and additive percentage using X-ray diffraction technique and field emission scattered electron microscopy respectively. The flexural strength and thermal shock behavior was also studied for each batch.

Dense magnesium aluminate spinel was successfully produced. The planetary milling and additive were found to enhance spinellisation process at lower temperature. The density and strength was also found to improve with milling and additive incorporation.

Contents

Certificate of examination.....	ii
Supervisor's Certificate	iii
Dedication	iv
Declaration of Originality	v
Acknowledgement	vi
Abstract.....	vii
Contents.....	viii
List of figures.....	xiii
Chapter 1.....	1
1.0 Introduction	1
1.1 Structure or crystallography of MgAl ₂ O ₄	3
I.Normal spinel (A ^{IV} B ₂ ^{VI} O ₄).....	4
II.Inverse spinel (B ^{IV} (AB) ^{VI} O ₄).....	4
III.Intermediate or random spinel (A _{1-x} B _x) ^{IV} (A _x B _{2-x}) ^{VI} O ₄	4
1.2 MgO-Al ₂ O ₃ phase diagram	5
1.3 Preparation of MgAl ₂ O ₄ spinel	6
I. Conventional oxide mixing (solid-solid reaction).....	6
II. Electrical fusion process	7
III. Wet synthesis techniques.....	8
IV. Other synthesis techniques	8
1.4 Importance of MgAl ₂ O ₄ spinel as a refractory material.....	9
I. Cement industry:	9
II. Iron and steel industry:.....	10
III. Glass industries:.....	10
IV. Other refractory applications:.....	10
Chapter 2.....	12
Literature review.....	12
2.0 Magnesium aluminate spinel.....	12
2.1 Formation and synthesis of magnesium aluminate spinel by solid state route	12
2.2 Synthesis through other non-conventional routes	17

2.2.1 Co-precipitation method	17
2.2.2 Sol-gel method.....	20
2.2.3 Other modified non-conventional techniques.....	22
2.3 Sintering of magnesium aluminate spinel	24
I. Solid state sintering	25
II. Liquid state sintering.....	25
III. Sintering in the presence of reactive liquid	25
IV. Reaction sintering or sintering with the chemical reaction	25
2.4 Effect of additives on formation and sintering of magnesia aluminate spinel	30
2.5 Effect of sintering on properties of magnesium aluminate spinel.....	36
Chapter 3.....	39
Motivation and objective.....	39
3.0 Motivation	39
3.1 Objective of the work.....	39
Chapter 4.....	40
Experimental methods and materials	40
4.0 Raw materials.....	40
4.1 Sample preparation processes	41
4.1.1 Weighing	41
4.1.2 Mixing	41
4.1.3 Drying.....	42
4.1.4 Milling	42
4.1.5 Pressing.....	42
4.1.6 Sintering.....	43
4.1.7 Grinding.....	44
4.2. Experimental process flow-chart.....	44
4.2.1 For milling compositions.....	44
4.2.2 For additive containing compositions.....	44
4.3 Methods used for characterization	46
4.3.1 Surface area measurement	46
4.3.2 Linear shrinkage measurement.....	47
4.3.3 Density and porosity measurement.....	47
4.3.4 Dilatometry study	48

4.3.5 Phase analysis study	48
4.3.6 Microstructure study.....	49
4.3.7 Flexural strength study	49
4.3.8 Thermal shock resistance study	50
4.4 List of equipments used.....	50
4.4.1. Electronic balance.....	50
4.4.2. Magnetic stirrer.....	51
4.4.3. Hot air oven	51
4.4.4. Electric arc furnace.....	51
4.4.5. Automatic hydraulic pressing machine	52
4.4.6. Dilatometer	52
4.4.7. Molds.....	52
4.4.8. Mortar pestle.....	53
4.4.9. Field emission scanning electron microscope.	53
4.4.10. Muti-purpose x-ray diffractometer	53
4.4.11. BET surface area analyzer	54
4.4.12. Universal testing machine	54
4.4.13. Glassware's and accessories.....	54
4.4.14. Planetary mill.....	55
4.4.15. Digital vernier caliper	55
Chapter 5.....	56
Results and discussions.....	56
5.1 Effect of planetary milling	57
5.1.1 Surface area variation with milling time	57
5.1.2 Densification study.....	57
5.1.3 Dilatometric study	58
5.1.4 Microstructural study.....	59
5.1.5 Phase analysis study	62
5.1.6 Flexural strength study	64
5.1.7 Thermal shock behaviour study.....	64
5.1.8 Conclusions	65
5.2 Effect of zinc oxide addition	66
5.2.1 Linear shrinkage study.....	66

5.2.2	Densification study	66
5.2.3	Dilatometry study	67
5.2.4	Microstructural study	68
5.2.5	Phase analysis study	72
5.2.6	Flexural strength study	74
5.2.7	Thermal shock behaviour study	74
5.2.8	Conclusions	75
5.3	Effect of zirconium dioxide addition	76
5.3.1	Linear shrinkage study	76
5.3.2	Densification study	76
5.3.3	Dilatometry study	78
5.3.4	Microstructure study	79
5.3.5	Phase analysis study	83
5.3.6	Flexural strength study	86
5.3.7	Thermal shock behaviour study	86
5.3.8	Conclusions	87
5.4	Effect of aluminium nitrate nonahydrate addition	88
5.4.1	Linear shrinkage study	88
5.4.2	Densification study	88
5.4.3	Dilatometry study	89
5.4.4	Microstructural study	91
5.4.5	Phase analysis study	94
5.4.6	Flexural strength study	95
5.4.7	Thermal shock behavior study	96
5.4.8	Conclusions	96
5.5	Effect of magnesium nitrate hexahydrate addition	98
5.5.1	Linear shrinkage	98
5.5.2	Densification study	98
5.5.3	Dilatometry study	99
5.5.4	Microstructure study	101
5.5.5	Phase analysis study	103
5.5.6	Flexural strength study	105

5.5.7 Thermal shock behavior study.....	105
5.5.8 Conclusions	106
Chapter 6	107
Summary of the work	107
Chapter 7	108
Future work	108
Bibliography	109
Publications originating from M.Tech (Research) work.....	126
Resume.....	127

List of figures

Fig.1.1 Crystallographic structure of MgAl ₂ O ₄ spinel.....	3
Fig.1.2 MgO-Al ₂ O ₃ Phase diagram	5
Fig.1.3 Formation of MgAl ₂ O ₄ from oxide reactants by counter diffusion in solid oxide reaction process.....	7
Fig.4.1 Raw materials(a) Fused magnesia (b) Reactive alumina.....	41
Fig.4.2 Pressed pellets and bars	42
Fig.4.3 Heating schedule during sintering.	43
Fig.4.4 Process flow chart for milling composition.....	45
Fig.4.5 Process flow chart for additive containing compositions.....	46
Fig.4.6 Thermal shock resistance experiment.....	50
Fig.4.7 Electronic balance.....	50
Fig.4.8 Magnetic stirrer.....	51
Fig.4.9 Hot air oven	51
Fig.4.10 Electric arc furnaces	51
Fig.4.11 Automatic hydraulic pressing machine	52
Fig.4.12 Dilatometer	52
Fig.4.13 Molds	52
Fig.4.14 Mortar pestle.....	53
Fig.4.15 Field emission scanning electron microscope	53
Fig.4.16 Multi-purpose x-ray diffractometer	53
Fig.4.17 BET surface area analyzer	54
Fig.4.18 Universal testing machine	54
Fig.4.19 Glassware's and accessories.....	54
Fig.4.20 Planetary mill.....	55
Fig.4.21 Digital vernier caliper.....	55
Fig.5.1 BET surface area of batch against milling time.	57
Fig.5.2 Bulk density vs. sintering temperature plot with the variation of milling time.....	58
Fig.5.3 Apparent porosity vs. sintering temperature plot with the variation of milling time.	58
Fig.5.4 Dilatometry plot of the samples with different milling time.	59

Fig.5.5 FESEM images of 1200 ⁰ C fired samples with different milling time.....	60
Fig.5.6 FESEM images of 1600 ⁰ C fired samples with different milling time.....	61
Fig.5.7 EDAX analysis of without milled 1600 ⁰ C sintered sample.	62
Fig.5.8 XRD plot of samples fired at 1200 ⁰ C.....	63
Fig.5.9 XRD plot of samples fired at 1400 ⁰ C.....	63
Fig.5.10 XRD plot of samples fired at 1500 ⁰ C.....	63
Fig.5.11 XRD plot of samples fired at 1600 ⁰ C.....	63
Fig.5.12 Flexural strength of 1600 ⁰ C fired samples with different milling time.....	64
Fig.5.13 Thermal shock behaviour of 1600 ⁰ C fired samples with different milling time.	64
Fig.5.14 Linear shrinkage with the addition of zinc oxide	66
Fig.5.15 Variation in bulk density against zinc oxide addition and sintering temperature.	67
Fig.5.16 Variation in apparent porosity against zinc oxide addition and sintering temperature. .	67
Fig.5.17 The dilatometry plot of the samples with variation of zinc oxide percentage.....	68
Fig.5.18 FESEM images of 1200 ⁰ C fired samples with different wt. % of zinc oxide.	69
Fig.5.19 FESEM images of 1600 ⁰ C fired samples with different wt. % of zinc oxide.	70
Fig.5.20 EDAX frame analysis of 1600 ⁰ C sintered sample without zinc oxide.....	71
Fig.5.21 EDAX analysis of 2 wt. % Zinc Oxide containing composition sintered at 1600 ⁰ C, (a) analysis of grain, spot A, (b) analysis of grain boundary, spot B and (c) analysis of grain boundary, spot C.	71
Fig.5.22 XRD plot of samples fired at 1200 ⁰ C.....	72
Fig.5.23 XRD plot of samples fired at 1300 ⁰ C.....	72
Fig.5.24 XRD plot of samples fired at 1400 ⁰ C.....	73
Fig.5.25 XRD plot of samples fired at 1500 ⁰ C.....	73
Fig.5.26 XRD plot of samples fired at 1600 ⁰ C.	73
Fig.5.27 Flexural strength of 1600 ⁰ C sintered samples.	74
Fig.5.28 Strength retainment of 1600 ⁰ C sintered samples after thermal shock.....	74
Fig.5.29 Linear shrinkage behavior with zirconium dioxide contained samples.	76
Fig.5.30 Variation of bulk density with zirconium dioxide addition.....	77
Fig.5.31 Variation of apparent porosity with zirconium dioxide addition.	77
Fig.5.32 Variation of relative density with zirconium dioxide addition.	78
Fig.5.33 The dilatometry plot of the samples with a variation of zirconium dioxide percentage.	79

Fig.5.34 FESEM images of 1200 ⁰ C sintered samples.	80
Fig.5.35 FESEM images of 1600 ⁰ C sintered samples.	81
Fig.5.36 EDAX of zirconium dioxide containing samples.	82
Fig.5.37 XRD plots of samples sintered at (a) 1200 ⁰ C (b) 1300 ⁰ C (c) 1400 ⁰ C (d) 1500 ⁰ C (e) 1600 ⁰ C with variation of zirconium dioxide percentage.	84-85
Fig.5.38 Variation of flexural strength with zirconium dioxide content for 1600 ⁰ C sintered samples.	86
Fig.5.39 Strength retainment of the compositions after thermal shock.	86
Fig.5.40 Plot of linear shrinkage vs. sintering temperature.	88
Fig.5.41 Variation of bulk density with sintering temperature and additive percentage.	89
Fig.5.42 Variation of apparent porosity with sintering temperature and additive percentage.	89
Fig.5.43 Dilatometry plots of aluminium nitrate nonahydrate containing batch.	91
Fig.5.44 FESEM micrograph of without additive batch.	92
Fig.5.45 Microstructure 1200 ⁰ C sintered 1wt.% aluminium nitrate nonahydrate containing sample.	92
Fig.5.46 Microstructure of 1200 ⁰ C sintered 2 wt.% aluminium nitrate nonahydrate containing sample.	93
Fig.5.47 Microstructure of 1600 ⁰ C sintered 1 and 2 wt.% aluminium nitrate nonahydrate containing batches.	93
Fig.5.48 XRD of aluminium nitrate nonahydrate batch (a)1200 ⁰ C sintered(b)1400 ⁰ C sintered and (c)1600 ⁰ C sintered.	94
Fig.5.49 Flexural strength of 1600 ⁰ C sintered sample.	96
Fig.5.50 Strength retainment additive containing batch after thermal shock.	96
Fig.5.51 Plot of linear shrinkage vs. sintering temperature for magnesium nitrate hexahydrate batch.	98
Fig.5.52 Plot of bulk density vs. sintering temperature for magnesium nitrate hexahydrate batch.	99
Fig.5.53 Plot of apparent porosity vs. sintering temperature for magnesium nitrate hexahydrate batch.	99
Fig.5.54 Dilatometry plots of magnesium nitrate hexahydrate containing batch.	100
Fig.5.55 Microstructure of the without-additive batch.	101

Fig.5.56 Microstructure of 1200 ⁰ C sintered 1 wt.% magnesium nitrate hexahydrate containing sample.	102
Fig.5.57 Microstructure of 1200 ⁰ C sintered 2 wt.% magnesium nitrate hexahydrate containing sample.	102
Fig.5.58 Microstructure of 1600 ⁰ C sintered 1 and 2 wt.% magnesium nitrate hexahydrate containing batches.	103
Fig.5.59 XRD of magnesium nitrate hexahydrate batch (a)1200 ⁰ C sintered(b)1400 ⁰ C sintered and (c)1600 ⁰ C sintered.	104
Fig.5.60 Flexural strength of 1600 ⁰ C sintered magnesium nitrate hexahydrate.	106
Fig.5.61 Strength retainment magnesium nitrate hexahydrate containing batch after thermal shock.	106

Chapter 1

1.0 Introduction

The progress and evolution of the human civilization are associated with discovery, invention and development of new materials. Modern era focuses on improving the condition of human life with taking into environmental aspects. With the progression of human civilization there will be discoveries and inventions that will never stop. From the beginning to till date there is evolution and discovery of materials that have shaped and changed the way of living of a society and civilization. Development of new materials and their processing has helped in the evolution of new technologies in every field of science. Ceramic materials have played a crucial role in development of human civilization. Ceramic include a vast range of materials. In order to simply that ceramic is divided in two groups –traditional ceramics and advanced ceramics. Traditional ceramics include pottery, structural clay products, clay based refractories etc. Advance ceramic include functional ceramics like ceramics for electrical, optical, magnetic applications etc., and structural ceramics that involves materials that can be used in both room and elevated temperature. In brief it can be said that without ceramic research in materials engineering is incomplete. In ceramic materials spinel forms an interesting field of research because of their properties and different engineering applications. Among all spinels magnesium aluminate spinel have prominent place because of its excellent combination of properties.

Magnesium aluminate spinel is an important industrial material among different refractory material because of its excellent corrosion and thermal shock resistance. It is the only compound that forms in MgO-Al₂O₃ system that has desirable characteristics for refractory application, along with environment friendliness. Other than the refractory application it has many applications such as humidity sensors, transparent ceramic, anode material in aluminium cell etc.[1.1, 1.2]

The Magnesium aluminate is a type of double oxide which generally has a general formula AB₂O₄, where A is divalent element and B is a trivalent element. There are more than 200 compounds that can be classified as spinels. But only a few are related with refractories system e.g. FeFe₂O₄, FeAl₂O₄, FeCr₂O₄, MgFe₂O₄, MgAl₂O₄, MgCr₂O₄ etc. Among these compounds MgAl₂O₄ and MgCr₂O₄ has good combination of physical and chemical properties to be used as material for making spinel containing refractories which has very high demand in industry. MgCr₂O₄ refractories having good physio-chemical properties are used in refractory application,

but there is a major disadvantage. It is carcinogenic in nature due to presence of Cr^{6+} ion. The presence of Cr^{6+} ion also bear the risk of contamination of ground water on disposal of the waste refractories and skin ulceration. For these reasons the MgAl_2O_4 which has similar properties like MgCr_2O_4 grabbed the attention as an alternative. MgAl_2O_4 is an environ friendly material. The thermal shock resistance of MgAl_2O_4 is better than the magnesite chrome refractory b .It has high chemical inertness and low linear thermal expansion than magnesium dichromate.[1.3-1.5] The typical properties of magnesium Aluminate spinel is listed in table 1.[1.3, 1.6]

Table 1. Typical properties of magnesium aluminate spinel.

Composition(wt.%)	MgO-28.3	
	Al ₂ O ₃ -71.7	
Molecular weight	142.2g	
True density	3.58g/cc	
Melting point(⁰C)	2135 ⁰ C	
Thermal expansion coefficient (X 10⁻⁶/⁰C)	100 ⁰ C	5.6
	500 ⁰ C	7.6
	1000 ⁰ C	8.4
	1500 ⁰ C	10.2
Thermal conductivity(W/mK)	25 ⁰ C	15
	100 ⁰ C	13
	500 ⁰ C	8
	1000 ⁰ C	5
Young's modulus(GPa)	240-284	
Bending strength(MPa)	Room temperature	110-250
	1400 ⁰ C	8-10
Hardness(GPa)	15	

1.1 Structure or crystallography of $MgAl_2O_4$

The crystallographic structure of the $MgAl_2O_4$ spinel is simple cubic with eight formula units in one cubic unit cell. The Structure of $MgAl_2O_4$ was first determined by Bragg and Nishikawa independently.[1.7, 1.8] The structure consist of a perfect cubic close packed array of oxygen ions with metal ions positioned in fourfold and six fold oxygen coordination. A maximum of 64 octahedral sites and 32 tetrahedral sites are possible in such a structure respectively. Due to these kind of structure with relatively few potential sites occupied by cations it allows a large deviations and solid solutions. A small subshell of magnesium aluminate spinel has total 4 oxygen ions positioned to form face centered cubic lattice. As result there are total four octahedral and eight tetrahedral interstices. The trivalent Al^{3+} ion occupy two octahedral sites and divalent Mg^{2+} occupy one tetrahedral site. So half of the octahedral sites and one-eighth of the tetrahedral sites are occupied by cations. Since eight such sub-cells form a unit cell, so total 32 oxygen ions with 16 trivalent ions filling half of the octahedral sites and 8 divalent ions filling one-eighth of the tetrahedral site constitutes a unit cell of $MgAl_2O_4$.The fig.1.1 shows the structure of the spinel.[1.9]

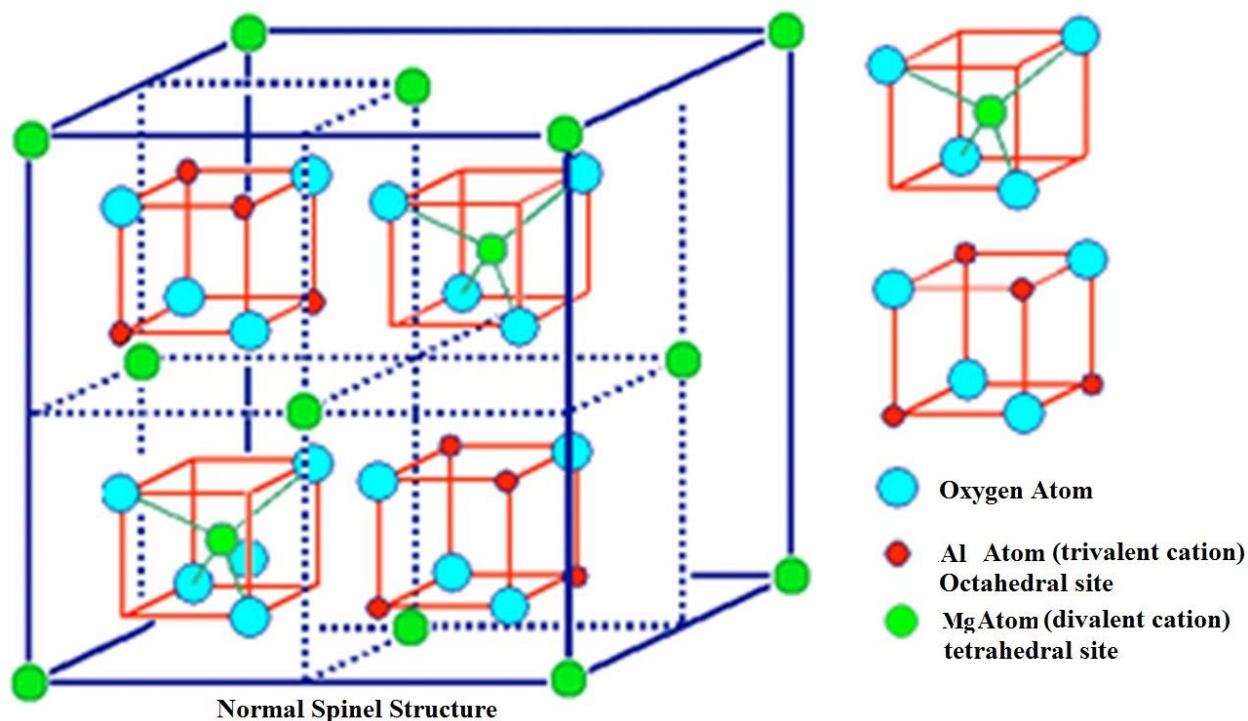


Fig 1.1 Crystallographic structure of $MgAl_2O_4$ spinel.

The occupation of sites in MgAl_2O_4 structure is governed by factor that bond strength of oxygen must be correct. Each Mg^{2+} ion present in tetrahedral site has a bond strength of $\frac{1}{2}$ and each Al^{3+} bond has strength of $\frac{1}{2}$. A single oxygen ion is coordinated by 3 Al^{3+} and 1 Mg^{2+} ions, making bond strength of 2, which is appropriate to the divalent oxygen ion.[1.10]. Structural measurements of magnesium aluminate and its solid solution were carried out by various researchers. The lattice parameter of MgO rich and stoichiometric spinel were nearly similar but with increase in alumina content it gradually decreased. The stoichiometric magnesium aluminate had a lattice constant of $8.064 \pm 0.002 \text{ \AA}$ whereas magnesia rich composition (alumina content up to 32.1 wt.% had a lattice constant of 8.06.[1.11, 1.12] But for alumina rich composition the lattice parameter reduced to 7.93 \AA . The reason for these decrease was stated as a second phase formation i.e. $\gamma\text{-Al}_2\text{O}_3$. [1.13]. Many researchers reported a constant lattice parameter for non-stoichiometric $\text{MgO} \cdot n\text{Al}_2\text{O}_3$ for n varying from 0.883 to 1. But for $n > 1$ the lattice constant decreases.[1.14].

In 1932, Barth and Posnjak proposed possibility of different cation arrangement in different types of spinels.[1.15] In addition to the normal spinel structure they observed two different kinds of arrangement. In accordance to these arrangements they categorized spinel in three different ways:

- I. **Normal spinel ($\text{A}^{\text{IV}}\text{B}_2^{\text{VI}}\text{O}_4$):** In this type of arrangement there are 32 oxygen ions. Out of 32 octahedral voids 16 are filled with trivalent ions. And out of 64 tetrahedral voids 8 are filled with divalent ions.
- II. **Inverse spinel ($\text{B}^{\text{IV}}(\text{AB})^{\text{VI}}\text{O}_4$):** In this type of arrangement the tetrahedral sites are filled with 8 trivalent ions. The octahedral sites are filled with remaining 8 trivalent and 8 divalent ions.
- III. **Intermediate or random Spinel (A_{1-x}B_x)^{IV}(A_xB_{2-x})^{VI} O_4 :** in this type of arrangement the both trivalent and divalent cations are distributed randomly over the available tetrahedral and octahedral voids.

(A=divalent cation, B =trivalent cation)

In general, all spinels are considered as random spinels. If the value of $X=0$ then it is normal spinel and for $X=1$ it is inverse spinel. to describe normal or inverse spinel a parameter λ is used which designates fraction of trivalent ions in tetrahedral voids. For normal spinel $\lambda=0$ and fully inverse spinel $\lambda= 1/2$.

1.2 MgO-Al₂O₃ phase diagram

To understand the properties of materials it is important to understand the phase relationships. The different phases present in equilibrium in a system as a function of temperature, pressure and composition are indicated in a phase diagram. For ceramic pressure is assumed to be constant as pressure variability is not important from application point of view. Phase diagrams also describe variation of different phases and their amounts against temperature and composition. Rankin and Merwin are the first to report about MgO-Al₂O₃ phase diagram. They discovered it while studying the CaO-MgO-Al₂O₃ system.[1.16] The phase diagram of MgO-Al₂O₃ is depicted in fig.1.2.[1.17, 1.18]

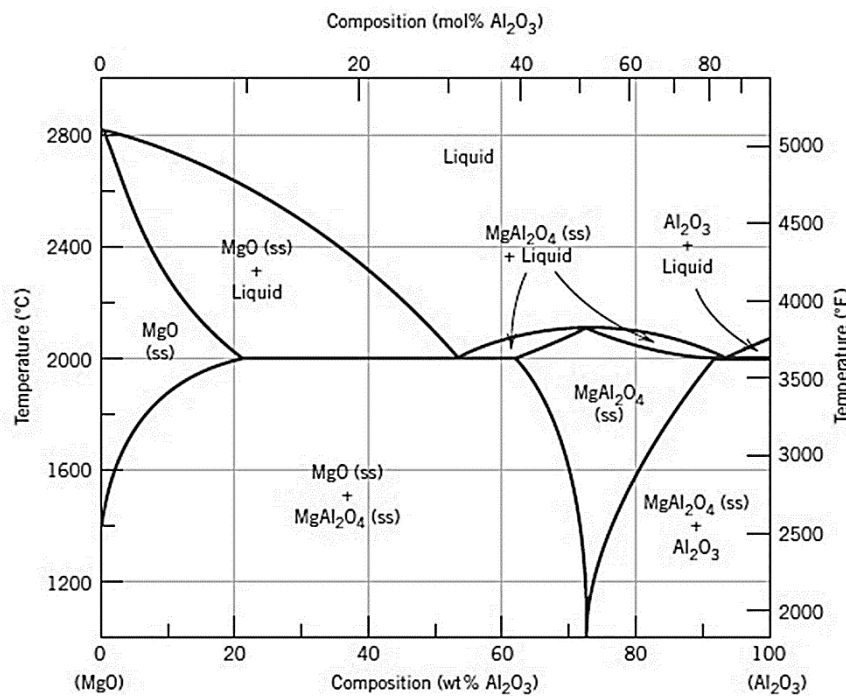


Fig. 1.2 MgO-Al₂O₃ phase diagram [1.17,1.18]

The MgAl₂O₄ is the only compound formed in MgO-Al₂O₃ system having a congruent melting point of 2135⁰C. The magnesia rich portion has a eutectic composition of 45 wt.% MgO and 55 wt.% Al₂O₃ and the eutectic temperature is 2030⁰C. The alumina rich portion has a eutectic composition of 97 wt.% Al₂O₃ and 3 wt.% MgO with a eutectic temperature of 1925⁰C. Alumina makes solid solution with spinel and highest solubility up to a composition of 93 wt.% Al₂O₃ and 7 wt.% MgO whereas, no such solid solution is reported with spinel.[1.19]

Many researchers did on the MgO-Al₂O₃ phase diagram and reported some deviations. The researchers divided the work into two separate systems namely, MgO-MgAl₂O₄ and MgAl₂O₄ – Al₂O₃. Roy, Roy and Osborn studied on MgAl₂O₄–Al₂O₃ system in 1953. They found that primary field of spinel solid solution extend up to 93.46 wt.% alumina content at eutectic temperature. But with cooling the solubility rapidly decreases. They reported exsolution of alumina from spinel lattice takes place with cooling up to 800⁰C.[1.20] Alper, McNally, Ribbe and Doman studied magnesia rich part of the MgO-Al₂O₃ system. They studied the system in N₂ atmosphere and observed a remarkable difference in the melting point of spinel phase. The reported melting temperature as 2105⁰C instead of 2135⁰C as reported earlier. Similar eutectic composition was reported with a eutectic temperature of 1995⁰C. They also reported about difference in solid solubility of MgO in spinel phase. Solubility was maximum at the eutectic temperature and extended up to 39 wt.% Magnesia and 61 wt.% alumina. They also reported about solubility of alumina in magnesia with a maximum limit up to 18 wt.% Al₂O₃. [1.21]

1.3 Preparation of MgAl₂O₄ spinel

Magnesium aluminate spinel does not occur in nature so they are synthesized by using a wide variety of techniques. This section will through a little light on these techniques along with formation mechanisms.

- I. **Conventional oxide mixing (solid-solid reaction):** This technique involves mixing of MgO and Al₂O₃ bearing compounds. Pressing them into certain shapes and then heating at high temperature for a prolonged period. The mechanism of spinel formation in this process involves a counter diffusion process that depends on a number of factors. At the beginning stage of MgAl₂O₄ formation reaction small crystals of spinel stoichiometry is nucleated on either MgO or Al₂O₃ grains. After the formation of this initial layer subsequent growth and thickening of spinel layer become difficult. This is because the reactants are now separated by an impassable spinel layer. So a counter diffusion process takes place Mg²⁺ ion diffuse away and Al³⁺ ion diffuse toward MgO-MgAl₂O₄ interface. Likewise, Al³⁺ ion diffuse away and Mg²⁺ ion diffuse toward MgAl₂O₄-Al₂O₃ interface.[1.3] The schematic for the counter diffusion process of MgAl₂O₄ formation is represented in Fig.1.3. This results in formation of 1 MgAl₂O₄ molecule in MgO-MgAl₂O₄ interface and 3 MgAl₂O₄ in MgAl₂O₄-Al₂O₃ interface.

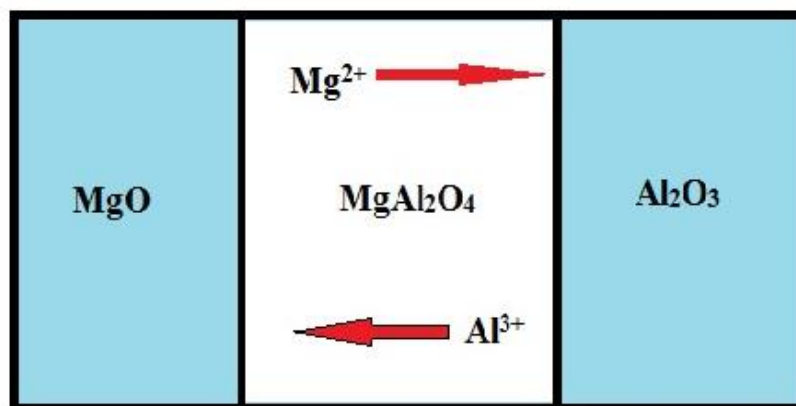
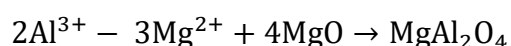


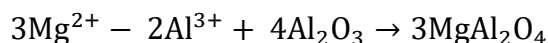
Fig. 1.3 Formation of $MgAl_2O_4$ from oxide reactants by counter diffusion in solid oxide reaction process.

The electro neutrality during the reaction is preserved diffusion of 3 Mg^{2+} ions for diffusion every 2 Al^{3+} ions. The reactions that occur at MgO - $MgAl_2O_4$ and $MgAl_2O_4$ - Al_2O_3 interface are stated below (as mentioned by Zhang and Lee) [1.3]:

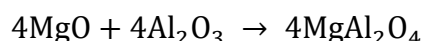
At MgO - $MgAl_2O_4$ interface:



At $MgAl_2O_4$ - Al_2O_3 interface:



The overall reaction:



- II. **Electrical fusion process:** The Electrofusion or electrical fusion process or EF process uses natural magnesite and calcined alumina as starting materials. The starting material were mixed and melted in an electric arc furnace by heating to a temperature greater than the melting temperature of the mixture. The reactants MgO and Al_2O_3 react in molten state to form spinel. The molten mass is then cooled to a solidified ingot which can be further crushed and ground to a further controlled particle size. Purity of spinel formed is more than conventional oxide mixing process. But the spinel powder formed by electrical fusion process has low surface reactivity so spinel formed require higher temperature to densify.

Another disadvantage of this process is that this process consumes a lot of energy and hence it is highly expensive.[1.3]

- III. **Wet synthesis techniques:** Wet synthesis techniques are used to prepare high quality spinel powders (both uniform and reactive). Some examples of wet synthesis techniques are sol-gel, hydrothermal synthesis etc. In sol-gel process reagents are mainly metal-organic compounds such as alkoxides. The starting point of this process is to prepare a homogenous sol containing the cationic ingredients. The next step is to dry the sol gradually and transform into a viscous sol having particles of colloidal dimensions. Finally, the sol is transformed to an amorphous solid gel. The gel is fired to remove the volatile components and to crystallize the final product. Spinel powder formed by this process are pure and homogenous and possess very high reactivity. Synthesis temperature is much lower than conventional oxide mixing process and EF. In spite of having these advantages it has a lot of disadvantages. The first reason is requirement of organic precursors and solvents which are harmful for environment. Another reason is it cannot produce product in industrial scale because these process is difficult to commercialize.[1.22-1.24]

Another wet synthesis technique which we mentioned about is hydrothermal technique. This technique involves reacting the precursor containing cationic ingredients in water/steam at appropriate pressure and temperature. The resulting spinel forming precursor after reaction are pyrolyzed at appropriate temperature. The spinel formed by this process are very reactive. Temperature required for this process can be as low as 500⁰C.[1.25]Main drawback of this process is the precursors which are harmful for environment and requirement of a high pressure autoclave. The technique is quite lengthy as pyrolysis takes time.

- IV. **Other synthesis techniques:**

In addition to the wet synthesis techniques there are also other techniques which are implemented to synthesize Magnesium aluminate spinel. Two novel methods among them are mechano- chemical alloying and molten salt synthesis. In mechano-chemical alloying appropriate raw materials are mixed in a high energy milling machine. The raw materials may be oxide hydroxide or carbonates containing the reactant cations. After milling a spinel forming precursors are obtained from which fine spinel can be obtained. The crystallization temperature for this method is less than 1200⁰C.[1.26]The technique which

can be used for synthesis of MgAl_2O_4 spinel is molten salt synthesis technique (MSS). This method uses low melting salts as reaction medium permitting mixing of the reactants in a liquid phase in atomic scale. Due to presence of liquid phase the diffusion process becomes quicker and the reaction is completed at much lower temperature. Besides this technique there are many other routes which are used for synthesis of spinel like co precipitation, auto combustion etc.[1.1, 1.27, 1.28]

Among all these processes the conventional oxide mixing technique still is the main route of production of spinel in industry because its economic advantage and easiness in commercialization.[1.2]

1.4 Importance of MgAl_2O_4 spinel as a refractory material

Even in 1980's Magnesium Aluminate spinel was a laboratory material for research and science. The first commercial application of spinel was not as a refractory material but as a chemical bond in periclase bodies.[1.2] The in situ spinel bond formed in periclase bodies containing high purity alumina provided outstanding resistance against deformation under load, slagging and spalling. Soon after that spinel was tried in open hearth furnace roofs in 1970s.[1.29] After that the demand of spinel increased in Japan and USSR in late 1980's.

- I. **Cement industry:** The first application of MgAl_2O_4 was done as a refractory material in Japan in cement rotary kilns as a replacement for magnesia chrome refractory which have environmental issues. Studies on the upper (feeding part) and lower transition zone of cement rotary kiln showed that life of this part was much lower compared to main sintering zone due to high thermal stress, wear and presence of liquid and alkali vapour. Application of periclase spinel bodies reported 2-3 times better life than the conventional magnesia chrome refractories.[1.30] In present scenario with increased in kiln diameter and rotational speed the rate of stress is much more. To overcome this process in situ magnesia aluminate spinel formation techniques are being employed. This technique led to gain sufficient flexibility and increased the life of the brick by reducing the crack formation and also improved the chemical inertness.[1.31,1.32] Use of spinel bonded periclase bodies and spinel clinkers in the burning and transition zone of rotary kiln increased the life of the kiln by 40-100%.[1.33]

- II. **Iron and steel industry:** Application of $MgAl_2O_4$ started with its application on the roof of open hearth furnaces in USSR. As open hearth furnaces are nearly obsolete this practice has stopped. The most important application of magnesium aluminate spinel is in the lining of steel ladles as alumina rich castables. The steel ladles are always exposed to high temperature corrosion, mechanical wear and thermal shock. Magnesium aluminate spinel possess all these characteristics which make it suitable for application in steel ladles. The $MgAl_2O_4$ spinel is added either as a preformed spinel or formed by reaction between MgO and Al_2O_3 (insitu spinel).[1.2] Beside steel ladles spinel is also used in impact pads, purging cones and well blocks, nozzles, wears and dams, lances, and slide gates. The major advantage of spinel addition in alumina castables is high corrosion resistance. The betterment in corrosion resistance is due to dissolution of spinel in slag. The MgO rich spinel showed much better corrosion resistance than stoichiometric one. The addition of spinel not only increase the corrosion resistance but also increase the hot strength. In alternative to addition of presynthesized spinel to alumina castables, in situ spinel can be formed. The insitu formation of spinel is associated with a volume expansion that counter balance the shrinkage of castables. In situ spinel are mainly applicable in side walls of steel ladle where there is requirement of high corrosion resistance, thermodynamic stability and flexibility. In addition to steel ladle spinel in present day are also used in blast furnace trough castables which increase the corrosion resistance and spalling resistance. Many new application of spinel are coming up in iron and steel industries. Use of spinel carbon refractories in ladle application are booming because of their high thermal shock and corrosion resistance.[1.34-1.36]
- III. **Glass industries:** The glass tank furnace regenerators exposed to severe thermal fluctuations and suffer high sulfate and alkali attacks. Use of spinel contained brick in glass tank regenerators was found to possess high strength even after infiltration of sulfate into the brick.[1.37] Use of spinel as an additive for bonding in fused spinel checker brick was reported to possess highest corrosion resistance.[1.38] Direct bonded pure $MgAl_2O_4$ based brick were found to have excellent corrosion resistance in crown lining and superstructures of oxy fuel fired glass melting furnaces.[1.39]
- IV. **Other refractory applications:** $MgAl_2O_4$ because of excellent properties are used in many important refractories application. Its application in copper smelting convertors increase the

life of convertor.[1.40]Magnesium aluminate spinel is also used as a substitute for magnesium chrome bodies in mineral processing kilns. This also led to decrease in problems of disposal of waste.[1.41] $MgAl_2O_4$ is also used as crucible material for reduction of uranium by “thermite reaction”. [1.42]Many researchers have synthesized and proposed magnesium aluminate spinel as a suitable anode material for metallurgical industry as a replacement for carbon anode.[1.43]

Apart from refractories magnesium aluminate spinel is also used in humidity sensors, IR sensors and optical domes, ballistic weapons, military and armor vehicles etc. Other applications include faceplate of CRT, polarimeter for LED, Watch crystals, Safety goggles, as components in optical computer and high-speed printer, High-pressure arc lamp and lens, pressure vessel sight glass, furnace sight glass.[1.44]

Chapter 2

Literature review

2.0 Magnesium aluminate spinel

As discussed in earlier chapter magnesium aluminate spinel is a material with immense technical applications owing to its excellent thermal, mechanical and chemical properties both at room and elevated the temperature. But magnesium aluminate spinel does not occur naturally, and so there is a need for an efficient method for its commercial-scale production. The commercially feasible method for its synthesis is the conventional oxide mixing (CMO), or solid – solid reaction, a technique in which powder MgO- and Al₂O₃-bearing compounds (e.g., oxides, hydroxides, or carbonates) are mixed, shaped & sintered at high temperature for extended times. The formation of spinel from its constituent oxides depends on a large number of factors [2.1]. Many researchers studied various parameters and their effects on reaction, reactant products, formation mechanism, etc. Some researchers also studied the spinel formation reaction by different methods other than solid state reaction. But still solid oxide reaction dominates other synthesis techniques because of its simplicity and applicability in mass production in industry[2.2].

2.1 Formation and synthesis of magnesium aluminate spinel by solid state route

The formation of magnesium aluminate spinel from its constituent oxide reactants is a counter diffusion process. This counter diffusion process occurs at two interfaces MgO-MgAl₂O₄, and MgAl₂O₄-Al₂O₃. the process consists of diffusion of 3 Mg²⁺ ions toward alumina side and 2 Al³⁺ ions towards magnesia side forming in total 4 MgAl₂O₄. [2.3] The thickness ratio between spinel formed in alumina and magnesia side is 3:1. This is due to the higher solubility of alumina in spinel. The formation reaction of magnesium aluminate spinel is always associated with dimensional expansion ~8% the main reason for this is the density difference between reactants and products[2.4].

Andrianov et al. studied [2.5] the expansion behavior of magnesium aluminate spinel in a designed apparatus and found 5% growth due to spinellisation. They reported that spinel formation was effected by the rate of diffusion. Colinas et al. studied [2.6] the formation of different spinel at different temperature by measuring the fraction of reaction completed as a function of time.

They found the rate of spinel formation followed the sequence $\text{MgAl}_2\text{O}_4 > \text{ZnAl}_2\text{O}_4 > \text{NiAl}_2\text{O}_4$. The cause of the increase in MgAl_2O_4 spinel formation was reported as the neutrality in site preference by Mg^{2+} cation which increases its mobility leading to higher rate of spinel formation. Mansour et al. studied [2.7] the effect of MgO and Al_2O_3 characteristics on spinel formation. He reported calcination temperature, calcination atmosphere, and raw materials played an important role in spinel formation. Eta alumina was reported to form spinel easily and formed spinel increased with the increase in the crystal size of the reactants. Mazzoni et al. studied [2.8] spinel formation and sintering using reducing atmosphere. They reported that presence of reducing atmosphere did not affect the spinel formation up to 1300°C . The spinel formation was complete at 1300°C in the stoichiometric composition. However, secondary phases were present in the non-stoichiometric composition. A weight loss was observed in Mg-rich spinel in CO atmosphere. They reported this weight loss due to volatilization of MgO during sintering in reducing atmosphere.

Different workers studied the mechanism of spinel formation. W.D. Kingery well described [2.9] various mechanisms for spinel formation from its constituent oxides. All the mechanisms show that rate of spinel formation being controlled by diffusion of divalent, trivalent and oxygen ions. The rate of transportation of electron/holes and oxygen gas along interfaces $\text{AO-AB}_2\text{O}_4$ or $\text{AB}_2\text{O}_4\text{-B}_2\text{O}_3$ also controlled the rate of formation of spinel. Navais et al. used [2.10] different atmospheric conditions for the formation of spinel. MgO vapors were diffused into Al_2O_3 in a vapor–solid reaction at 1 atmospheric hydrogen pressure. Consistently increased amount of spinel was obtained with increasing temperature and time. The properties and compositions of spinel formed were found to be different at different layers.

Carter et al. studied [2.11] the mechanism of solid state reaction of spinel formation using molybdenum wires as inert markers. He confirmed that spinel formation reaction occurred due to counter diffusion of Mg^{2+} and Al^{3+} ions in the rigid oxygen lattice. This mechanism of spinel formation was later verified by Rossi et al. [2.12] Different parameters affecting solid state reaction of spinel formation was studied by Yamaguchi et al. They reported [2.13] that the reaction follows a parabolic law. No distinct effect of the specimen, single crystal or polycrystalline was found in the reaction. The thickness ratio of formed spinel layer was found to increase at a higher temperature. The spinel formed in contact with alumina was found to have higher alumina content. The activation energy of spinel formation was found to be 92kcal/mol . They also reported spinel

formation to spinel to be occurred by diffusion of 3 Mg^{2+} and 2 Al^{3+} ions. The role of oxygen in solid state reaction of $MgAl_2O_4$ spinel formation was studied by Nakano et al.[2.14] They prepared spinel by close contact with oxygen-rich MgO and Al_2O_3 polished surfaces piece in an argon atmosphere. The soaking time was 170hrs at $1650^{\circ}C$. To study the distribution of oxygen ion in the resulted mass, spark source mass spectroscopy was used. An oxygen enriched spinel was obtained on MgO side; however, the concentration of oxygen was low at the interfaces and next alumina side spinel layer. They confirmed the diffusion of Mg and Al ions in rigid oxygen lattice as the main reason for the growth of spinel from these observations.

Whitney II et al. used [2.15] the cleaved and polished surface of single crystals to see interdiffusion between MgO and Al_2O_3 . They reported that rate of spinel formation to be dependent on temperature. The rate varied with a rate constant of $k=1.19 \times 10^2 \exp(-88000/RT)$ above $1750^{\circ}C$. The rate constant k was determined as $1.17 \times 10^4 \exp(-125000/RT)$ for a temperature less than $1750^{\circ}C$. They also reported that change in diffusion mechanism was responsible for the change in activation energy for spinel formation. The interdiffusion coefficient of Al ion in MgO was studied in the temperature range $1565-1900^{\circ}C$. It was reported that interdiffusion is directly proportional to temperature, mole fraction of cation vacancy and was found to be independent of the crystallographic orientation of alumina. Murphy et al. investigated [2.16] the mechanism of cation diffusion in magnesium aluminate spinel. The transportation mechanism of Al^{3+} and Mg^{2+} ions through $MgAl_2O_4$ lattice was investigated by atomic scale simulation in a computer. Both cation and the interstitial process were considered. They reported Mg^{2+} ions to be more mobile than Al^{3+} ions. The preferred mechanism for Al ion diffusion was reported as vacancy mechanism.

Ghosh et al. investigated [2.17] the effect of particle size of MgO and Al_2O_3 on the spinel formation with permanent linear change on heating (PLCR) and microstructure in Al_2O_3 - $MgAl_2O_4$ -C refractory. They reported spinel formation to be very much dependent on particle size and reactivity of the starting materials. Spinel formation was found to occur in between alumina grains which acted as bond. $MgAl_2O_4$ was found to improve the strength and control PLCR of the refractory in stoichiometric nature. Szczerba et al. studied [2.18] the influence of raw materials morphology on properties of magnesium -spinel products. They mainly investigated the effect of clinker morphology on properties magnesia-spinel product. Two types of magnesia clinkers and fused magnesia was used along with fused spinel. The product containing a high amount of spinel

produced high open porosity, gas permeability and low crushing strength irrespective of the type of magnesia used.

Zhang et al. examined [2.19] the effect alumina polymorphism on the synthesis of magnesium aluminate spinel. Three different kinds of alumina were used- α Al_2O_3 , γ Al_2O_3 , and ρ Al_2O_3 . The magnesia used was analytical grade magnesia. The γ Al_2O_3 was found best for sintering and synthesis of spinel. The main reason for this may be due to its starting crystal structure similar to spinel. Haldar et al. prepared [2.20] magnesium aluminate spinel aggregates from Indian magnesite and calcined alumina in single firing stage. They achieved around 94% densification after sintering at 1600°C . Sarkar et al. used [2.21] different commercial grade magnesia and alumina to prepare magnesium aluminate spinel by single stage firing. Spinel formation was completed at around 1500°C for all compositions. Purer compositions led to higher expansion and low density with porous microstructure. Kong et al. synthesized [2.22] spinel by activated high energy ball milling process. They used commercially available 99.9% pure MgO and Al_2O_3 powder. They chose a stoichiometric composition and did 12 hr. of planetary milling. Milling significantly enhanced the reaction between MgO and Al_2O_3 . 98% theoretical density was obtained by sintering at 1550°C for 2hrs. Orosco et al. studied [2.23] magnesium aluminate synthesis in a chlorine atmosphere. They used 99.99% pure MgO and Al_2O_3 reactants. The presence of chlorine reduced the spinel synthesis temperature. The presence of chlorine in the atmosphere led to the crystallization of spinel in between 800 to 1000°C . Tavangarian et al. used [2.24] lansfordite and gibbsite in 1:2 ratio to prepare stoichiometric spinel. They mechanically activated the mixture by using planetary ball mill. Single phase nano- spinel powder was obtained after 6-10hrs of planetary milling at 1000 and 1200°C after annealing for 1 hr. The reduction in particle size by milling increased spinel formation due to increase in contact surface area which accelerated the diffusion reaction of spinel formation. Tripathi et al. studied [2.25] the effect of MgO reactivity on synthesis and densification of magnesium aluminate spinel. They used two types of magnesia one calcined at 1100°C and another sintered magnesia. Spinel produced from sintered magnesia show better densification than the calcined magnesia. Spinel formation to densification ratio was better in calcined magnesium composition due to higher spinel formation rate as a result of lower crystallite size. Ting et al. [2.26] tried to identify the rate controlling mechanism in the sintering of MgAl_2O_4 compositions. They considered the defect reactions and constructed Brouwer diagram to correlate densification rates to defect concentrations. They reported intrinsic defects as Schottky types and

oxygen vacancies the principle charge compensating defect in MgO-rich composition. The oxygen lattice diffusion through vacancies was concluded as rate controlling mechanism.

Sarkar et al. studied [2.27] effect of attritor milling on densification of magnesium aluminate spinel in both single and double stage sintering process. 99.5% densification was achieved after 6hrs of attrition milling. Calcination was done at 1400 and 1600°C. Higher calcination temperature was not found beneficial for densification. Kostic et al. [2.28] sintered magnesium aluminate spinel bodies containing 60, 80 and 90% spinel. They concluded degree of densification to be directly proportional to initial spinel content. Addition of even 0.5wt.% CaO: SiO₂ enhanced the densification to a great extent. Grain growth was also increased with 0.5wt.% the addition of CaO: SiO₂. Kim and Saito studied [2.29] the effect of grinding on the synthesis of MgAl₂O₄ spinel from Mg(OH)₂ and Al(OH)₃. They reported that formation of the amorphous phase of starting material after 60mins of grinding. Over 15mins of grinding produced MgAl₂O₄ phase at 780°C. However, the reactivity of mixture did not improve after 30 mins of grinding as over grinding led to aggregation of particles. Mustafa et al. studied [2.30] sintering of spinel forsterite bodies using talc, calcined magnesite, and reactive alumina. The spinel phase was found either within forsterite or on the rims of forsterite or prismatic crystals between the boundaries.

Ganesh et al. reported [2.31] on the influence of processing parameters on formation and densification of MgAl₂O₄. They used 3 different sources of alumina and magnesia. The degree of hydration of precursor material had a strong influence on spinel formation. Spinel percentage greater than 70% in calcined powder was found to be good for densification. The presence of finer spinel particles led to high rate of sintering. Zhihui et al. studied [2.32] the effect of mechanical activation of Al₂O₃ on the synthesis of magnesium aluminate spinel by reaction sintering alumina and magnesia. They used α -Al₂O₃ synthesized from gibbsite heated at 1400°C for 4 hr. The α -Al₂O₃ was mechanically activated by milling for 12hr, 24hr, and 36hrs. They reported improving in bulk density value with increase in milling time of Al₂O₃. However, the effect of milling for more than 24hrs was not eminent in the bulk density values. Tavangarian and Emadi synthesized [2.33] nanocrystalline magnesium aluminate spinel powder by mechanical activation of precursor powder containing Al₂O₃ and MgCO₃. The subsequent annealing mechanical activation led to the formation of a single phase nanocrystalline magnesium aluminate powder. Liberation of CO₂ from MgCO₃ increased surface reactivity. The crystallite size of prepared spinel was 25-45nm.

2.2 Synthesis through other non-conventional routes

A lot of literature are available in the fabrication of magnesium aluminate spinel. The synthesis of spinel by different routes, raw materials were studied by many workers in different conditions. Some of the methods which were used are co-precipitation, sol-gel, combustion synthesis, etc.

Mitchell developed a chemical method of spinel preparation by mixing aluminium hydroxychloride $\text{Al}(\text{OH})_5\text{Cl}\cdot 2\text{-}3\text{H}_2\text{O}$ and $\text{Mg}(\text{OH})_2$ suspension in water. The rapid reaction resulted in an amorphous gel which on drying produced solid mass. The solid was milled and heat treated at 900°C which produced white fine partially crystallized spinel.[2.34]

2.2.1 Co-precipitation method

Among non –conventional techniques of spinel synthesis, co-precipitation is an important method. High purity powders can be produced by this method. A highly reactive homogenous sinterable powder with uniform particle size distribution and controlled morphology can be produced by this method. Mukherjee et al. prepared[2.35] spinel from hydroxides of aluminium and magnesium in the pH range 6.5-10. Stoichiometric spinel was obtained at pH 9. They also reported that at a lower pH concentration of Al ion was higher which decreased after pH 9. 100 mins at 1200°C led to complete spinellisation. Co-precipitation of magnesium aluminate spinel was also studied by Bratton et al. [2.36] He co-precipitated in the pH range 9.5-10. He used Mg^{2+} : Al^{3+} ion concentration solution obtained from hydroxide precipitation from chloride solutions. The precipitate was a mixture of gibbsite $[\text{Al}(\text{OH})_3]$ and Mg-Al double hydroxide $[2\text{Mg}(\text{OH})_2\text{Al}(\text{OH})_3]$. Calcination of this mixture between $350\text{-}400^\circ\text{C}$ resulted in an amorphous phase, but calcination above 400°C resulted in crystallization of spinel phase. After studying on spinellisation behavior of a mixture of magnesium oxalate precipitate and aluminium hydroxide, he reported that delay in spinel formation in this case up to 800°C .The complexity of the oxalate decomposition was reported as the cause of the delay. Mechanism of spinel formation from co-precipitated hydroxides was studied by Gusmano et al. [2.37] They used Mg-Al hydroxycarbonate with Mg^{2+} : $\text{Al}^{3+} = 2:1$, $\text{Al}(\text{OH})_3$ and AlOOH to synthesize magnesium aluminate spinel. They reported decomposition of mixed hydroxide around 220°C . Around 280°C Al-hydroxide transformed to η alumina. These transition products than reacted to form transition phase which decomposed to magnesium aluminate spinel at about 400°C . Nicolai et al. developed [2.38] an

industrially feasible modified co-precipitation technique. They used Mg salts and sodium meta-aluminate to produce active spinel powders. Popovic et al. [2.39] synthesized spinel through co-precipitation of magnesium hydroxide with pseudoboehmite and thereafter calcining the produced gel. The coprecipitate formed was a mixture of double hydroxide $[2\text{Mg}(\text{OH})_2 \text{Al}(\text{OH})_3]$, pseudoboehmite $[\text{AlOOH}]$ and aluminium trihydroxide $[\text{Al}(\text{OH})_3]$; calcination of the mixture resulted in poorly crystallized primary spinel phase around 450°C . This spinel converted to crystalline secondary spinel around 850°C due to solid state reaction between γ alumina and magnesia oxide.

Wang et al. used [2.40] a controlled chemical co-precipitation technique in aqueous solution based on thermodynamic modelling to synthesize nano-sized metastable precursor of magnesium aluminate spinel. At pH 10 and temperature 25°C hydroxides of magnesium and aluminium were precipitated from chloride solutions. Calcination at 1000°C for 10hrs produced pure spinel phase of specific surface area $47.4\text{m}^2/\text{gm}$. Thermal decomposition of spinel from hydrated nitrate mixture was studied by Messier et al. [2.41] They used magnesium nitrate hexahydrate and aluminium nitrate nonahydrate as a precursor to form a stoichiometric spinel. The mixture was melted at 130°C and quenched to solidify, crushed, dried and heat treated to decompose at 400°C . The powder obtained was reported to be highly active with small crystallite size. Tomilov et al. [2.42] tried to determine the chemical and structural transformation during thermal decomposition of double hydroxide to understand the formation condition of magnesium aluminate spinel. They obtained highly dispersed thermolysis product at 800 and 1000°C . They reported that Mg-Al hydroxide precipitate composition to be dependent on co-precipitation method that predetermines the spinel formation mechanism. Takeo et al. studied [2.43] the spinel formation by decomposition of freeze dried sulfate. They used $\text{Mg}(\text{SO}_4)6\text{H}_2\text{O}$ and $\text{Al}_2(\text{SO}_4)_3 \cdot 17\text{H}_2\text{O}$ as a source of magnesia and alumina. They reported transformation of crystalline Al sulfate to crystalline anhydride on heating which on further heating transformed to amorphous alumina. Similarly, Mg sulfate transformed to amorphous MgO. The formed amorphous oxides reacted and produced spinel even at 840°C . Zenbee et al. studied [2.44] similar investigation and reported decomposition of a mixed amorphous sulfate $\text{MgAl}_2(\text{SO}_4)_{4.8-9}\text{H}_2\text{O}$ to spinel above 1000°C . Chae et al. [2.45] supported the reaction of spinel formation at 1000°C from mixed sulfate hydrate in amorphous oxide state. They calculated the crystallite size after calcining at 1000°C for 1 hr. as 280\AA and activation energy of spinel formation to be 36.5kcal/mol between $900-1000^\circ\text{C}$. Healy et

al. used [2.46] hydrothermal processing using acetate and nitrate route to study the spinel formation reaction.

Zawrah et al. [2.47] synthesized magnesium aluminate spinel powders using stoichiometric aluminium and magnesium chlorides at 80⁰C by co-precipitation. They obtained a mixture of Mg-Al double hydroxide with traces of gibbsite and brucite in the co-precipitated spinel powders. The particle size of the co-precipitated powder was 25-60nm. After heat treatment of the coprecipitate at 1000⁰C crystalline spinel powder was obtained. They also studied the effect of MnO₂ and ZnO on densification. About 94% and 96% theoretical density was achieved with ZnO and MnO₂ addition respectively. Improvement in mechanical properties was also reported with ZnO and MnO₂ addition. Khalil et al. studied [2.48] the sintering, mechanical and refractory properties of magnesium aluminate synthesized by co-precipitation process and sol-gel process. He used magnesium nitrate and aluminium nitrate as a precursor in coprecipitation method and aluminium hydroxide and magnesium chloride in case of the sol-gel process. He concluded firing at 1300⁰C to be sufficient for spinel formation for both the process. Spinel prepared via sol-gel route were reported to have lower particle size compared to co-precipitation method. He also studied the addition of zirconia and chromia; the addition of chromia and zirconia was reported to improve mechanical properties. However, the addition of a mixture of chromia and zirconia was reported to have the highest benefit. Wajler et al. investigated [2.49] the formation of magnesium aluminate spinel precursor powder prepared by a co-precipitation method using magnesium nitrate and aluminium nitrate and ammonium carbonate. During coprecipitation only crystalline phase formed was ammonium downsonite (NH₄Al(OH)₂CO₃.H₂O). A second phase (Mg₆Al₂(CO₃)(OH)₁₆.4H₂O) was reported to appear after ageing. At 940⁰C, they obtain MgAl₂O₄ along with MgO and Al₂O₃. Guotian Ye et al. used [2.50] a combination of sol-gel and coprecipitation process to prepare magnesium aluminate spinel powder using aluminium isopropoxide [Al(-O-i-C₃H₇)₃] and magnesium acetate tetrahydrate [Mg(CH₃COO)₂.4H₂O] as starting materials. They obtained pure spinel phase using this technique at 900⁰C. Mosayebi et al. [2.51] employed surface assisted co-precipitation method to produce high surface area nanocrystalline magnesium aluminate spinel at low temperature. They used magnesium nitrate hexahydrate and aluminium nitrate nonahydrate and pluronic P123 triblock copolymer (as a surfactant) as starting material. The increase in pH and reflux temperature and time increased the surface area and decreased the particle size. They also

reported that increase in calcination temperature increased crystallite size and particle size due to sintering.

Alvar et al.[2.52] synthesized mesoporous nanocrystalline $MgAl_2O_4$ spinel via surfactant assisted precipitation route. They used aluminium nitrate nonahydrate, magnesium nitrate hexahydrate as precursor and N-Cetyl-N,N,N-trimethylammonium bromide and ammonium hydroxide as surfactant and precipitation agent respectively. They reported that addition of surfactant influenced the spinel structural properties. Use of surfactant reduced crystallite size and increase surface area and thermal stability. Li et al. [2.53] used ammonium carbonate as a precipitator to produce magnesium aluminate spinel precursor from magnesium nitrate and aluminium nitrate. The precursor was composed of ammonium dawsonite hydrate $[NH_4Al(OH)_2CO_3 \cdot H_2O]$ and hydrotalcite $[Mg_6Al_2(CO_3)(OH)_{16} \cdot 4H_2O]$ which transformed to spinel at $900^\circ C$. The sintering of the $1100^\circ C$ calcined powder at $1550^\circ C$ for 2hrs produced dense spinel of 99% theoretical density.

2.2.2 Sol-gel method

Many researchers studied the synthesis of magnesium aluminate spinel via a sol-gel route. The sol-gel route has the advantage among different other routes; as it can produce pure ultrafine powders at low temperature. Besides this, it can also incorporate soluble inorganic salts into the matrix either by actual chemical reaction or by simple entrapment in the gel matrix. In organometallic sol-gel route, two organometallics are hydrolyzed in a controlled environment with vigorous stirring which results in a translucent gel. Later the fluid of the gel is drained out to produce an amorphous gel which on heating crystallizes and produce the desired phase at a much lower temperature.

Carole et al.[2.54] used the sol-gel technique to produce magnesium aluminate spinel for optical applications. They hydrolyzed Mg-Al alkoxide mixture or mixture of Al-alkoxide and Mg nitrate solution thereafter spray drying it in an inert atmosphere. They obtained homogenous spheroidal amorphous particles; spinel formation was reported at $1000^\circ C$. Lepkova et al. [2.55] used the sol-gel technique to produce 97% spinel at $1000^\circ C$ using $Mg(NO_3)_2 \cdot 6H_2O$ and $Al(OC_4H_9)_3$ as a precursor. During hydrolysis combination of additives like B_2O_3 , TiO_2 were added as alcoholate to intensify the spinel formation. Around $500-600^\circ C$ amorphous phase was obtained. Crystallization of amorphous phase occurs at around $900^\circ C$. Wang et al. [2.56] used the

freeze-drying technique to prepare high sintered magnesium aluminate spinel from alkoxide precursors. They used aluminium isopropoxide to prepare an aluminium sol. Magnesium methoxide was introduced thereafter up to stoichiometric composition into the alumina sol. The excess water evaporated out, and organic matters and sol was freeze dried and calcined to produce spinel powder. Spinel formation was reported to occur at 430⁰C. Varnier et al. [2.57] used the sol-gel technique to produce high-quality magnesium aluminate spinel. They used heterobimetallic n-butoxide as precursor, intermediate alumina or magnesia phase formation was eliminated. Hydrolysis of molecular precursor $[\text{MgAl}_2(\text{O}^n\text{Bu})_8]_n$ with polyethelene glycol produced a reproducible transparent gel. Decomposition of glycol occurred at 150 to 500⁰C, and pure fine crystallites of spinel were formed at 700⁰C.

The addition of mineralizers on spinel formation via sol-gel route was studied by Kadogawa et al. [2.58] They prepared magnesium aluminate using $\text{Al}(\text{NO}_3)_3$ and $\text{Mg}(\text{NO}_3)_2$ with a small amount of $\text{Si}(\text{OC}_2\text{H}_5)_4$ and mineralizers like LiCl, NaCl, KCl, etc. The spinel formation reaction started at 800⁰C. LiF was reported to have the highest influence on spinel formation. Singh et al. [2.59] used combined gelation-coprecipitation method to prepare spinel from a mixture of sulfates of aluminium and magnesium. They reported spinel formation to start at 600⁰C and completed at 1000⁰C. They obtained 95% densification in pressed calcined bodies sintered at 1450⁰C for 3hrs. Magnesium aluminate spinel was produced by Waldner et al. [2.60] using $\text{Al}(\text{OH})_3$ and MgO or $\text{Mg}(\text{OH})_2$ with tetra ethanolamine. Calcination of the polymeric precursor at 500⁰C led to very fine material which got converted to magnesium aluminate and γ -alumina at 700⁰C for 2hrs. At 900⁰C, a homogenous material was obtained which transformed into spinel at 1200⁰C after 2hrs of soaking.

Saberi et al. [2.61] used sol-gel citrate technique to synthesize magnesium aluminate spinel. They studied the influence of heat-treatment atmosphere on the formation of magnesium aluminate spinel. Nano-size magnesium aluminate spinel in the range 20-100nm was produced when they used argon atmosphere. Use of argon atmosphere slowed down the heat generation from combustion reactions, which helped in the production of nano-size MgAl_2O_4 powder. Sanjabi et al. [2.62] also synthesized nanocrystalline magnesium aluminate spinel using a modified sol-gel technique. They used aluminium nitrate, magnesium nitrate, citric acid and diethylene glycol monoethyl ether as a precursor material. They investigated the formation of spinel at different

calcination temperature 700,800 and 900⁰C.The 800⁰C 2h calcined powder showed optimum properties with a crystallite size of 11 nm and surface area 154m²/g. Pei et al. [2.63] developed a low cost efficient aqueous sol-gel technique to synthesize fine magnesium oxide and magnesium aluminate spinel powders. They used citrate precursors derived from magnesium chloride, aluminium nitrate and citrate as a precursor. The citrate precursor decomposed to Magnesium oxide and spinel at 400⁰C.The heat treatment of spinel precursor at 1200⁰C lead to the formation of cubic MgAl₂O₄ phase. The particle size of spinel formed was reported in the range of nanometer and micrometer size. Nassar et al. [2.64] used sol-gel auto combustion technique to prepare magnesium aluminate spinel using oxalic acid, urea, and citric acid as fuel. Pure phase spinel was synthesized at 250⁰C.Nano –sized MgAl₂O₄ with crystallite size 27.7,14.6 and 15.65nm were produced at 800⁰C.

2.2.3 Other modified non-conventional techniques

Besides sol-gel and coprecipitation, many researchers have worked and developed many other routes and techniques to prepare magnesium aluminate spinel. Suyama et al. [2.65] used spray pyrolysis technique to prepare magnesium aluminate spinel. The reaction temperature of 740-1030⁰C was used by them. They used alcohol and alcohol-water system. The alcohol –water system was reported to produce spinel of poorer crystallinity and lower surface area.Spinel synthesis by flame spray pyrolysis was studied by Brickmore et al. [2.66] They used double alkoxide in alcoholic solutions as precursors. Nano size spinel with surface area 20-45m²/gm was obtained at 600⁰C.They reported the formation of powder due to nucleation and grain growth of oxide species in the vapour phase. Kang et al.[2.67] used colloidal solution to prepare magnesium aluminate spinel using filter expansion aerosol generator and aqueous solution. They also reported that crystallinity of formed spinel was not dependent on alumina or magnesia source. Good crystallinity was obtained for particles calcined with a soaking period. Very high surface area particles were obtained from colloidal solutions compared to aqueous solution due to higher nucleus concentration in colloidal solutions. Spinel formation by decomposition of a double alkoxide Mg[Al(OR)₄]₂ in supercritical fluid ethanol, was studied by Pommier et al. [2.68] They reported the formation of partly crystallised submicronic powder at around 350⁰C and 15 MPa. The crystallinity was found to increase with reaction temperature and time. The increase in ethanol content leads to better crystallinity and smaller particles and agglomerates. Kanerva et al. studied

[2.69] the crushing strength of MgAl_2O_4 granules. They use MgO and $\text{Mg}(\text{OH})_2$ as magnesia precursor and $\text{Al}(\text{O})\text{OH}$ and $\alpha\text{-Al}_2\text{O}_3$ as alumina precursor. Spinel granules were prepared via dispersion manufacturing and spray drying process. The granules were heat treated between 1000-1400⁰C. The highest strength was obtained from spinel prepared by using $\text{Mg}(\text{OH})_2$ as Mg Precursor and $\text{Al}(\text{O})\text{OH}$ as Al precursor.

Effect of seeding on spinel formation was studied by Pasquier et al. [2.70] through different methods using different sols, nitrate solutions, and alkoxides. A decrease in crystallization temperature of spinel was reported due to isostructural seeding. The nucleation and epitaxial growth mechanism were attributed for this. Ghosh et al. studied [2.71] seeding effect on formation of MgO-rich spinel with 20wt.% spinel incorporation. They reported improvement in thermo-mechanical properties of the MgO-rich spinel refractory material.

Choi et al. used [2.72] the self-propagating high-temperature synthesis (SHS) method to synthesize magnesium aluminate spinel. Variable conditions such as mixing of fines, preheating temperature, amount of ignition catalyst were optimized. They reported 48 hr. mixing time, 800⁰C preheating temperature and 20 wt. % as the most in effect parameters. Ping et al. used [2.73] SHS technique to prepare magnesium aluminate spinel. They used reagent grade MgO powder and metallic alumina as starting material. Very high purity spinel with 92% theoretical density was achieved at 1600⁰C.

Tong et al. [2.74] prepared nanocrystalline MgAl_2O_4 by a convenient salt assisted combustion process using low-toxic glycine as fuel, magnesium nitrate hexahydrate, and aluminium nitrate nonahydrate as raw materials. They reported to obtain optimal condition to synthesize nanocrystalline magnesium aluminate oxide. Glycine/metal/salt = 2:1:1 using LiCl (salt assistant) and calcination temperature 700⁰C was reported perfect for the synthesis. They also studied the crystal growth dynamics of MgAl_2O_4 and reported the activation energy of nanocrystals to be 39.1kJ/mol. Gomez et al. [2.75] did a comparative study of microwave and conventional processing of MgAl_2O_4 based materials. They reported 90% spinel formation by both the methods. However, the microwave heating was reported to be faster than conventional heating resulting in the better microstructure.

Ganesh et al. studied [2.76] the effect of processing route on microstructure and mechanical properties of magnesium aluminate spinel. They concluded calcination of 1hr at 1400⁰C could

produce 89% spinel via temperature induced gelation process. They obtain stable slurries by using surface passivated MgAl_2O_4 powder with 45vol% solid loading. 95-98% theoretical density was achieved by sintering at 1650°C for 1 hr. Behera et al. [2.77] synthesized magnesium aluminate spinel via auto ignition of citrate-nitrate gel. They used 1:1 hydrated nitrates of Mg and Al as precursors. Auto-ignition of the gel produced a black color mass, which on calcination at 650°C for 9hrs yielded crystalline MgAl_2O_4 spinel. They also reported calcination at higher temperature lead to increasing order of spinel.

Fazli et al. [2.78] used the molten salt method to prepare nanocrystalline MgAl_2O_4 spinel. They used nano alumina, magnesia and lithium chloride as starting materials. They reported 850°C and 3h soaking as optimum temperature to prepare nano-crystalline MgAl_2O_4 using LiCl via the molten salt method. The optimum salt to oxide ratio was reported as 5:1. The particle size of synthesized MgAl_2O_4 nanocrystal was in the range of 30-50nm. Kutty et al. [2.79] used a non-conventional soft chemical method to prepare nanocrystalline MgAl_2O_4 . They used oxalic acid as an organic template and nitric acid as an oxidizing agent. They used 1:2 molar ratio of Magnesium nitrate hexahydrate and aluminium nitrate nonahydrate as raw materials. They reported obtaining MgAl_2O_4 nanocrystals at around 700°C which was quite low in comparison to conventional processes.

2.3 Sintering of magnesium aluminate spinel

The definition of sintering is given as- “Thermal treatment of powder or compact at a temperature below the melting point of the main constituent in order to increase its strength by bonding the particles together”. Sintering results in an increase in strength, conductivity and density.

Generally, sintering can be divided into a number of stages namely, initial stage, intermediate stage, and final stage. Initial sintering stage is accompanied by large curvature gradient near the inter-particle neck, tangential contact between particles and interconnected pores. The initial stage sintering ends with coalescing of particles. The next stage is the intermediate stage which is marked with interconnected cylindrical pore structure along the grain junctions. Grain growth with possible pore isolation occurs at the end of an intermediate stage of sintering. 70-92% densification occur at this stage. The open pore network that was formed during the initial stage of sintering breaks up during this stage. The beginning of the last or final stage of sintering is

marked with the appearance of isolated pores. The rate of sintering is slow during this stage. Mass transport from grain boundaries to the pores eliminates the isolated pores. But the presence of gaseous phase in the pores limits the end point density.

Sintering is generally divided into three categories depending on the mechanism involved-

- I. Solid state sintering
- II. Liquid state sintering
- III. Sintering in the presence of reactive liquid.
- IV. Sintering with chemical reaction or reactive sintering

I. Solid state sintering:-In solid state sintering transfer of material from one part to other leads to the occurrence of densification without the presence of any liquid phase. The main driving force of sintering is lowering of the free energy due to the reduction of surface area by the elimination of solid vapour interfaces by solid-solid interfaces.

II. Liquid state sintering:-In liquid phase sintering densification occur in the presence of a liquid phase which serves as a bond for the body. Liquid phase sintering is used in the system where solid-solid sintering is difficult due to poor diffusion of material transport. Sintering with liquid phase must be controlled critically or else there may be a distortion of the body due to additional complications arising from the liquid phase.

III. Sintering in the presence of reactive liquid: -This sintering mechanism is quite similar to liquid phase sintering, but essential requirement is the solubility of the solid phase in the liquid medium at sintering temperatures. The essential part of this is a solution- reprecipitation of the solids which leads to increase in grain size and density.

Essential requirement of this sintering technique are-

- Presence of appreciable amount of liquid
- Solubility of solid phase in formed liquid and
- Complete wetting of solids by the liquids.

IV. Reaction sintering or sintering with the chemical reaction: - It is a type of sintering in which chemical reaction between the starting materials and densification of powder compact are achieved in a single heat treatment step.

Densification of magnesium aluminate is important as the formation reaction of magnesium aluminate is associated with a volume expansion which opposes the densification process. So, in general, a two-step firing process is used. The first stage is the calcination stage during which spinel formation occurs. The formed spinel is then crushed, milled and reshaped and sintered in the second firing step. Research on sintering of MgAl_2O_4 by different sintering methods, spinel formed by different processes, the effect of different sintering parameters, the effect of additives, and effect of stoichiometry is going on from a long time. However, commercial viability and sophistication involved is increasing with time. Sintering also effects development different properties. Many researchers have also worked on the characterization of spinel sintered at various conditions.

Bailey et al. studied [2.80] the formation of spinel and its densification taking MgO and Al_2O_3 as starting material. They calculated activation energy for spinel formation as 90.5kcal/mol . They developed a new method in order to minimize the effect of volume expansion during spinellisation. They named it as “Partial reaction technique” in which 55-70% spinellisation was completed in the first firing, retaining sufficient degree of reactivity of material which would benefit in sintering in next firing. They reported obtaining 95% theoretical density after sintering at 1640°C . They also reported that sintered product had an average grain size of 15.6μ , lattice parameter 8.083\AA , cold MOR of 24000psi , modulus of elasticity $29.1 \times 10^6 \text{psi}$ and coefficient of thermal expansion $8.38 \times 10^{-6} / ^\circ\text{C}$ in the temperature range $25-700^\circ\text{C}$. Densification behavior of magnesium aluminate spinel via co-precipitation route and mixed route sintered at $1600-1750^\circ\text{C}$ with soaking time 30-240mins was studied by Ruthner et al. [2.81] He reported achieving 92% true density after sintering at 1750°C for 4 hrs. for spinel synthesized via co-precipitation route from chloride solutions. Chisato et al. [2.82] studied the factors influencing the densification of magnesium aluminate spinel. They reported particle size of the starting materials to have the highest influence on sintering. They synthesized spinel with density value more than 3.3gm/cc through a commercially accepted process. Sintering of magnesia spinel using vibromilling and thermal treatment of the starting materials was studied by Dunaitseva et al. [2.83] They reported vibromilling to improve densification and reported 1200°C calcined powder to produce higher density after sintering at 1600°C . Serry et al. [2.84] used a two stage firing process for pure magnesia; spinel bonded magnesia, pure spinel, and pure corundum bodies. They reported periclase and spinel to be present as clusters with direct bonding in magnesia-rich composition.

Microstructure with closed porosity was reported for pure spinel body than that of the spinel bonded body. Kitagawa et al. studied [2.85] the mass transport mechanism of $\text{MgO} \cdot 2.4\text{Al}_2\text{O}_3$ spinel by the scratch smoothening method. They found that mass transport in spinel to be controlled by the transport of oxygen ions either as volume or surface diffusion. However, the overall transport was reported to be low because of low transport through the surface. They concluded that oxygen ion is the slowest diffusing species, this sluggish mechanism of mass transport was reported as a reason for slow densification process of spinel.

Bratton et al. investigated [2.86] the initial sintering kinetics of spinel synthesized from magnesium aluminium hydroxide co-precipitation, calcined at 1100°C for 4hrs. He calculated the activation energy for initial stage sintering as 116kcal/mol with spinel formation energy of $100\text{-}107\text{kcal/mol}$. He also concluded that the initial sintering rate was controlled by Al^{3+} ions. In the temperature range $1050\text{-}1300^\circ\text{C}$, he reported volume diffusion as the operating mechanism and apparent diffusion-coefficient was calculated as $D = 18.6 \exp [(-116 \text{ kcal/mol})/RT] \text{ cm}^2/\text{sec}$ for initial sintering. They also determined the sintering and grain growth kinetics in the temperature range $1300\text{-}1600^\circ\text{C}$ for same spinel powder with 96% densification. A sharp increase in density was reported with an initial soaking period, but prolonged soaking flattened densification for all sintering temperatures. Sintering process was found to be volume diffusion controlled one and apparent diffusion-coefficient was calculated as $D_v = 157 \exp [(-118 \text{ kcal/mol})/RT] \text{ cm}^2/\text{sec}$. The grain growth was calculated using the relationship $G^2 - G_0^2 = kt$ (where G_0 = initial grain size and G = instantaneous grain size).[2.87] The densification kinetics of spinel sintered under rate controlled conditions was investigated by Johnson et al. [2.88] They reported the sintering of finely divided magnesia-rich spinel, cold-pressed to 50% theoretical density, with densification rate as controlling variable. The kinetics for 60-90% theoretical density was described as a rate independent correspondence of temperature and density as $\ln D = 1.96 + 1.48 \times 10^{-3} T$ and a linear densification and heating rate correspondence $dD/Ddt = 1.48 \times 10^{-3} dT/dt$. They reported that spinel ceramics sintered at constant densification rate synthesized from active powders produced bloating when the initial heating rate was too fast on reheating.

Sintering of magnesium aluminate spinel depends on a number of factors and parameters such as general time, temperature and sintering rate. Petkovic et al. studied [2.89] the effect of magnesia powder activity on sintering of spinel. They used three types of magnesia and commercial alumina

powder as raw materials. They produced partially synthesized spinel at 1200 and 1300⁰C. The partially synthesized alumina was then sintered at 1600 and 1700⁰C in a vacuum. Smaller particle size was reported to produce more spinel but at a higher temperature and prolong soaking the advantage was found to be gradually reduced. The main reason for this was reported as the initiation of the sintering process due to higher fineness which reduced the reaction. They also reported the quantity and structure of presynthesized spinels an important parameter for sintering of spinel.

Kanai et al. investigated [2.90] the effect of body composition on sintering and developed strength of magnesium aluminate spinel. Sintering at 1600⁰C for 4 hrs. they reported magnesia rich and stoichiometric compositions to show higher density and uniform texture in comparison to alumina rich composition. The obtained highest bending strength for stoichiometric composition and lowest in the case of alumina rich spinel. Teoreanu et al. [2.91] worked on single stage sintering of spinel using different source sources of alumina and magnesia. Effect of additives like B₂O₃, Cr₂O₃ and MgCl₂ was also studied by them. Higher densification was observed for the batch containing calcined alumina and sintered magnesia irrespective of the additive. Sarkar et al. [2.92] used solid state oxide reaction for densification of magnesium aluminate spinel using three different sea water magnesia and commercial alumina. They reported achieving 99% theoretical density for highest purity material after attrition milling to a surface area of 9.3m²/gm. The properties like hot MOR, thermal shock resistance, etc. was reported best for the purest grade material.

Recrystallization and grain growth are two important terms in ceramics literature. Both these terms are related to increasing in grain size. In recrystallization abnormal or discontinuous grain growth may occur due to consumption of smaller grains by larger ones. However, in grain growth the grain size increases maintaining a same grain size distribution. Many researchers studied on recrystallization and grain growth of magnesium aluminate spinel by changing different parameters. Budnikov et al. studied [2.93] sintering and recrystallization of high purity magnesia alumina spinel produced by hot pressing. They used temperature range of 1200-1600⁰C pressure range of 60-300kg/cm² and holding time 10-30mins. They reported spinel with theoretical density at temperature 1500⁰C and above. Around 1450-1600⁰C intensive recrystallization was reported. Recrystallization rate of 10⁻⁶cm/sec was reported for grain size 2-6μ when hot pressed at 1400⁰C

with a pressure 300kg/cm^2 for 10-30mins. Rossi et al. studied [2.12] epitaxial growth of spinel by solid oxide reaction. They used a periclase crystal sandwiched between two sapphire crystals as a reaction couple and heat them at 1650°C for 250hrs in air. They obtained two spinel layers one from each oxide, with thickness ratio supporting the counter diffusion of cations. They observed that sapphire grown spinel had a similar orientation as sapphire, but periclase grown spinel was independent of the orientation of the periclase crystal. The mechanism of material transport through spinel periclase interface was reported as the main parameter which decided the degree of epitaxy. The growth of magnesium aluminate spinel was studied by Grabmier et al. using Czochralski method [2.94]. They produced single crystal of magnesium aluminate with MgO: Al_2O_3 molar ratio 1:1 to 1:3.2 with a pulling rate of 0.5cm/hr. The Higher rate of pulling was reported to entrap gas bubbles. Lattice constant of $8.089\pm 0.002\text{\AA}$ was reported for stoichiometric spinel. Two lattice parameters were reported for alumina rich composition due to the existence of two separate types of spinel in a single crystal. Ming et al. [2.95] took non-stoichiometric magnesium aluminate spinel to study grain growth by grain boundary migration. They obtained grain boundary mobility 100-1000 times higher in MgO rich compositions compared to Al-rich composition in the temperature range $1200\text{-}1800^\circ\text{C}$. The mobility was varied by less than 10 times over composition $1 < n < 1.56$ for $\text{MgO} \cdot n\text{Al}_2\text{O}_3$ composition.

Spinel with non-stoichiometric compositions are also important it has got a lot of commercial applications. But very fewer literature is available in its study. Bailey et al. [2.96] varied alumina content from 71.66-93.46 wt.%. They used partial reaction technique to prepare spinel around $1100\text{-}1150^\circ\text{C}$ and sintered in the range $1640\text{-}1685^\circ\text{C}$. With the increase in alumina content, they observed a decrease in lattice parameter till precipitation of free corundum phase. They obtained spinel phase up to 85% alumina content and also achieved maximum grain size and minimum thermal expansion for that composition. A sharp improvement in mechanical properties was observed for compositions containing 85% alumina with free corundum phase. The authors also studied [2.97] magnesia rich spinel systems and compared them against stoichiometric spinel. They reported the presence of little excess magnesia was extremely beneficial for stoichiometric spinel. The presence of a distinct second phase was suggested to restrain the grain boundary motion which produced highly sintered small grained spinel body. The also suggested excess magnesia less than 10% was sufficient to enhance densification.

Proverbio et al. investigated [2.98] nonstoichiometric spinel with composition $MgO_{1.5}Al_2O_3$. They focused on densification behavior, phase evaluation and microstructure development during sintering of spinel. They obtained 95% relative density after sintering at $1300^{\circ}C$ for 6 hrs. for spinel synthesized via hydrolysis of alkoxide calcined at $900^{\circ}C$. In between $1100-1400^{\circ}C$ precipitation of corundum phase was reported with larger grain size. An increase in spinel grain size was also reported resulting in heterogeneous microstructure with discontinuous grain growth. But in second stage sintering at $1500^{\circ}C$, they reported a homogenous microstructure with fine grain size. An increase in solubility of alumina in spinel phase was observed with increasing temperature. The grain growth of spinel was reported to be restricted by finely distributed second phase alumina which resulted in a fine homogenous microstructure in the final product.

2.4 Effect of additives on formation and sintering of magnesia aluminate spinel

Additives have great influence on ceramic processes. Additives are nothing but foreign substances which are intentionally added to a matrix to enhance effects to ceramic processes. For $MgAl_2O_4$ system additives are important from many aspects such as the formation of spinel, sintering, grain growth, and properties, etc. Additives are most important for formation and sintering of spinel. Additives promote sintering as they react with the system to make a solid solution or new compound or liquid phase by reacting with batch composition. Both interstitial and substitutional effect may occur in solid state solution causing a vacancy or strain in the lattice which promotes densification process. The introduction of a lower valence cation creates anion vacancy or cation interstitial which increases diffusivity which leads to increase the sintering rate. Such phenomenon can be observed when Li_2O is incorporated in MgO [2.99]. In a similar way cation vacancies are created when higher valence cations are incorporated. Incorporation of higher valence cation increases the diffusion rate which further enhance sintering and related processes. Some additive form liquid phase which acts as lubricant enhancing the mass transfer by diffusion in comparison to solid state sintering. The wetted solid particles are attracted by the capillary force of attraction which leads to higher densification.

Many researchers are studying the effect of the addition of additives on formation and densification of magnesium aluminate spinel from a long time. Effect of salt vapour on synthesis and crystal growth of $MgAl_2O_4$ was studied by Noda et al. [2.100]. They reported increase

spinellisation in the presence of salt vapour from 74-90%. However, the influence was reported to be complex. The addition of salt vapour increased crystal growth specially alkali fluorides. Effect of additives like B_2O_3 , V_2O_5 , P_2O_5 , MoO , WO_3 , MgF_2 , and LiF was studied by Helmut et al.[2.101] using 2wt.% additive addition on the formation of spinel in the temperature 1200-1400⁰C. Among these additives V_2O_5 and B_2O_3 was reported to have maximum effect. Additives like MnO_2 , MgO , CaO , and NiO were reported to have very less or almost negligible effect. Many additives like Li_2O , SiO_2 , CoO and Cr_2O_3 was reported to hinder the reaction.

Kostic et al.[2.102] investigated the influence of AlF_3 and CaF_2 on reaction sintered magnesium aluminate spinel. They reported substitution of O^{2-} ion by F^- ion in the lattice which created more cation vacancy which intensified cation diffusion completing spinellisation process in much lower temperature. However, a higher concentration of fluorine ion was found to be detrimental as it led to producing MgF_2 . Bakker et al.[2.103] used 1.5% AlF_3 and reported to complete spinellisation reaction within 1000⁰C using hydroxides. The addition of AlF_3 was also studied by Sarkar et al. [2.104] They used oxide reactants with 3% AlF_3 addition. The addition of AlF_3 was found to lower the spinel formation temperature from 1400 to 1100⁰C. Sintering was also reported to start at a lower temperature with the higher amount of AlF_3 addition. Sarkar et al. also studied [2.105] the densification of reaction sintered and presynthesized stoichiometric spinel using various oxide additives. They used oxide additives namely B_2O_3 , TiO_2 , V_2O_5 , and Cr_2O_3 and calcined co-precipitated spinel. The greatest beneficial effect was reported for TiO_2 addition followed by Cr_2O_3 addition. They also reported that additives B_2O_3 and V_2O_5 to have detrimental effects on densification. Sarkar et al. also studied [2.106, 2.107] the effect of various additives on phase composition and densification of reaction sintered spinel with $MgO:Al_2O_3$ molar ratio 2:1, 1:1 and 1:2. The addition of additives was found to have no effect on phase formation. However, the densification was greatly influenced by additives. TiO_2 , Cr_2O_3 , Dy_2O_3 , etc. was found to increase sintered density whereas V_2O_5 was found to inhibit sintering of all compositions. Effect of chloride ions on sintering of spinel was studied by Homano et al. [2.108] using hydroxide reactants. They found chlorine ions to help in decomposition of hydroxides and decrease in spinel formation temperature finally aiding in sintering. The addition of $AlCl_3$ in conventional double oxide densification process of magnesium aluminate spinel was studied by Ganesh et al.[2.109]. They reported having a similar effect with $AlCl_3$ addition like AlF_3 addition. However, the addition of $AlCl_3$ also improved the sintered density. The reason for improved sintered density was reported

due to the formation of OH^- ions over Al_2O_3 particle surface due to hygroscopic nature of AlCl_3 . These OH^- ions get removed at a higher temperature causing an increase in defect concentration improving sintered density.

Ghosh et al. [2.110] studied the effect of ZnO addition on reaction sintered MgAl_2O_4 . The added ZnO as an additive up to 2wt.%. The addition of ZnO was reported to improve thermal shock resistance. 99% theoretical density was achieved with 0.5wt.% ZnO addition at 1550°C . They reported that addition of ZnO caused anion vacancy by entering the spinel structure resulting in higher densification and strength. ZnO incorporation was also found to restrict grain boundary migration which resulted in reduced grain size. Yu et al. also studied [2.111] the addition of zinc oxide on magnesium aluminate spinel prepared from alumino ferrous waste slag and $\text{Mg}(\text{CO}_3)_4 \cdot \text{Mg}(\text{OH})_2 \cdot 5\text{H}_2\text{O}$. They reported producing 93% MgAl_2O_4 phase with the addition of 2 wt.% ZnO. They achieved a bulk density of 3.36g/cc and bending strength 136.2 MPa.

Effect of MgSO_4 on magnesium aluminate spinel was studied by Sarkar et al. [2.112] They reported improvement in solid solubility of corundum into spinel in the presence of MgSO_4 . The addition of MgSO_4 was also reported to improve strength both at room and elevated temperature due to the high rate of sintering. However, thermal shock resistance was reported to deteriorate with MgSO_4 addition. They also studied [2.113] the addition of Cr_2O_3 on properties of reaction sintered spinel in both stoichiometric and non-stoichiometric compositions. They choose three different compositions with MgO: Al_2O_3 molar ratio 1:1, 1:2, 2:1. Upto 4 wt.% Cr_2O_3 was added. The addition of Cr_2O_3 was reported to be very effective on alumina rich composition sintered at 1550°C . Thermal shock resistance was found to improve with 1wt.% Cr_2O_3 addition. They also reported Cr_2O_3 to help in grain growth of all the compositions.

Mohammadi et al. studied [2.114] MgCl_2 addition on formation and sintering of stoichiometric MgAl_2O_4 . They reported an increase in spinel phase formation with MgCl_2 addition. They also observed a decrease in average grain size of spinel with MgCl_2 addition. MgAl_2O_4 nano particles were reported to form on the surface of larger grains due to the reaction of ultra-fine MgO from MgCl_2 with Al_2O_3 .

Ugur et al. investigated [2.115] the incorporation of SnO_2 on magnesia spinel composites. The incorporation was reported to increase mechanical properties significantly. The reported improvement in mechanical properties mainly due to the formation of Mg_2SnO_4 phase,

microstructural change, transformation in the type of fracture and decrease in average MgO grain size as the effective parameters. Effect of yttria addition on thermal shock behavior of magnesium aluminate spinel was investigated by Posarac et al. [2.116] They reported an increase in density and thermal shock resistance with an increase in the amount of yttria. The improvement in thermal shock resistance was reported due to the formation of $YAlO_3$ phase which had a lower thermal expansion coefficient in comparison to spinel. Formation of this new phase caused residual stress which was beneficial for thermal cycling. Sarkar et al. studied [2.117] the addition of Y_2O_3 in stoichiometric and magnesia rich spinel ($MgO:Al_2O_3$ 1:1 and 2:1). They found Y_2O_3 addition beneficial for sintering of stoichiometric $MgAl_2O_4$ spinel. They concluded lattice strain caused by substitution of Al^{3+} by Y^{3+} as the reason for enhanced densification. Aguilera et al. studied [2.118] the addition of $CaCO_3$ up to 30 mol% in a stoichiometric mixture of MgO and Al_2O_3 . They studied the formation of $MgAl_2O_4$ up to $1400^\circ C$. They reported the formation of pure spinel phase along with traces of calcium aluminate phase in the sintered product. The influence of CaO and moisture in the precursor on formation and densification of magnesium aluminate spinel was studied by Ganesh et al. [2.119] They reported to obtain bulk density value $>3.35 g/cc$, porosity $< 2\%$ and water absorption less than 0.55% in stoichiometric spinel composition containing $CaO > 0.9\%$. They observed better sintering properties in batches containing $CaO > 0.9$.

Alvarez et al. studied [2.120] the effect of the addition of LiCl on magnesium spinel formation. They reported that presence of Li^+ and Cl^- enhanced reaction kinetics of spinel formation. Diffusion of aluminium into magnesia was reported to accelerate in the presence of Li^+ . The reason for this was reported as vacancy creation due to the dissolution of Li^+ which improved atomic mobility and enhanced crystal growth. Rozenburg et al. studied [2.121] interaction between LiF and $MgAl_2O_4$ spinel during sintering. They concluded that reaction between LiF and $MgAl_2O_4$ involves a sequence of reaction that involves transient liquid phase at elevated temperature. The LiF addition was reported to be beneficial for sintering of $MgAl_2O_4$ due to the formation of transient liquid phase and reformation of $MgAl_2O_4$ at a higher temperature. They also studied the sintering kinetics of LiF doped $MgAl_2O_4$. They studied [2.122] about the activation energies associated with spinel formation and densification on the addition of LiF. They concluded that main limiting factor in sintering of spinel was oxygen diffusion. The addition of LiF created oxygen vacancies which enhanced the densification process. The activation energy of spinel formation was also reported to get lowered in the presence of LiF.

Hamid et al. [2.123] worked on the processing of cast particulate composite of insitu generated alumina by adding MnO_2 to molten aluminium. Magnesium was also added to improve wetting of alumina particles by molten aluminium. They reported obtaining MgAl_2O_4 and $\alpha\text{-Al}_2\text{O}_3$ phase in the composite. The addition of MnO_2 was reported to improve mechanical strength due to the formation of MnAl_6 phase at high temperature. The addition of TiO_2 and MnO_2 on magnesium aluminate was studied by Baik et al. [2.124] They reported TiO_2 to have a better impact on densification in comparison to MnO_2 . The addition of TiO_2 on sintering of MgAl_2O_4 was studied by Yu et al. [2.125] They studied the TiO_2 addition in the range 0.2-2wt.%. They achieved increasing densification up to 1.5wt.% TiO_2 addition. They concluded reason for this as exsolution of alumina and dissolution of TiO_2 in the spinel lattice. Sarkar et al. [2.126] studied TiO_2 addition on magnesium aluminate spinel with $\text{MgO}:\text{Al}_2\text{O}_3$ molar ratio 1:1,1:2,2:1. They reported higher densification on Al-rich and stoichiometric spinel with TiO_2 at 1550°C . But the higher amount of TiO_2 was reported to have deteriorating effect at elevated temperature due to the occurrence of grain growth. Hot strength was reported to decrease with TiO_2 addition due to increasing in the roundness of grain and presence of impurities and TiO_2 along the grain boundaries. Yan et al. studied the [2.127] effect of the addition of TiO_2 on microstructure and strength of porous spinel prepared using magnesite and $\text{Al}(\text{OH})_3$ as raw material. The $\text{MgO}:\text{Al}_2\text{O}_3$ was 2.53. They found the addition of TiO_2 lead to the formation of the liquid phase at a higher temperature (1600°C). They concluded that increasing amount of TiO_2 lead to more liquid phase formation which decreased porosity and improved strength.

Tripathi et al. [2.128] synthesized magnesium aluminate spinel from calcined alumina and calcined magnesia. They studied the effect of the addition of Dy_2O_3 on stoichiometric spinel composition. They found Dy_2O_3 to mainly enhance densification without effecting spinellisation. The addition of Dy_2O_3 was also found to influence microstructure. They reported uniform, and compact microstructure with small intergranular pores in Dy_2O_3 contained samples.

The addition of SiO_2 on magnesium aluminate spinel was investigated by Zografou et al. [2.129] They reported the addition of SiO_2 in Mg-rich spinel was detrimental for spinel formation as it reduces the anion vacancy formation by consuming free magnesia to produce forsterite phase. However, the addition of SiO_2 in Al-rich spinel leads to liquid phase formation which accelerated the grain boundary diffusion thus enhancing the densification process. Yi et al. [2.130] reported

that addition of SiO_2 not beneficial for spinel formation due to the formation of some intermediate compounds. But they found SiO_2 incorporation to promote densification at elevated temperature. Kim et al. [2.131] used SiO_2 , TiO_2 and CaCO_3 as additive up to 4wt.% in the stoichiometric composition. They found the addition of TiO_2 for densification. SiO_2 and CaCO_3 were reported to present in grain boundary in the microstructure. However, TiO_2 was reported to react with spinel and present in both grain boundary and grain. They achieved the highest densification with TiO_2 addition.

Futija et al. [2.132] found that incorporation of fine zirconia enhanced the bending strength and fracture toughness. They also studied the effect of the addition of zirconia on densification and fracture toughness of the sample. They reported improvement in densification with the addition of zirconia above 1.4vol%. The addition of zirconia above 6.6vol% was reported to improve bending strength. Fracture toughness was reported to improve with incorporation of zirconia % in between 12.5-15.1vol%. The transformation of zirconia was stated as the reason for improved fracture toughness at a higher temperature. Tsuboi et al. [2.133] also worked on zirconia addition on the $\text{MgO-Al}_2\text{O}_3$ system by varying the $\text{MgO:Al}_2\text{O}_3$ ratio. They reported higher strength value in all zirconia contained compositions. However, compositions containing higher alumina along with zirconia was reported to have the highest strength. Ganesh et al. [2.134] used double stage sintering process to prepare MgAl_2O_4 spinel. The addition of yttria partially stabilized zirconia on the synthesis of MgAl_2O_4 and sintering was investigated. They reported improvement in density, hardness and fracture toughness values with zirconia addition. Quenard et al. [2.135, 2.136] prepared $\text{ZrO}_2\text{-MgAl}_2\text{O}_4$ composite through combustion synthesis technique using 1–30% ZrO_2 . Mechanical strength was reported to improve with increasing amount of ZrO_2 content, even 1% incorporation of ZrO_2 was reported to increase strength to a great extent. Sahin and Aksel et al. [2.137, 2.138] also found improvement in strength, modulus of elasticity, fracture toughness, and fracture surface energy for $\text{MgO-MgAl}_2\text{O}_4$ composites with the incorporation of 3 mol% Y_2O_3 and varied % of zircon. $\text{MgAl}_2\text{O}_4\text{-ZrO}_2$ composite was prepared using calcined alumina and magnesia (1400 °C), 4 mol% Y_2O_3 to stabilize ZrO_2 by Lodha et al. [2.139] The $\text{ZrO}_2/\text{Y}_2\text{O}_3$ % was varied from 0 to 20. Solid oxide reaction with 3 h attrition milling was used for processing. An increase in density and flexural strength value was reported by them. Kim [2.140] worked on ZrO_2 incorporation in the $\text{MgO-Al}_2\text{O}_3$ system and non-stoichiometry. He reported that inclusion of ZrO_2 in the $\text{MgO-Al}_2\text{O}_3$ system increased the concentration of cation vacancies on either side. The

increase in vacancy concentration resulted in an acceleration in diffusion process and formation of spinel.

2.5 Effect of sintering on properties of magnesium aluminate spinel

The process of sintering is associated with densification and grain growth which occur due diffusion of mass. Sintering changes microstructure which in turn effects the properties. Sintering of magnesium aluminate spinel in single stage firing is difficult in solid state sintering as the formation of magnesium aluminate spinel is always associated with volume expansion. To overcome this, many researchers used different techniques. Use of intermediate mechanical milling, sintering additives, etc. are most prominent among all. Sintering is associated with densification which directly effects strength and thermos-mechanical properties.

Kanerva et al. [2.69] evaluated the cold crushing strength of $MgAl_2O_4$ granulated beds prepared using two different Mg precursors and three different Al precursors by spray drying. The sintering temperature 1000-1400⁰C.They reported an increase in cold crushing strength with increase in temperature, Highest strength was reported for $MgAl_2O_4$ granules prepared using $AlOOH$ and $Mg(OH)_2$ as a precursor.

Wan et al. [2.127]investigated the effect of the addition of TiO_2 as an additive on sintering properties like strength and porosity on porous $MgAl_2O_4$ ceramic. They use aluminium hydroxide and magnesite as raw materials. A maximum of 2wt.% TiO_2 was used as additive. Sintering was done at 1600⁰C for 3hrs.They reported an increase in strength value with increase in TiO_2 addition A maximum compressive strength of 23.1MPa and flexural strength of 11.8MPa was reported for 2wt.% TiO_2 containing sample.

Lodha et al. [2.139]studied the effect of zirconia addition on mechanical properties of magnesium aluminate spinel. They used 4 mol % Y_2O_3 to stabilize ZrO_2 .The amount of ZrO_2/Y_2O_3 was varied from 0-20wt.%. The sintering temperature was 1550-1650⁰C with a soaking period of 2hrs.They reported an increase in flexural strength of $MgAl_2O_4$ both at room temperature and elevated temperature with addition of ZrO_2 .Flexural strength ~190MPa was reported to achieve with 20wt.% the addition of ZrO_2 .

Ma et al.[2.141] investigated the effect of rare earth oxide Sm_2O_3 on magnesium aluminate spinel. They used 2.5-7.5 wt.% Sm_2O_3 as an additive. They used an intermediate planetary milling

process of 3hrs. The sintering was done at 1580⁰C for 4hrs. They reported achieving a bulk density of 3.13g/cc and compressive strength of 209.4 MPa with 7.5 wt.% Sm₂O₃ addition.

Ganesh et al. [2.142] investigated the effect of synthesis technique on properties of nanocrystalline MgAl₂O₄ and ZrO₂ contained MgAl₂O₄. The use both conventional solid state reaction and combustion technique to compare the results. The sintering temperature was 1625⁰C with 3hr soaking time. They reported higher flexural strength and fracture toughness in combustion process prepared samples. The presence of tetragonal zirconia was reported as the reason for improved mechanical properties.

Ugur et al. [2.115] tried to improve the mechanical properties of MgO-MgAl₂O₄ composites by using 5-30 wt.% of SnO₂. They sintered the samples at 1600⁰C for 2hrs. They reported obtaining significant improvement in mechanical properties like strength, modulus of elasticity, fracture toughness, and fracture surface energy. They reported to highest strength with 0-5 wt.% incorporation of SnO₂ in MgO-MgAl₂O₄ composites.

Zhang et al. [2.143] studied the sintering behavior of magnesium aluminate spinel by varying alumina content. The increase in alumina in the composition was reported to make the sintering process difficult. They reported precipitation of corundum from magnesium aluminate spinel at 1400⁰C for the composition containing 85% alumina. The precipitation of corundum was reported to hinder the process of sintering. However, at sintering temperature above 1600⁰C the corundum was reported to get dissolved in spinel.

Li et al. [144] studied the sintering behavior, changes in microstructure, physical and mechanical properties of spinel/SiC pellets sintered at different temperature with different holding time in vacuum. They used talc, aluminium and graphite as raw materials. 6h of ball milling was done in argon atmosphere to produce stoichiometric spinel containing 27.26% SiC. They obtained best results for samples annealed at 1200⁰C for 1 hr. Samples when sintered above 1300⁰C was reported to get decomposed to different phases. The 1200⁰C sintered samples was reported to have mean grain size of 34nm, hardness of 1.6GPa and cold crushing strength 118 MPa. Sarkar et al. studied [2.145] the effect of stoichiometry and fineness of composition on densification of magnesium aluminate spinel. The milling time was varied from 2-6 hrs. The sintering temperatures were 1550, 1600, 1650⁰C. They reported higher sintering Mg-rich composition. The milling was

reported to enhance sintering in all compositions. Highest density was reported to achieve for 6hr. milled compositions.

Various researchers used different new sintering techniques, methods and additives to improve the sintering properties of magnesium aluminate spinel. But commercial viability, availability of raw materials, additives, and processing cost were the main factors which determined the success of the research work.[2.104, 2.117, 2.146-2.154]

Chapter 3

Motivation and objective

3.0 Motivation

Magnesium aluminate spinel is a technically important material for its unique properties both at room and elevated temperatures. But it is deprived of wide commercial success because of the volume expansion associated with spinel formation, the requirement of purity raw materials and a two stage firing process which increases the production cost. Beside this, no natural of magnesium aluminate source is available for commercial extraction. Many literatures are available on the synthesis of magnesium aluminate spinel, as described in chapter 2, but very less literature are available on synthesizing magnesium aluminate spinel in a single stage reaction sintering method using commercially available raw materials. Also, very limited literature is available on the evaluation of strength and thermal shock properties of the spinel developed. Literature also does not throw much light on the effect of the addition of additives like zinc oxide, zirconium oxide, magnesium nitrate, aluminium nitrate, etc. in reaction sintering method. So, in the present work, the following objectives were selected for the study.

3.1 Objective of the work

- To prepare reaction sintered magnesium aluminate spinel from commercial grade reactants.
- To study the spinellisation and sintering behavior of the stoichiometric composition in a single stage firing process in the temperature range 1200-1600⁰C.
- To study the effect of planetary milling on densification and spinel formation by varying the milling time for 0.5,1,1.5, and 2 hr. respectively.
- To study the effect of additives, like zinc oxide, zirconium dioxide, magnesium nitrate hexahydrate, aluminium nitrate nonahydrate, etc.
- Evaluation of phase and microstructure using X-ray diffraction and Field emission scanning electron microscopy.
- To study the spinel formation and sintering process using dilatometer.
- Evaluation of densification behavior, strength and thermal shock resistance properties.

Chapter 4

Experimental methods and materials

4.0 Raw materials

Commercial grade alumina (source Almatris, India) and fused magnesia (Chinese source) were used as raw materials. The detail physio-chemical properties of these raw materials are mentioned in table 4.1.[4.1, 4.2] The additives used were ZnO, ZrO₂, Al(NO₃)₃.9H₂O, Mg(NO₃)₂. 6H₂O. The purity of the additives is mentioned in table 4.2.[4.3, 4.4] A maximum 2 wt.% of each additive was used. From table 4.1 it can be observed that alumina is 99.8% pure with traces of SiO₂, Fe₂O₃, CaO, MgO, etc. The specific surface area of the alumina powder used was 8.9g/m². The fused magnesia used was 97.14% pure with traces of impurities like CaO, SiO₂, and Al₂O₃, etc. Magnesia fines were relatively coarser than alumina.

Table 4.1. Physio-chemical properties of the starting material [4.1,4.2]

Constituent Oxide(%)	Alumina fines	Fused magnesia
SiO ₂	0.05	0.47
Al ₂ O ₃	99.8	0.12
Fe ₂ O ₃	0.03	0.063
CaO	0.05	1.46
MgO	0.06	97.14
Na ₂ O+K ₂ O	0.10	
Specific surface area, m ² /gm	8.9	
Particle size D ₅₀ , μ	0.5	28
True density (g/cc)	3.98	3.58

Table 4.2 Purity of the additives used [4.3,4.4]

Additives	Purity	Density(g/cc)
Zinc oxide	$\geq 99.5\%$	5.61
Zirconium dioxide	97%	5.85
Magnesium nitrate hexahydrate	$\geq 98\%$	1.464
Aluminium nitrate nonahydrate	$\geq 98\%$	1.72

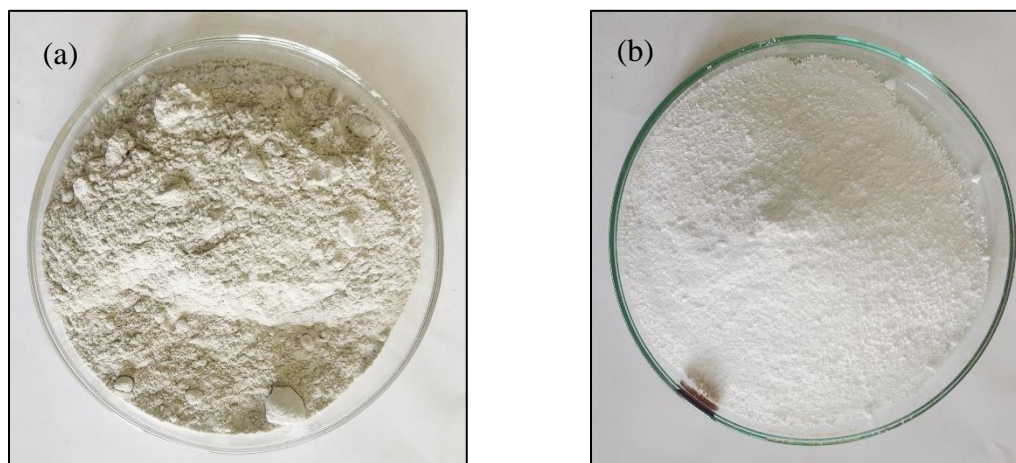


Fig 4.1 Raw materials(a) Fused magnesia (b) Reactive alumina

4.1 Sample preparation processes

The processes which were used for the preparation of samples are mixing, drying, milling, pressing, and sintering. The detail description of processes are as follows-

4.1.1 Weighing

A Mettler Toledo electronic balance was used to weigh the raw materials and additives before mixing. The accuracy of the balance was up to the 4-digit decimal place.

4.1.2 Mixing

The weighed composition was mixed in an alcoholic medium (isopropyl alcohol, purity $\geq 99\%$) using a magnetic stirrer. The mixing increases homogeneity of the mixture. The alcohol to the solid mass ratio used was 3:1. A maximum of 6hrs of mixing was done.

4.1.3 Drying

The thoroughly mixed mixture was then dried in a hot air oven. The hot air oven uses thermally heated air to maintain the temperature inside the oven. The drying was done at 80°C and 110°C. Drying gives strength to green body and helps in quick evaporation of volatile matter in composition.

4.1.4 Milling

For the milling study, a planetary ball mill was used to mill the samples. A maximum two hour of milling was done. The milling balls used was zirconia balls. The ball to mixture ratio was 1:4. To avoid heating during milling the machine was scheduled to stop automatically after every half an hour of milling. The milling was done at 300rpm.



Fig.4.2 Pressed pellets and bars

4.1.5 Pressing

The pressing was done to compact the particles of a loose mix and dried powder together by applying some external pressure. A binder was used to compact the particles properly. In the current work, uniaxial pressing was done using an automatic hydraulic press. The applied pressure was 150MPa and 4wt.% polyvinyl alcohol (6wt.% concentration) was used as a binder. Acetone and stearic acid solution (4% conc.) was used for cleaning and lubrication respectively. Three types of stainless steel mold were used. The dimensions of each mould are mentioned in table 4.3.

Table 4.3 Types of mold used

Sl. No.	Mold type	Dimensions
1.	Cylindrical	15mm(diameter)
2.	Rectangular	25mm X 6mm
3.	Rectangular	60mm X 6mm

4.1.6 Sintering

The sintering of the pressed specimen was done in a programmable electric arc furnace in an air atmosphere. The heating schedule used during sintering process is shown in Fig 4.3. The sintering was done at 5 different temperatures 1200,1300,1400,1500 and 1600°C respectively. The dwell time at peak temperature was 4hrs.

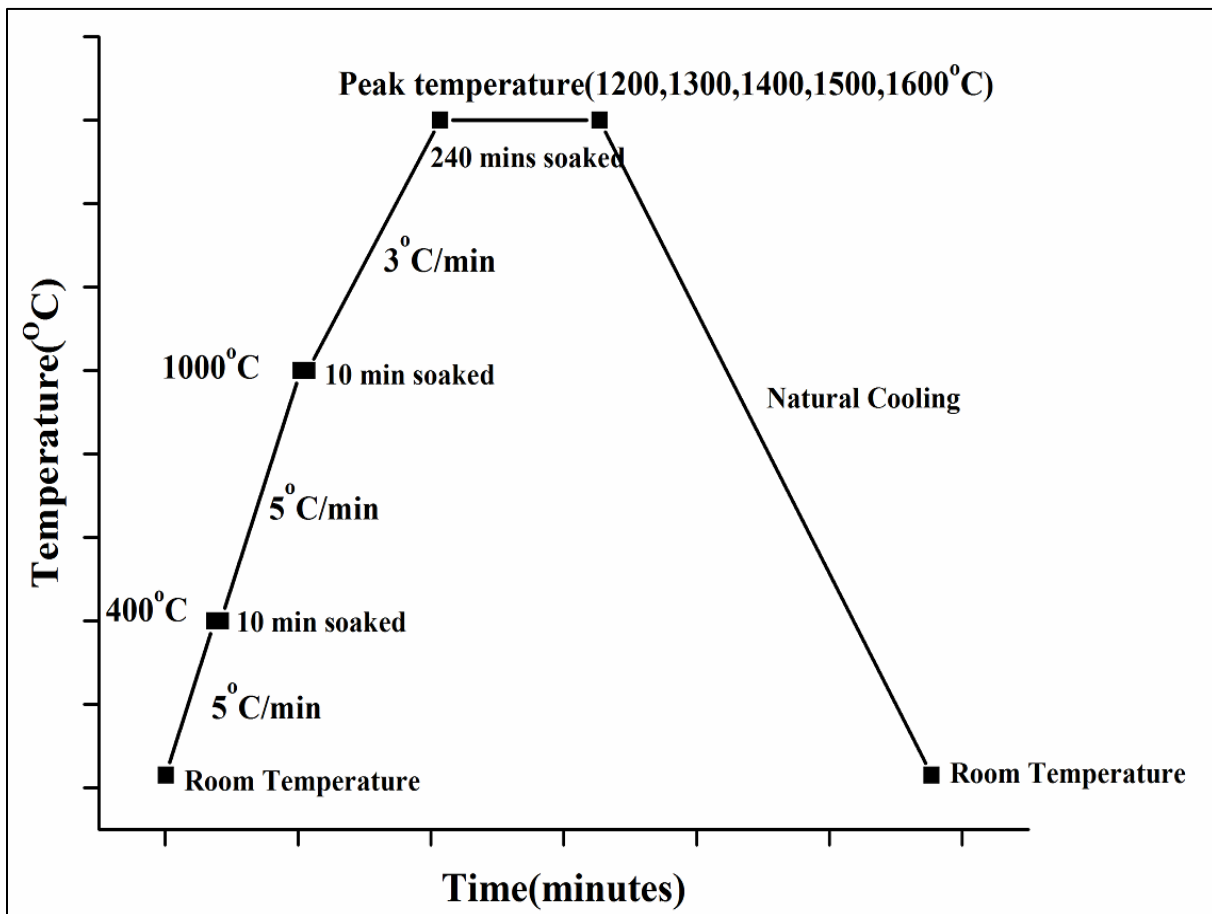


Fig.4.3 Heating schedule during sintering.

4.1.7 Grinding

Grinding of the sintered pellets was done for X-ray analysis using a mortar pestle. Grinding was done until the pellet was ground to very fine powder.

4.2. Experimental process flow-chart

4.2.1 For milling compositions

For the preparation of magnesium aluminate spinel stoichiometric composition was chosen. So, 71.7 wt.% Al_2O_3 and 28.3 wt.% MgO was weighed, mixed and stirred using a magnetic stirrer in alcohol medium (isopropyl alcohol, purity $\geq 99\%$) for 2 hrs. The mixture was then dried in a hot air oven at 80°C for 24 hrs. The dried powder was then divided into 5 equal parts and milled for 0, 0.5, 1, 1.5, and 2 hrs. respectively using a planetary milling machine in alcoholic medium with balls to mass ratio 1:4. The milled powder was then dried again in hot air oven at 80°C for 24 hrs. The dried powders were pressed into cylindrical pellets and bars of dimension 15 mm (dia.) X 15 mm (height) and 60 mm X 6 mm X 6 mm respectively with 150 MPa pressure in an automatic hydraulic press using 4 wt.% PVA (6 wt.% conc.) as a binder. The pellets were then sintered in the temperature range $1200\text{--}1600^\circ\text{C}$ with 4 hrs dwell time at peak temperature. The sintered pellets were characterized by bulk density, apparent porosity, phase, microstructure analysis, etc. The rectangular bar samples were sintered at 1600°C for 4 hrs. The sintered bars were then characterized for flexural strength and thermal shock resistance study. The spinel formation and sintering were also studied by using a dilatometer. For dilatometry study, rectangular bar samples pressed at 150 MPa in a stainless steel mold of dimension 25 mm X 6 mm X 6 mm were used. The experimental flow diagram for the preparation of magnesium aluminate spinel by using planetary milling is shown in fig. 4.4 for better understanding.

4.2.2 For additive containing compositions

Similar methodology as mentioned in section 4.1.1 were used for sample preparation of additive containing compositions. But here instead of milling 0.5, 1, 1.5, 2 wt.% of additives were added and stirred again in the alcoholic medium for better mixing. The stirred mixture was then again dried at 80°C for 24 hrs. Fig 4.5 shows the process flow chart of a single additive containing batch for better understanding. Four different additives zinc oxide, zirconium dioxide, aluminium nitrate nonahydrate, magnesium nitrate hexahydrate were used. The percentage of additive was varied

from 0-2 wt.% in each case. Density, microstructure, phase, flexural strength, thermal shock resistance was studied after sintering in the temperature range 1200-1600°C. The effect of the additives on spinel formation and densification was studied using dilatometer

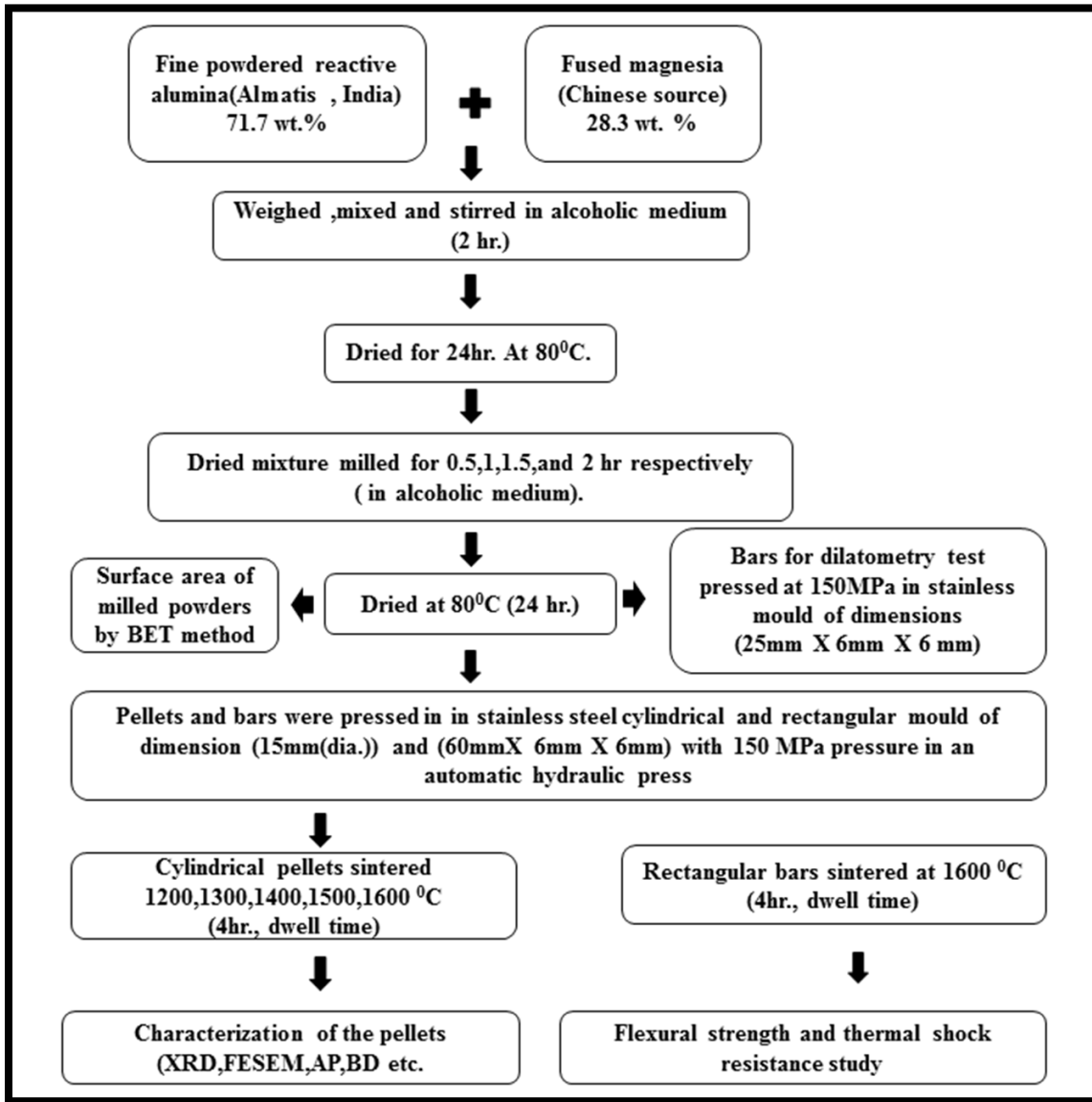


Fig.4.4 Process flow chart for milling composition.

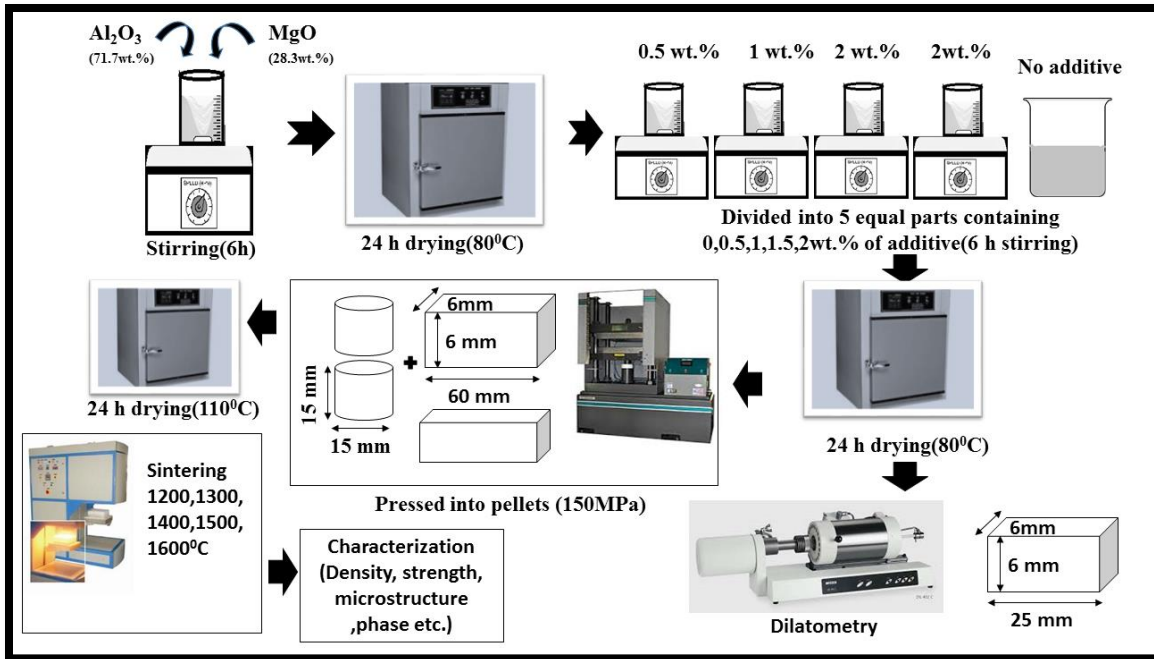


Fig.4.5 Process flow chart for additive containing compositions.

4.3 Methods used for characterization.

4.3.1 Surface area measurement

Sintering characteristics can be predicted by knowing the surface area of ceramic powder. BET (Brunauer, Emmet and Teller after the developers of the basic calculations) method is a precise method to measure the surface area. The BET method involves adsorbing a monolayer of nitrogen gas onto the surface of particles, then measuring the amount of nitrogen that is released when that monolayer is vaporized. Based on this nitrogen quantity adsorbed, the surface area of the sample can be calculated from the BET equation:

$$\frac{1}{V_g} \frac{x}{1-x} = \frac{(c-1)}{cV_m} x + \frac{1}{cV_m}$$

Where-

V_g = volume of gas adsorbed.

V_m = volume of gas adsorbed at monolayer coverage.

$x = P/P_0$

P = Ambient pressure,

P_o = Total pressure,

c = a constant that is related to the heat of adsorption.

BET surface area of raw combustion powder as well calcined powder was measured using 5-point method by AUTOSORB 1, (Quantachrome) (Model No: Nova 1200 BET).

4.3.2 Linear shrinkage measurement

The linear shrinkage of cylindrical sintered sample was measured to see the densification rate. The diameter before and after firing was measured using a digital Vernier caliper. The linear shrinkage percentage was then calculated using the following formula –

$$\text{Linear shrinkage percentage(\%)} = \frac{D_o - D_s}{D_o} \times 100$$

Where

D_o = Diameter of the cylindrical sample before sintering.

D_s = Diameter of the cylindrical sample after sintering.

4.3.3 Density and porosity measurement

Bulk density and apparent porosity were measured using Archimedes principle. Both boiling water method and vacuum method was used. The medium used was water in both the cases. Cylindrical pellets of 15mm diameter and 15mm height were used for this purpose. The dry weight soaked weight and suspended weight were measured in a Mettler Toledo electronic balance. The bulk density and apparent porosity were calculated using the following equations –

$$\text{Bulk density(g/cc)} = \frac{W}{W-S}$$

$$\text{Apparent porosity(\%)} = \frac{W - D}{W - S} \times 100$$

Where

W = Soaked weight of the sample.

D = Dry weight of the sample.

S = Suspended weight of the sample.

The relative density was also measured for additive containing sample. The relative density was calculated using the formula-

$$\text{Relative density} = \frac{\text{Bulk density}}{\text{Specific gravity of the composition}} \times 100$$

The specific gravity was calculated using the formula-

$$\text{Specific gravity} = \rho_{\text{additive}} \times \% \text{ of additive} + (100 - \% \text{ of additive}) \times \rho_{\text{spinel}}$$

The density of spinel (ρ_{spinel}) was taken as 3.58g/cc.

4.3.4 Dilatometry study

For dilatometry study, rectangular bar shaped samples prepared. The bars were pressed at 150 MPa using stainless steel mold of dimension 25mm X 6mm X 6mm in an automatic hydraulic press. The pressed samples were put inside a dilatometer. A dilatometer measured the linear dimensional change of sample with respect to dynamic temperature. The dilatometry study was done in an inert argon atmosphere up to a maximum temperature of 1450°C. The heating rate used was 10°C/min. The data obtain from dilatometer was plotted using Origin graph analysis software.

4.3.5 Phase analysis study

X-ray diffraction technique was used to study the phases present in the compositions after sintering. The technique involves irradiation of a beam of monochromatic X-ray radiation on the sample and recording the position and intensity of diffracted beam as a function of goniometer position(2θ). The main principle on which it works is Bragg's law-

$$\lambda = 2d\sin\theta$$

Where λ =wavelength of X-rays, d =interplanar spacing or d -spacing=position of the diffraction angle.

For X-ray analysis sintered sample were ground into powder using an agate mortar. The ground powder was placed on a sample holder and was irradiated by a monochromatic X-ray beam from an X-ray tube. Cu-K α radiation of wavelength(λ) =1.5406Å passed through nickel filter was used. The range of scanning angle (2θ) used was 20-60°. The step size used was 0.05 and scanning rate was 2°/min. The generator voltage and current were set 35KV and 25mA respectively. The X-

ray diffraction pattern obtained was analyzed using Philips Xpert highscore software. XRD of 1200,1300,1400,1500 and 1600⁰C sintered sample was done to see the change in spinel phase formation with temperature, milling and additives addition.

4.3.6 Microstructure study

Field emission scanning electron microscope (FESEM) was used to see the microstructure of fractured samples sintered at 1200⁰C and 1600⁰C. A field emission scanning electron microscope uses a high energy focused beam of electron produced by field emission gun(FEG) for generating an image.As the wavelength, of the electron is very small a very high magnification can be achieved in field emission electron micrisocopy.The electron beam on interaction with the specimen produces secondary images and back scattered images. The samples with milling were observed under secondary electron(SE) mode. However, the sample with additives was observed in back scattered electron(BSE) mode. The samples were gold coated for 240sec in a sputter coater in an argon atmosphere for observation.

EDAX analysis was also carried out for the samples using an EDAX detector attached to the microscope. The EDAX or energy dispersive X-ray spectroscopy is a technique to analyze the elemental or chemical composition of a specimen. The technique analyzes the X-ray emitted due to excitation of atoms of the certain portion of the specimen due high energy electron beam or X-rays interaction with the specimen using an analyzer to determine the elemental composition of the specimen.

4.3.7 Flexural strength study

The flexural strength of material is its property which gives the maximum stress the material can bear before it yields in a flexure test. The flexural strength was measured using three-point bending method. The strength was calculated using the formula –

$$\text{Flexural strength}(\sigma) = \frac{3FL}{2BD^2}$$

Where F= Force (N)

L= Span length of the sample between two supports (mm).

B= Breadth of the sample (mm).

D= Height of the sample (mm).

σ = Flexural strength (N/mm² or MPa)

For flexural strength measurement, rectangular bar shaped samples were used. The dimensions of the sample were 60mm X 6mm X 6mm. The samples were pressed at 150 MPa in an automatic hydraulic press using a stainless steel mold. The pressed samples were sintered at 1600°C for 4 hrs. in an air atmosphere. The flexural strength of sintered sample was determined in a universal testing machine.

4.3.8 Thermal shock resistance study

For thermal shock resistance study, 150MPa pressed 1600°C sintered samples were used. Each thermal shock cycle involved heating of the sample to 1000°C for 10mins in an electric arc furnace and quenching at room temperature for 10mins. The flexural strength retained by the sample after 2,4,6, and 8 cycles of thermal shock were measured. The dimension of the sample used for thermal shock study was 60mm X 6mm X 6mm.



Fig.4.6 Thermal shock resistance experiment

4.4 List of equipments used

The detail description of all equipment used during the work is mentioned as below-

4.4.1. Electronic balance

Company/Make – Mettler toledo/Switzerland make.

Maximum capacity-220g

Model-ML 203T.

Readability-1 mg.



Fig.4.7 Electronic balance

4.4.2. Magnetic stirrer

Company Model/Make-

Tarson spinot magnetic stirrer cum hot plate/India make.

Maximum capacity-5 ltrs.

Dimensions-18cm X 18 cm.



Fig.4.8 Magnetic stirrer

4.4.3. Hot air oven

Company /Make-

Weiber achmas technology private Ltd. /India make.



Fig.4.9 Hot air oven

4.4.4. Electric arc furnace

Company model/Make -

1. Jay crucibles raising heart furnace/India make

Maximum temperature-1400⁰C.

2. Baisakh raising hearth furnace/India make

Maximum temperature-1700⁰C.

3. Jay crucibles chamber furnace/India make

Maximum temperature-1400⁰C.



Fig.4.10 Electric arc furnaces

4.4.5. Automatic hydraulic pressing machine

Company model/Make-Carver automatic hydraulic press/USA make

Maximum load-15 tons



Fig.4.11 Automatic hydraulic pressing machine

4.4.6. Dilatometer

Company model/Make- Netzsch DL402 C dilatometer/Germany make.

Vacuum tight horizontal pushrod.



Fig.4.12 Dilatometer

4.4.7. Molds

Three types of stainless steel molds were used-

- (a) Cylindrical mold –Dimension-15mm diameter.
- (b) Rectangular mold- Dimension- 60mm X 6mm.
- (c) Rectangular mold-Dimension-25mm X 6mm.



Fig.4.13 Molds

4.4.8. Mortar pestle

Mortar pestle was used to grind the pellet to powder for x-ray analysis.



Fig.4.14 Mortar pestle

4.4.9. Field emission scanning electron microscope.

Company model/Make- Nova Nanosem FEI/USA make

Equipped with EDAX (Bruker USA make)

Beam landing energy down to 50KV



Fig.4.15 Field emission scanning electron microscope

4.4.10. Multi-purpose X-ray diffractometer.

Company model/Make- Rigaku multi-purpose x-ray diffractometer/ Japan make.

-Cu-K α radiation ($\lambda=1.5406\text{\AA}$)

-Nickel filter



Fig.4.16 Multi-purpose X-ray diffractometer

4.4.11. BET surface area analyzer

Company model/Make-Quantachrome /AUTOSORB-1 BET analyzer/USA make.

Surface area range- $>0.05\text{m}^2/\text{g}$

Max. degassing temperature- 350°C



Fig.4.17 BET surface area analyzer

4.4.12. Universal testing machine

Company model/make -Tinius olsen universal testing machine/USA make.



Fig.4.18 Universal testing machine

4.4.13. Glassware's and accessories

Different types of glasswares such as beaker, measuring cylinder, petri dish, funnel, etc. were used to carry out the experiment.



Fig.4.19 Glasswares and accessories

4.4.14. Planetary mill

Company model/Make-Planetary Mill PULVERISETTE 5 classic line/

Germany make

-300 rpm rotation.

-zirconia balls.



Fig.4.20 Planetary mill

4.4.15. Digital Vernier caliper

Company model/Make- Mitotuyo ABSOLUTE Digimatic

Caliper Series 500/USA make.

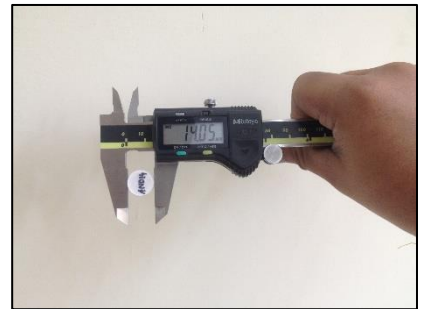


Fig.4.21 Digital Vernier caliper

Chapter 5

Results and discussions

This chapter includes detail discussions of results of all the experiments undertaken. The chapter comprises of 5 sections. The first section is on the effect of planetary milling; the second section discusses the effect of zinc oxide. The third section discusses the effect of zirconium dioxide on reaction sintered spinel. The fourth and fifth section are on the effect of in situ generated alumina and magnesia from nitrate precursor added as an additive.

The chapter also includes a description of all the characterization results obtained like surface area after milling, bulk density, apparent porosity sintered samples of each batch, and phase analysis by X-ray diffraction technique, microstructure by field emission scanning electron microscopy. The spinel formation reaction was studied by dilatometry technique as the spinel formation is associated with a volumetric expansion. The detail discussion of this is mentioned in subsection 3 for each section.

The reason for variation of properties is also discussed in detail in each subsection with proper reasoning.

The effect of milling and additives on strength and thermal shock behavior was also studied and discussed in subsection 6 and 7 of each section.

Section-I

5.1 Effect of planetary milling

5.1.1 Surface area variation with milling time

Increase in milling time increases the surface area of the raw mix (Fig. 5.1) as the particle size decreased with the increase in milling time. The extent of increase in surface area is very rapid at the initial stage of milling i.e. from 0 to 1hr but as the milling time is increased the effectiveness of milling decreases. The incremental increase in surface area value from 1.5 to 2 h milling is relatively less which might be due to agglomeration of the particles.[5.1] Milling above 2 h, was not considered in this study.

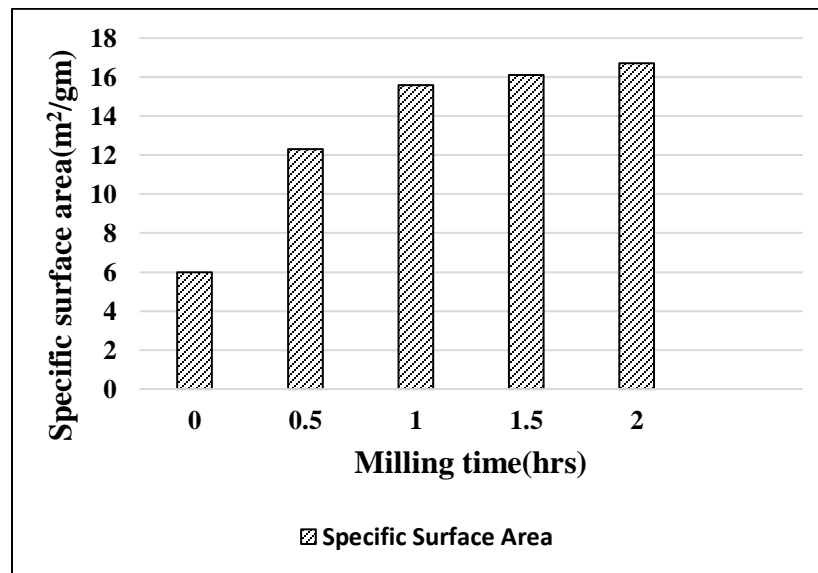


Fig. 5.1 BET surface area of batch against milling time.

5.1.2 Densification study

Increase in sintering temperature resulted in increased density (Fig. 5.2) and lower porosity (Fig. 5.3) values for all the compositions due to a greater extent of sintering. But milling was found to be strongly affecting the densification behavior. At lower temperatures, milling was found to reduce the density values greatly, and the decrease was found to be more with increasing milling time. This is due to a greater extent of spinel formation reaction and associated expansion in the composition when the sintering was poor.

Higher the milling time finer was the material, greater was the spinel formation, with higher expansion and lower density values. But at higher temperatures, say 1600⁰C, sintering is strongly higher for the milled batch, because of the finer materials resulting in denser fired samples. A maximum density equal to 96% of theoretical density (bulk density 3.44g/cm³) was achieved for 2 h milled samples fired at 1600⁰C. Apparent porosity values (Fig.5.3) fully support the densification character of the samples with milling time and firing temperature.[5.1]

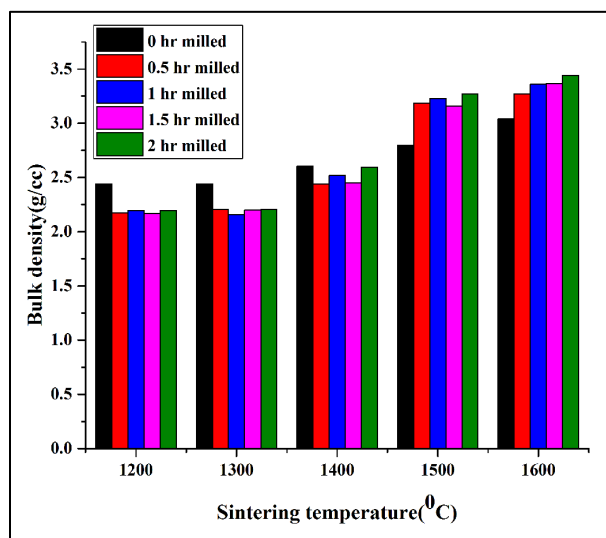


Fig.5.2 Bulk density vs. sintering temperature plot with the variation of milling time

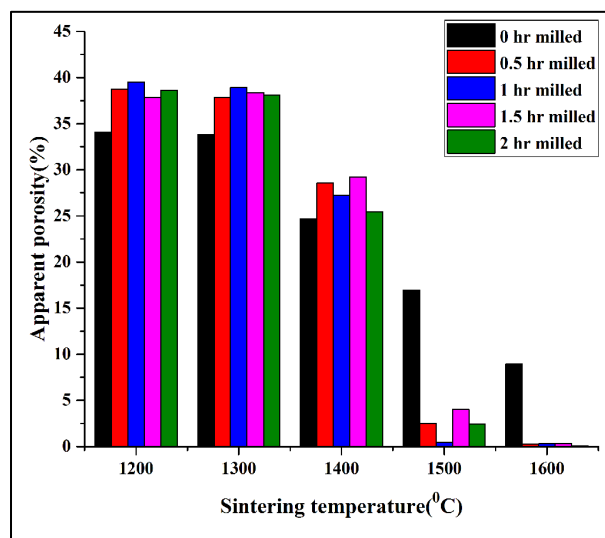


Fig.5.3 Apparent porosity vs. sintering temperature plot with the variation of milling time.

5.1.3 Dilatometry study

The dilatometry study shows (Fig.5.4) an increasing length of the sample with increasing the temperature due to reversible thermal expansion properties of starting materials. A sharp expansion peak was observed for all the samples above 1100⁰C, which is due to the volumetric expansion associated spinel formation reaction. On further increase in temperature, sintering in the compositions starts. Shrinkage due to sintering and expansion due to spinel formation run parallel. At higher temperatures, sintering process enhances due to increased mass transfer and expansion behavior of spinel formation is overtaken by shrinkage due to sintering. Thus, the dilatometry curve takes a downward turn at the high temperatures. This feature is common to all the powders milled at different times. Again with the increase in milling time, it has been found that the

expansion peak increases to a higher dL/L_0 value, indicating the greater extent of spinel formation and expansion associated with the spinel formation is more than the shrinkage of from sintering. But milling above 1 h showed a lower expansion peak but much higher shrinkage value, indicating a higher densification rate compared to that of expansion from spinel formation. 2 h milled batch showed minimum expansion with very high shrinkage value. This spinel formation reaction and its sintering in a single firing is a case of reaction sintering. It is established[5.2, 5.3] that for reaction sintering process, the reaction is dependent on L^{-1} or L^{-2} and densification depend on L^{-3} or L^{-4} , where L is the size of starting material. Now as the milling is increased, the sizes of the starting powders are decreased and so the densification is enhanced preferentially compared to that of spinel formation. Hence, spinel formation expansion peak is reduced with the increase in shrinkage behavior associated with densification.[5.1]

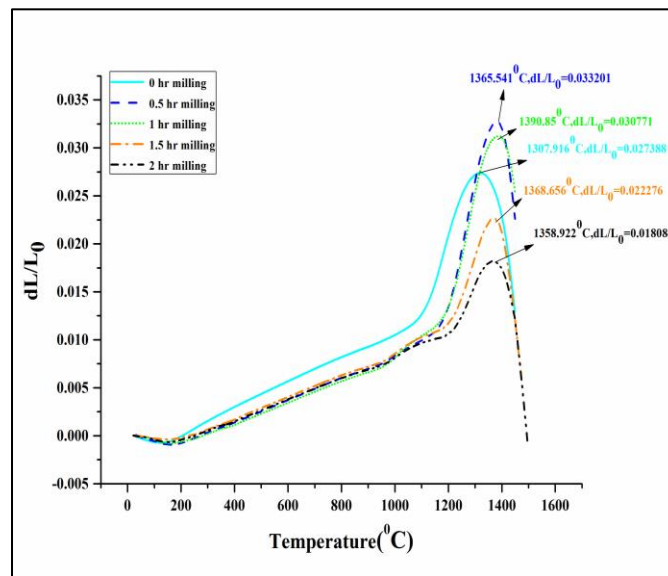


Fig. 5.4 Dilatometry plot of the samples with different milling time.

5.1.4 Microstructure study

FESEM photomicrographs show that the samples fired at 1200°C (Fig. 5.5) are highly porous, and the grains are very small (average grain size calculated was 0.3 micron). Pores are present mainly as intergranular in nature. Milling was found to enhance the average size of the sintered grains (average grain size calculated was 0.85 micron), but the overall features are nearly same. Increase in sintering temperature to 1600°C (Fig. 5.6) grossly changed the microstructural features of the sintered samples. All the samples are well compact irrespective of milling time.

Sample without any milling was found to have higher porosity and pores are inter-granular and intra-granular in nature. But milling of 2 hr. has resulted in more compact grain structure with a lesser extent of porosity and the pores are mainly intra-granular in nature. [5.1]

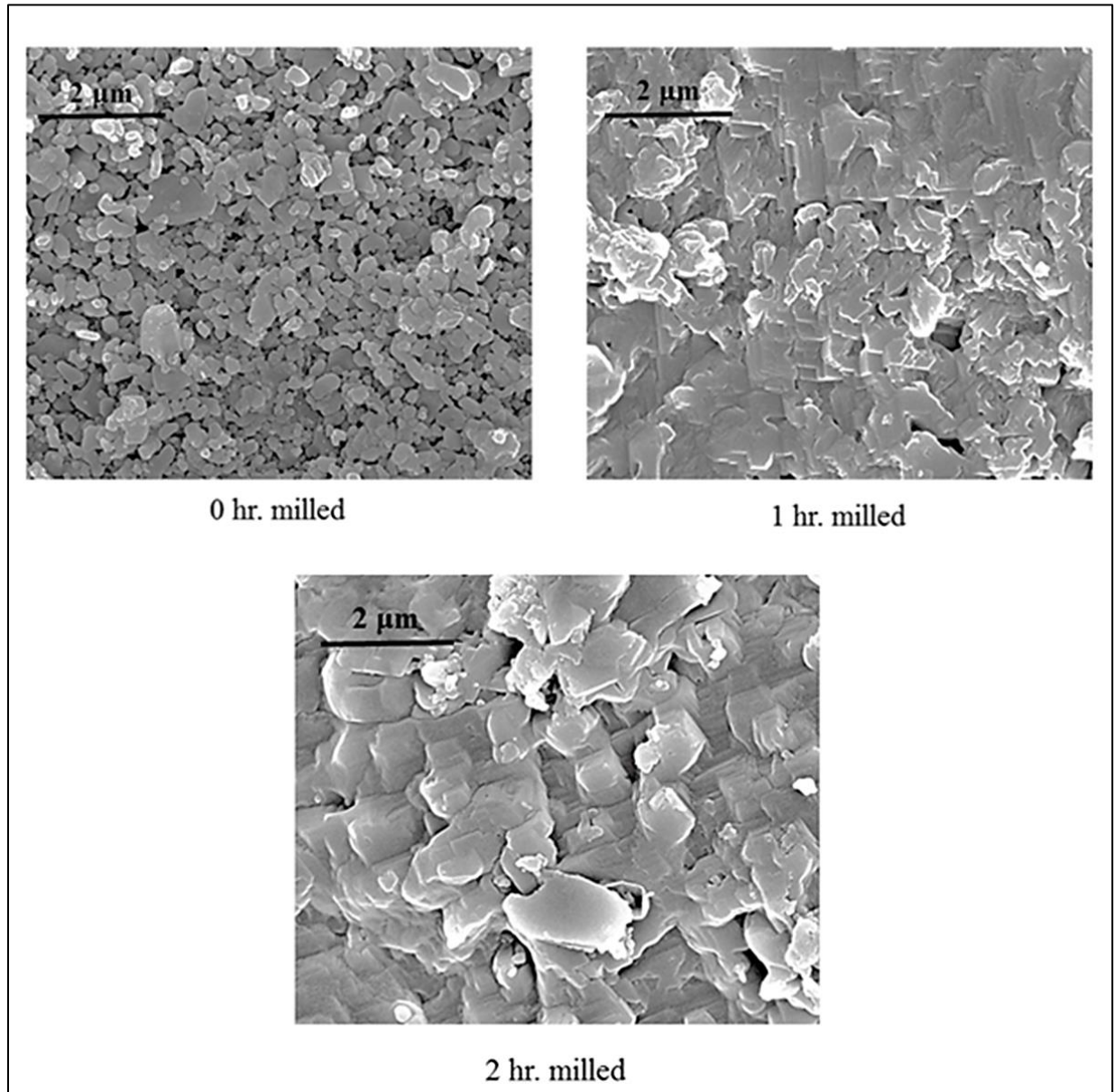


Fig 5.5. FESEM images of 1200^oC fired samples with different milling time.

EDAX study on the sintered samples showed that only magnesium, aluminium, and oxygen ions were present. No calcium ion was found, but gold ions were observed coming from the gold coating on the samples. EDAX study of the without milled 1600⁰C sintered sample is provided as Fig.5.7. [5.1]

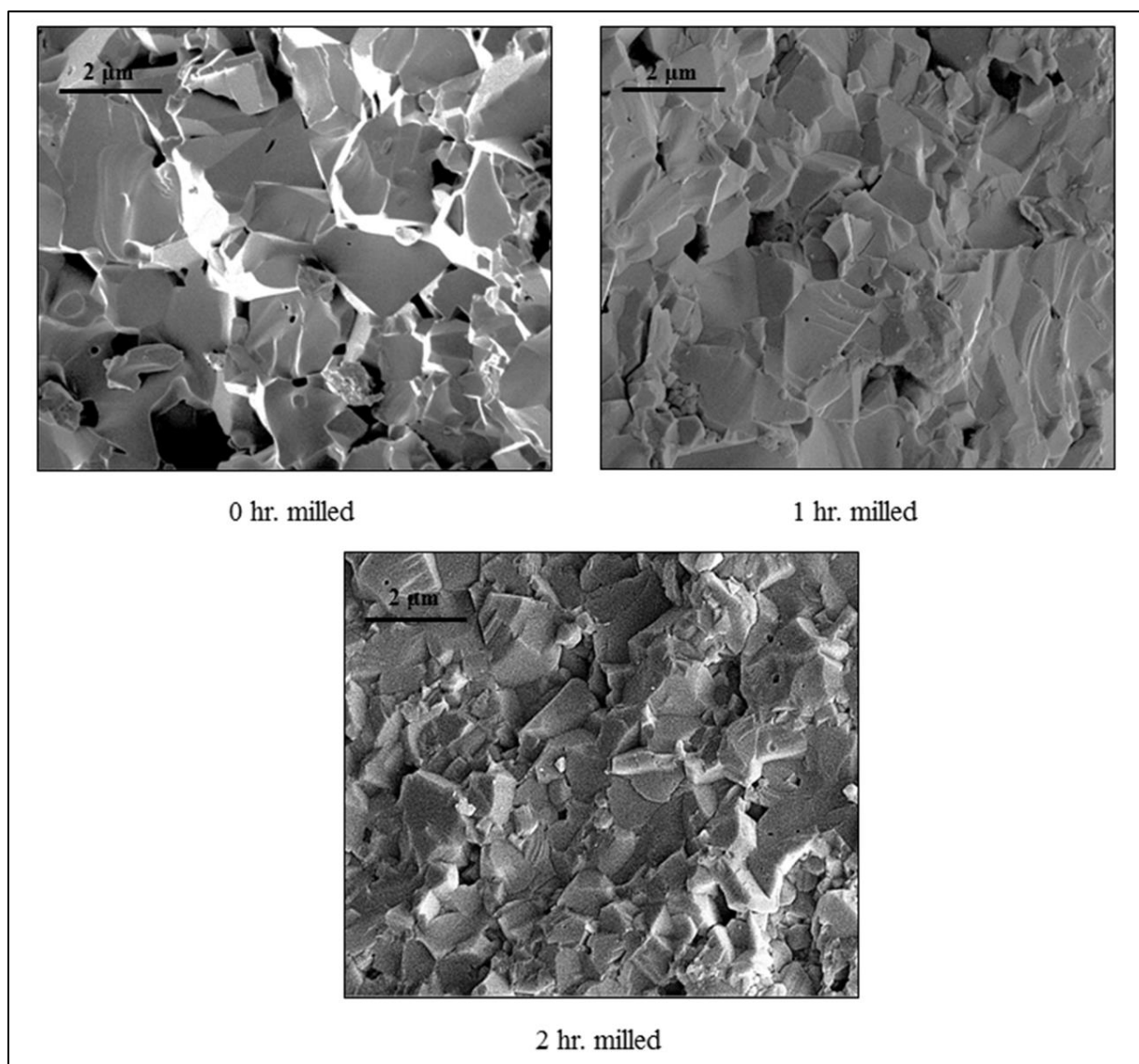


Fig 5.6. FESEM images of 1600⁰C fired samples with different milling time.

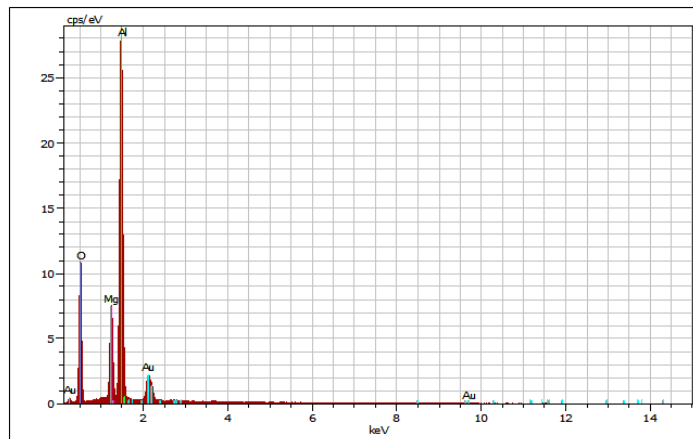


Figure 5.7. EDAX analysis of without milled 1600⁰C sintered sample.

5.1.5 Phase analysis study

Phase analysis study shows the presence of spinel phase in the 1200⁰C fired compositions, which confirms that the spinel phase formation starts below 1200⁰C (Fig. 5.8). At 1200⁰C, spinel phase is present with the reactant corundum and periclase phases and on increasing temperature spinel phase peak intensity has increased with a decrease in peak intensities of the reactant phases. The introduction of milling has a great effect on increasing the spinel formation reaction. At 1200⁰C, the reactant phases were found for the milled samples, but the peak intensities were much reduced.

The intensity of spinel phase in 1200⁰C sintered without milled batch were found to be very low may be due to the initiation of spinel reaction in the batch, which results in poorly crystalline spinel phase and a lesser amount of reactant phases present. Again, for the milled samples the intensity of the spinel phase was found to be stronger due to a greater extent of reaction (resulting in better crystallization of spinel phase) amongst the fine particles produced by milling. Complete spinel formation was observed at 1400⁰C, even for 0.5 h milling (Figure 5.9); whereas a little amount of free reactant phases mainly periclase was observed in the unmilled batch even after firing at 1500⁰C and 1600⁰C (Fig. 5.10 and 5.11). This might be due to formation of solid solution by excess alumina in spinel structure at high temperature. Complete spinellisation of the milled sample occurred at 1400⁰C due to increasing in the surface area leading to increasing reactivity of the reactants. With the increase in milling time increase in spinel phase, peak intensity is observed due to a greater extent of spinel phase formation.[5.1]

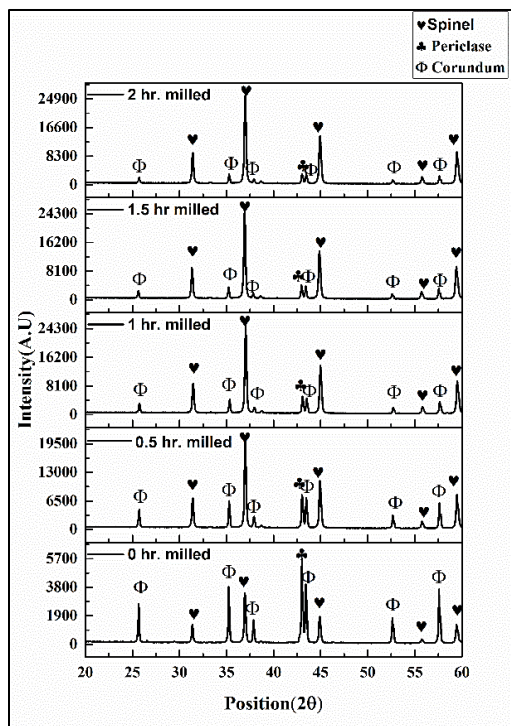


Fig.5.8. XRD plot of samples fired at 1200°C

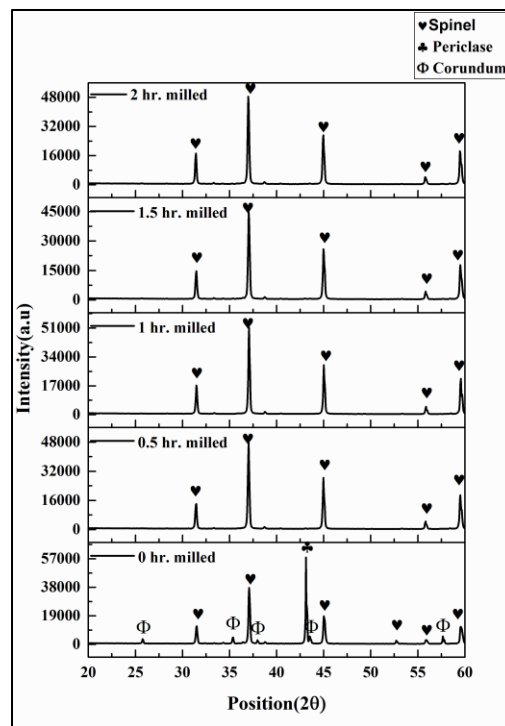


Fig 5.9. XRD plot of samples fired at 1400°C

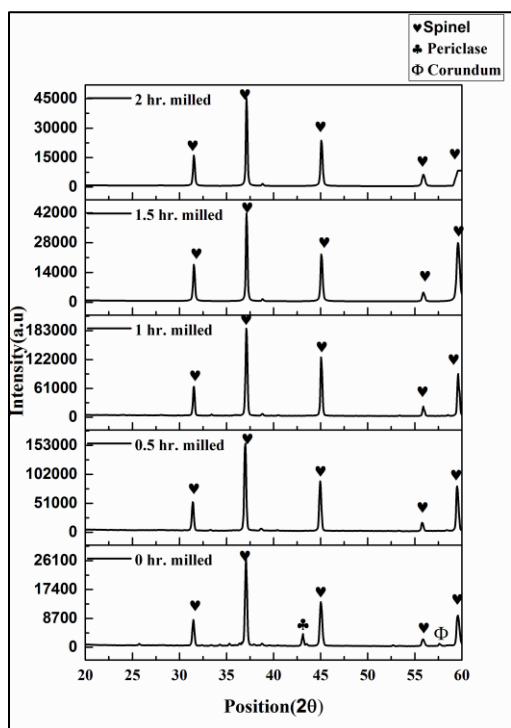


Fig 5.10 XRD plot of samples fired at 1500°C

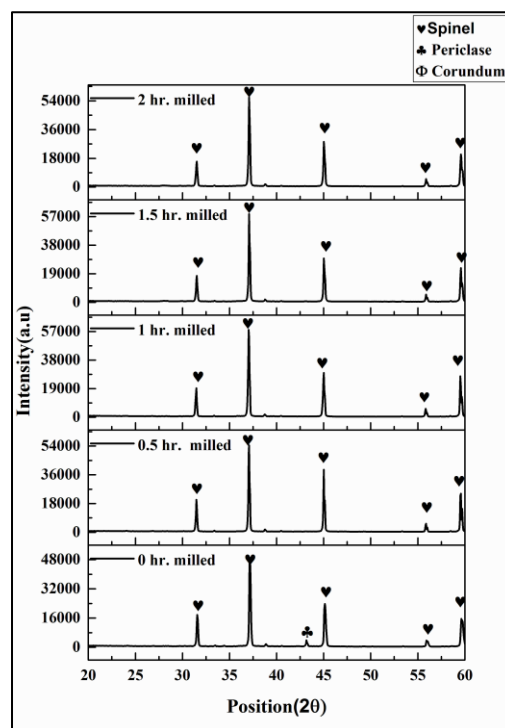


Fig 5.11. XRD plot of samples fired at 1600°C.

5.1.6 Flexural strength study

Flexural strength of 1600°C fired samples was found to increase with the increase in milling time, as shown in Fig.5.12. Enhancement of densification with the increase in milling time is responsible for such increase in strength. The increase in strength was very high at relatively lower milling hrs.; strength increased from 62 MPa to 122 MPa (nearly double) for increasing milling time from 0.5 to 1 hr. Highest strength of 140 MPa was observed for 2h milled samples whereas 0 h milled samples had only 54MPa of flexural strength.[5.1]

5.1.7 Thermal shock behavior study

Thermal shock behavior of both milled and non-milled samples fired at 1600 °C was studied by measuring the retained bending strength values after 0, 2, 4, 6, 8 thermal cycles. The bending strength values against the number of cycles are plotted in Fig.5.13. It is clearly observed that the milled samples retained more strength compared to unmilled samples after thermal shock. This may be associated with the higher densification and strength of the milled products. The increase in milling time had the direct effect on thermal shock behavior. Samples milled for a longer time retained more strength than the samples milled for lesser time. The 2 h milled samples had the highest strength retainment, has 63MPa even after 8 cycles, whereas without milled batch had a strength retainment of 29 MPa only, which is less than half of the 2 h milled samples.[5.1]

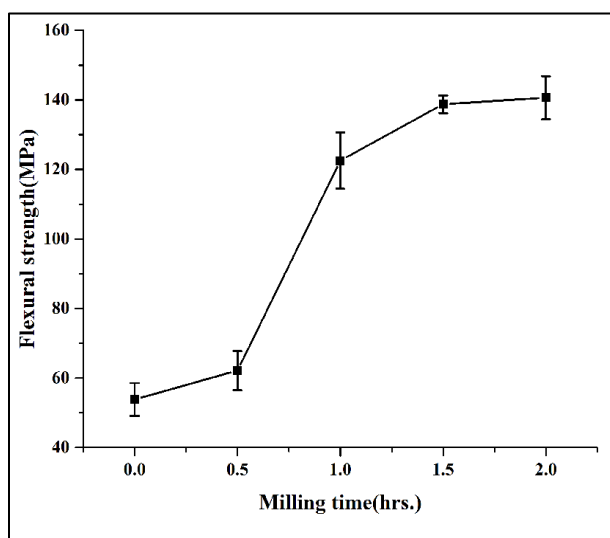


Fig 5.12. Flexural strength of 1600°C fired samples with different milling time.

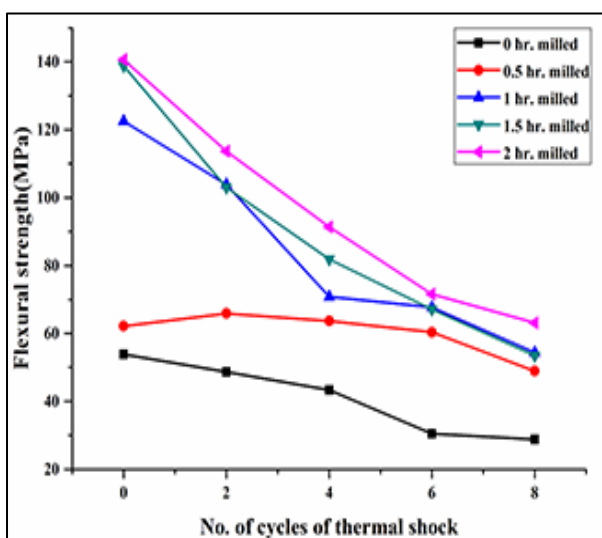


Fig. 5.13 Thermal shock behavior of 1600°C fired samples with different milling time.

5.1.8 Conclusions

- Milling was found to be very effective during initial hours and increasing milling time has a much-reduced effect on increasing the surface area.
- Free reactant phases were observed in the without milled batch even after firing at 1500⁰C whereas introduction of milling resulted in only spinel phase even at 1400⁰C.
- Density values were very low at low temperatures for the milled batches due to a greater extent of spinel formation and associated expansion. But at high temperature, once spinel formation is completed, milled batches showed much higher density values due to greater sintering from higher fineness.
- Microstructural features show well compact and less porous structure for the milled samples.
- Strength and retainment of strength after thermal shock was found to be double or more for the 1600⁰C fired 2-hour milled samples compared to that of without milled ones.

Section-II

5.2 Effect of zinc oxide addition

5.2.1 Linear shrinkage study

The linear shrinkage study (Fig.5.14) shows that addition of zinc oxide resulted in higher shrinkage at a higher temperature and a maximum of 6.5% at 1600°C for 2wt. % zinc oxide containing batch; whereas at low temperature (1200°C) the samples without zinc oxide exhibit higher shrinkage value. The addition of zinc oxide accelerated the spinellisation process even at a low temperature which was accompanied by a volumetric expansion. But as the spinellisation process was completed earlier due to accelerated spinellisation, the densification process was enhanced by the presence of zinc oxide resulting in higher shrinkage at a higher temperature. [5.4]

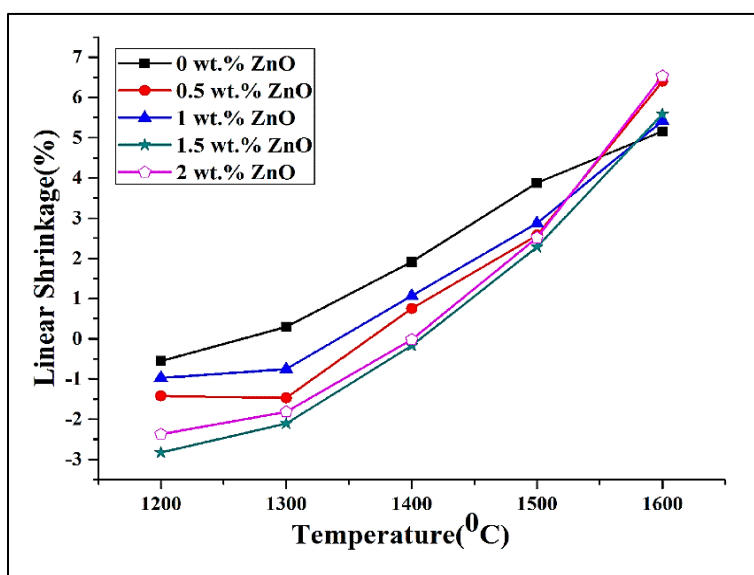


Fig.5.14 Linear shrinkage with the addition of zinc oxide.

5.2.2 Densification study

Increase in sintering temperature resulted in an increase in density (Fig. 5.15) and lower porosity (Fig. 5.16) values for all the compositions due to a greater extent of sintering. But zinc oxide addition was found to affect the densification behavior strongly. At lower temperatures, zinc oxide addition reduced the density values due to a greater extent of spinel formation reaction and associated expansion. But at higher temperatures, say 1600°C, zinc oxide addition enhanced the

sintering strongly. A maximum density of 3.17g/cm^3 was obtained for 2 wt. % Zinc oxide containing samples sintered at 1600°C . Apparent porosity values (Fig.5.16) fully support the densification character of the samples with zinc oxide addition and sintering temperature. The addition of zinc oxide creates anion vacancy in Al_2O_3 [5, 6], which helps the increased diffusion of the anion, oxygen which results in completion spinellisation reaction at a lower temperature.[5.4]

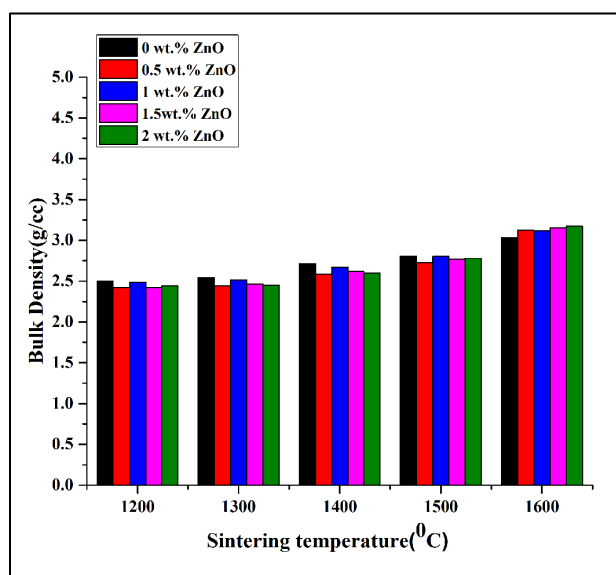


Fig.5.15 Variation in bulk density against zinc oxide addition and sintering temperature.

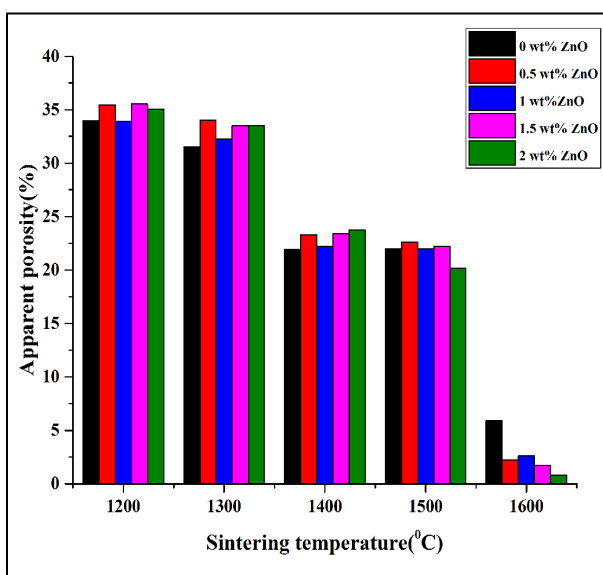


Fig.5.16 Variation in apparent porosity against zinc oxide addition and sintering temperature.

2.3 Dilatometry study

The dilatometry plot shows (Fig.5.17) that addition of zinc oxide lowered the densification temperature which is clearly visible as the shrinkage starts at a lower temperature. With the increase in temperature, expansion due to spinel formation and shrinkage due to sintering run parallel. At higher temperatures, sintering process dominates due to increased mass transfer and expansion behavior of spinel formation is overtaken by shrinkage due to sintering. Thus, the dilatometry curve takes a downward turn at the higher temperatures. This feature is common to all the compositions containing zinc oxide. [5.4]

It was found that an increase in zinc oxide percentage increased the shrinkage value due to higher densification. The shrinkage from sintering began at a little lower temperature for zinc oxide

contained samples due to higher densification rate in the presence of zinc oxide compared to the spinellisation rate.[5.5, 5.6]

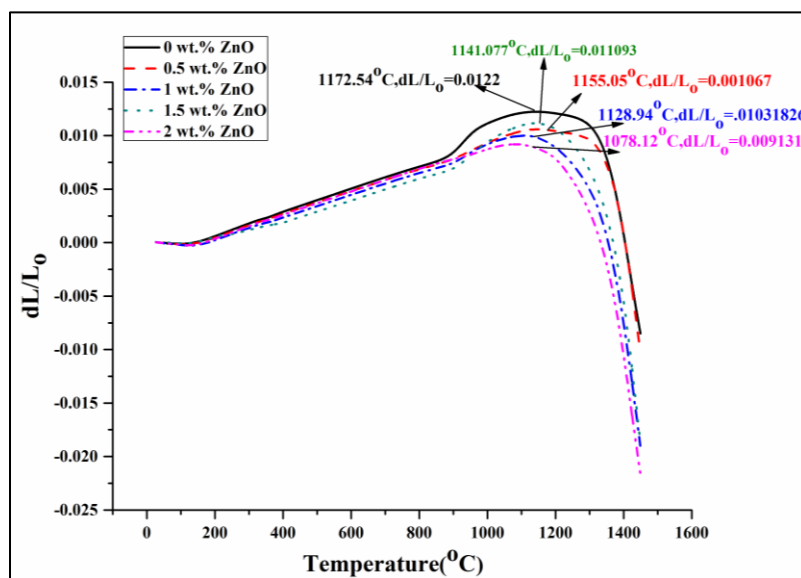


Fig 5.17 The dilatometry plot of the samples with variation in zinc oxide percentage.

5.2.4 Microstructure study

FESEM photomicrographs of the fractured surface show that the samples fired at 1200°C (Fig.5.18) are highly porous, and the grains are small. The addition of zinc oxide had a negligible effect at this temperature. Again zinc oxide addition was found to influence the microstructure strongly for 1600°C sintered products (Fig. 5.19). Sample without Zinc oxide addition was found to have higher porosity and both the inter-granular and intra-granular in nature. But the addition of zinc oxide resulted in more compact grain structure with a lesser extent of porosity at 1600°C. The pores were mainly intra-granular in nature. [5.4]

EDAX frame analysis study done on 1600°C sintered samples show that only magnesium, aluminium, and oxygen ions are present in samples without Zinc oxide [Fig.5.20]. But gold (Au) ions are observed in the EDAX analysis, coming from the gold coating on the samples. EDAX study of 2 wt. % zinc oxide containing sample sintered at 1600°C is shown in Figure 5.21. Spot A, as marked in microstructural photomicrograph (Fig 5.19), represents a spinel grain which was found to contain magnesium, aluminium and oxygen ions with no presence of zinc ion (Figure 5.21A). It indicates that the grains in zinc oxide containing samples are pure spinel and have nearly no Zn ion in it. Again spots B and C, as marked in figure 5.19, which mark the different

regions of the grain boundary and grain of the ZnO-containing sample sintered at 1600°C respectively, was found to contain Zn ions along with magnesium, aluminium and oxygen ions [Fig.5.21 B and 5.21C]. The presence of Zn ions in the grain boundaries and grain indicates that zinc ions diffused in the MgAl_2O_4 structure and acted as a barrier for grain boundary migration and grain growth which lead to uniform and dense microstructure in the case of zinc oxide containing samples at a higher temperature.[5.4, 5.5]

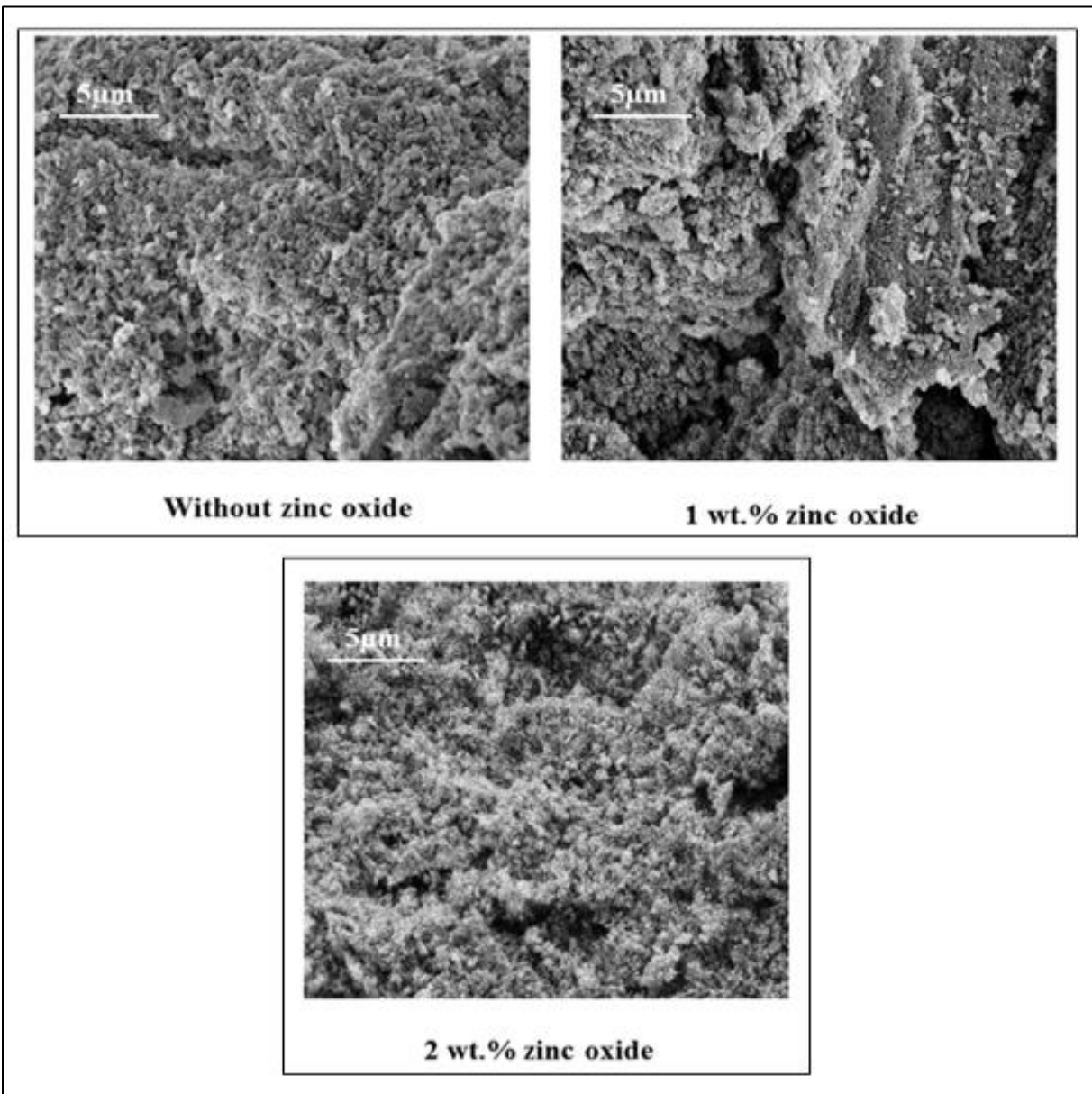


Fig 5.18 FESEM images of 1200°C fired samples with different wt. % of zinc oxide.

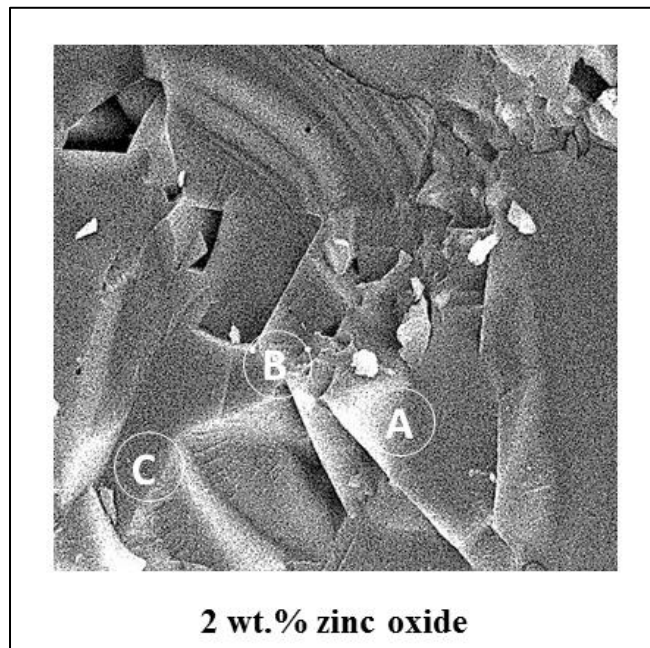
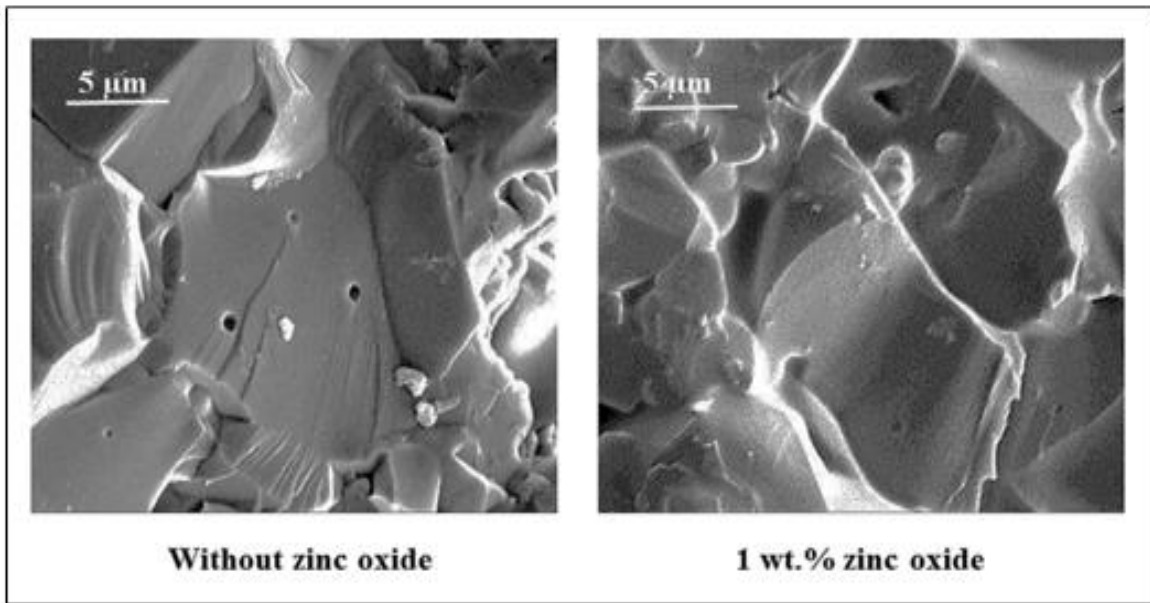


Fig 5.19 FESEM images of 1600°C fired samples with different wt. % of zinc oxide.

5.2.5 Phase analysis study

The presence of spinel phase in the 1200°C fired compositions confirms that the spinel formation started below 1200°C (Fig. 5.22). At 1200°C, spinel was present with the reactant corundum and periclase phases but with increasing temperature, spinel phase peak intensity has increased with a decrease in the reactant phases. The addition of zinc oxide had a great influence on enhancing the spinel formation reaction. At 1200°C, the reactant phases were present with much-reduced intensity for the ZnO-containing samples. Spinel formation increased at 1300, 1400, 1500 °C even for 0.5 wt. % zinc oxide incorporation (Figure 5.23, 5.24 and 5.25); whereas the high intensity of free reactant phases was observed in the batch without zinc oxide. Complete spinellisation of the zinc oxide contained samples occurred at 1600°C (Fig.5.26) whereas reactant phases were still present in the without additive batch. The ionic radius and the ionization potential of Zn^{2+} and Mg^{2+} are similar, due to which Zn^{2+} and Mg^{2+} may have substituted each other [$Zn^{2+}=88\text{pm}$, $Mg^{2+}=86\text{pm}$], thus enhancing the diffusion process resulting in more spinel formation. Also, the addition of zinc oxide creates anion vacancy in Al_2O_3 , which may have accelerated the spinellisation reaction.[5.4, 5.5, 5.7]

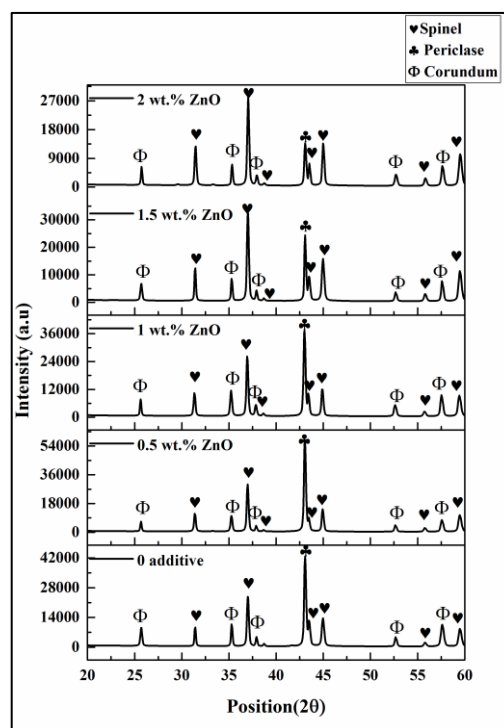
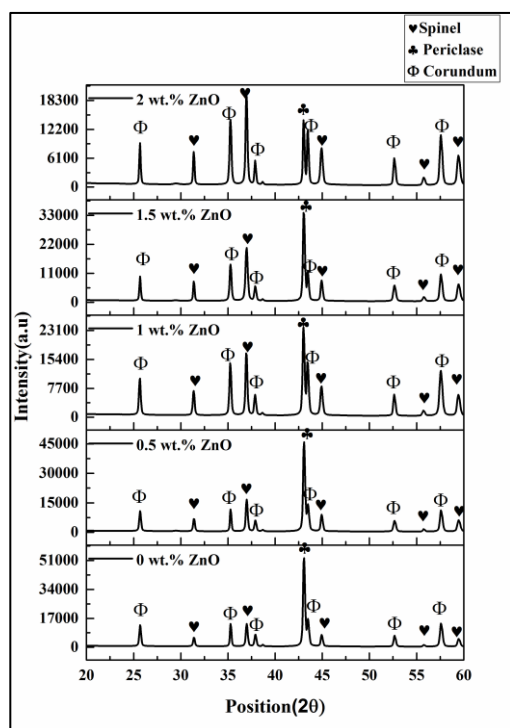


Fig.5.22 XRD plot of samples fired at 1200°C Fig.5.23 XRD plot of samples fired at 1300°C

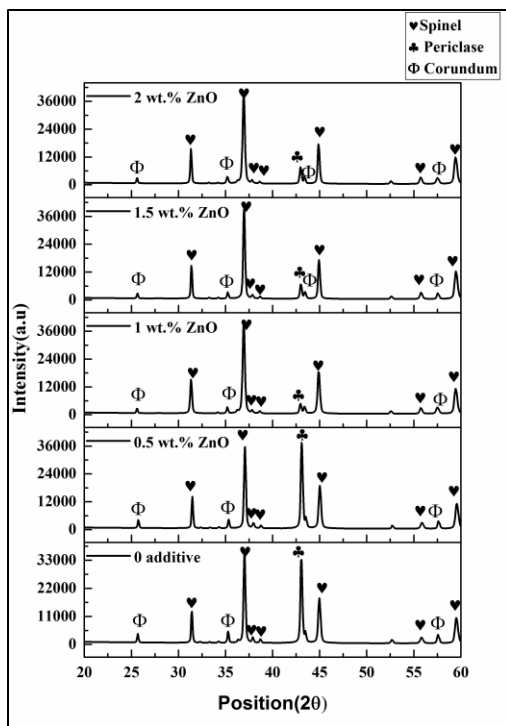


Fig.5.24 XRD plot of samples fired at 1400°C

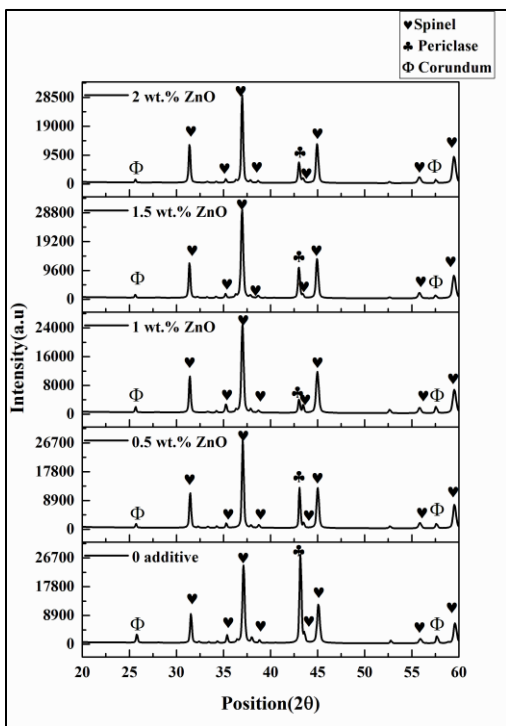


Fig.5.25 XRD plot of samples fired at 1500°C

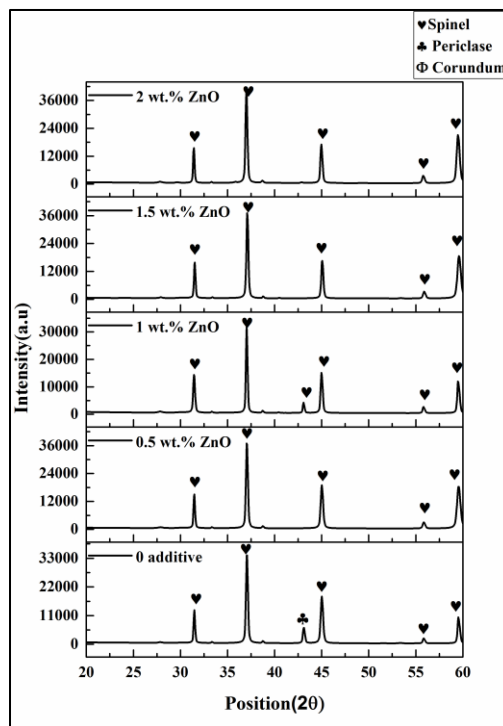


Fig.5.26. XRD plot of samples fired at 1600°C.

5.2.6 Flexural strength study

Flexural strength study of 1600⁰C sintered samples shows that increase in zinc oxide addition improved the flexural strength of the samples (Fig. 5.27). The flexural strength of 2 wt. % zinc oxide containing sample was found to be 240 MPa whereas the sample without zinc oxide had the strength of only 53 MPa. The incorporation zinc oxide has improved the densification of spinel by modifying the microstructure with smaller and uniform grains and resulted in higher strength. The increase in strength was found to rise with the increase in zinc oxide content in the composition. However, the incremental effect on strength with the increase in zinc oxide content was found to be reduced by higher amounts of ZnO. [5.4]

5.2.7 Thermal shock behavior study

Fig.5.28 represents the strength retainment capacity of the 1600⁰C sintered samples after thermal shocks. As the flexural strength, results show that presence of zinc oxide has increased the strength of the samples. The strength of zinc oxide containing samples was much higher even after thermal shock cycles compared to those samples without ZnO. The strength of all samples both zinc oxide containing and without zinc oxide decreased drastically after 4 cycles of thermal shock. But even, in that case, the strength was more for zinc oxide containing samples. After 8 cycles of thermal shock, the strength of all samples decreased, but the 2 wt. % Zinc oxide containing samples retained the strength better than the other ones even after 8 cycles.[5.4]

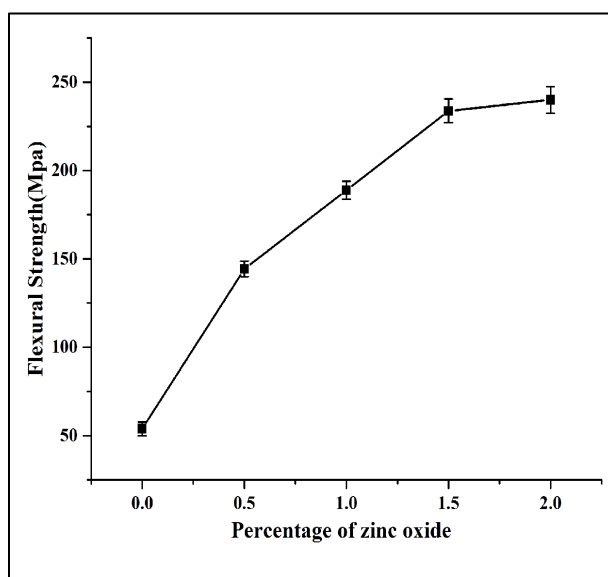


Fig.5.27 Flexural strength of 1600⁰C sintered samples.

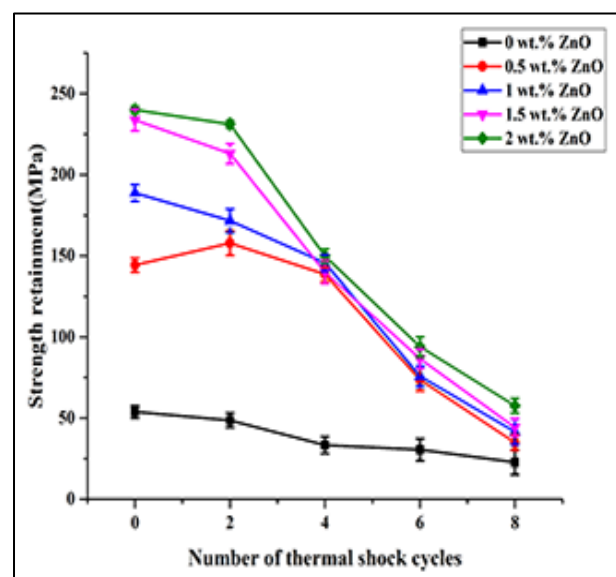


Fig.5.28 Strength retainment of 1600⁰C sintered samples after thermal shock.

5.2.8 Conclusions

- High linear shrinkage was observed with the addition of ZnO at higher temperature whereas at low temperature (1200⁰C) the samples without ZnO exhibits greater shrinkage value.
- The introduction of ZnO resulted in only spinel phase but in non-ZnO samples, reactant phases were present even after firing at 1600⁰C. ZnO containing batch had a lower intensity of reactant phase compared to non-ZnO batch.
- The Greater extent of spinel formation and associated expansion resulted in low-density at low temperature with increase in ZnO contain, but at high temperature (1600⁰C) ZnO doped samples showed higher density due to greater sintering resulting from defects.
- Microstructural features show well compact and less porous structure for the ZnO doped samples with traces of Zn present in EDAX of 1600⁰C sintered samples.
- Flexural strength and thermal shock resistance were improved with ZnO addition.

Section-III

5.3 Effect of zirconium dioxide addition

5.3.1 Linear shrinkage study

Fig.5.29 represents linear shrinkage behaviour of the different compositions at different sintering temperatures. Addition of ZrO_2 was found to cause more expansion compared to that of the without additive batch which may be due to increased spinel formation. All ZrO_2 added samples have the highest expansion at $1300^{\circ}C$. Again an increase in sintering temperature resulted in a sharp increase in the shrinkage curve which may be due to the greater densification of spinel grains in the presence of ZrO_2 at high temperatures and at $1600^{\circ}C$ the ZrO_2 containing samples exhibit much higher shrinkage values compared to samples without ZrO_2 . [5.8]

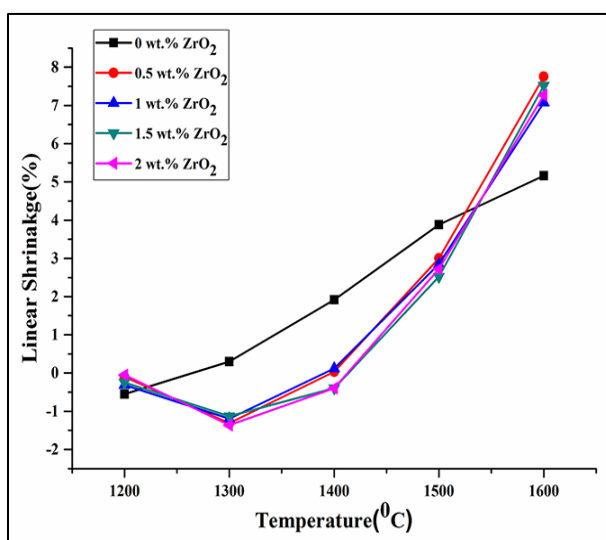


Fig.5.29 Linear shrinkage behaviour of zirconium dioxide contained samples

5.3.2 Densification study

Variation in bulk density values of different batches sintered at different temperatures are shown in Fig.5.30. The increase in sintering temperature was found to increase the bulk density and decrease the porosity due to a greater extent of sintering at higher temperatures. Bulk density values of the ZrO_2 containing compositions remained lower than that of the without additive composition till $1500^{\circ}C$. However, a strong increase in density values were observed for ZrO_2 containing compositions from $1500^{\circ}C$. Highest density was achieved for 0.5 wt. % ZrO_2 containing samples sintered at $1600^{\circ}C$. [5.8]

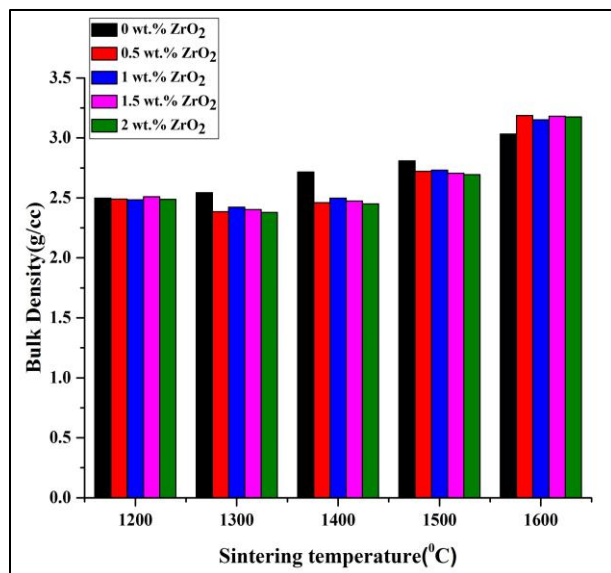


Fig.5.30 Variation of bulk density with zirconium dioxide addition.

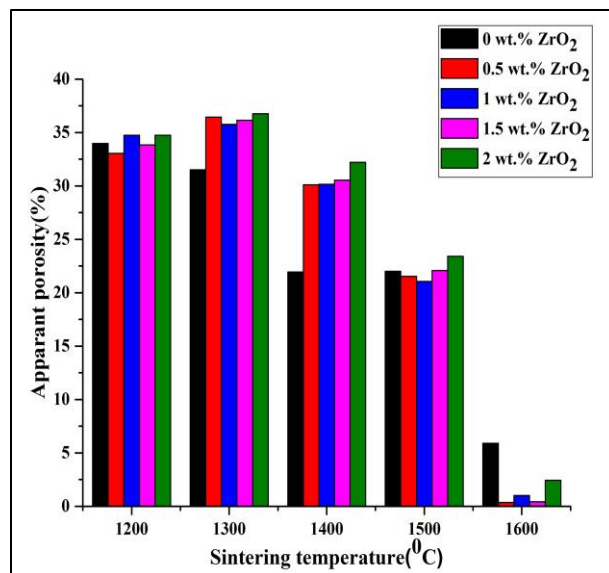


Fig.5.31 Variation of apparent porosity with zirconium dioxide addition.

Apparent porosity values (Fig.5.31) support the densification behaviour. The porosity of all samples was found to increase at low temperatures, due to the spinellisation reaction which is accompanied by a volume expansion. But at higher firing temperatures, when spinellisation is completed, sintering overtakes the spinellisation reaction, so there is a fall in apparent porosity values, above 1400°C. At 1600°C, very low porosity values were observed in ZrO₂ contained samples due to higher sintering. But porosity was found to be higher for higher ZrO₂ containing samples, due to a greater extent of micro-cracks generation caused by the presence of ZrO₂ in grain boundaries.[5.8]

Percent relative densification of the batches is shown in Fig.5.32. Spinel formation is associated with a volumetric expansion that results in decreased densification; again sintering will cause shrinkage in the batch resulting in increased densification (relative density). Relative density values of the without ZrO₂ batch was found to increase with increasing firing temperature above 1200°C. Whereas ZrO₂ containing compositions showed decreasing relative density values upto about 1400°C and then densification increased with increasing temperature. This marginally lower densification (relative density) of ZrO₂ containing compositions at lower temperatures compared to the without ZrO₂ containing composition is associated with the greater spinel formation. Bulk density values differ from the relative density values as the specific gravity of ZrO₂ is much higher than spinel and increases the specific gravity of the ZrO₂ containing compositions. The lower

relative density values of ZrO_2 containing compositions continued till about $1500^\circ C$. But at $1600^\circ C$, the relative density of the ZrO_2 containing samples are higher than the without ZrO_2 composition, which indicates that ZrO_2 enhances the densification process of spinel at a higher temperature. This may be due to the presence of high-density ZrO_2 in the grain boundaries which may have hindered the grain growth at higher temperature leading to greater densification, as observed in microstructural and EDAX studies. The increase in ZrO_2 content more than 0.5 wt. % was also not found to help in densification process. Greater amount of ZrO_2 was found to reduce the density values due to the expansion caused by more spinel formation and an increase in micro-cracks due to the presence of Zirconia in the grain boundaries.[5.6, 5.8, 5.9]

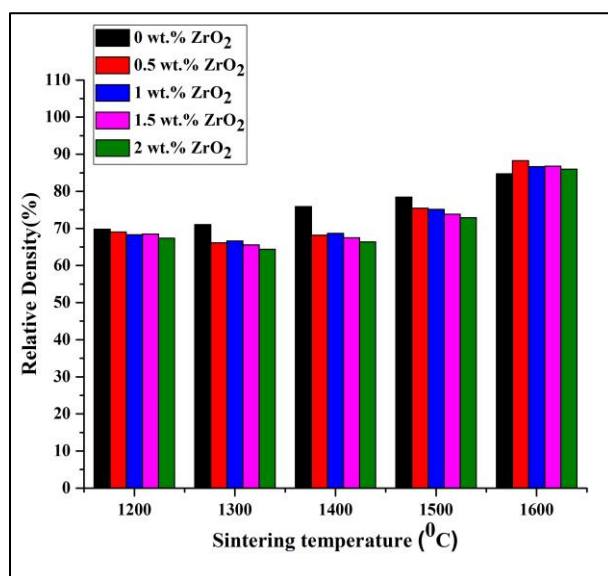


Fig.5.32 Variation of relative density with zirconium dioxide addition.

5.3.3 Dilatometry study

The dilatometry plot clearly shows (Fig.5.33) that addition of ZrO_2 accelerates the spinellisation reaction. With the increase in temperature, expansion due to spinel formation and shrinkage due to sintering run parallel. At higher temperatures, sintering process enhances due to increased mass transfer and expansion behavior of spinel formation is overtaken by shrinkage due to sintering. Thus, the dilatometry curve takes a downward turn at the high temperatures. This feature is common to all the compositions with or without containing zirconia. The addition of ZrO_2 has resulted in more spinellisation compared to densification because of which there is a sharp increase in dL/L_0 value for ZrO_2 containing samples. Also, it was observed that increase in ZrO_2 content

has increased the temperature at which shrinkage rate (due to sintering) overtakes the expansion rate (due to spinel formation). Hence, a higher amount of spinel forms and densification is delayed with increasing amount of ZrO_2 . The increase in spinellisation due to Zirconia addition may be due to cation vacancy created by substitution of Mg^{2+} or Al^{3+} by Zr^{4+} , which accelerated the spinellisation reaction at a lower temperature.[5.8, 5.10]

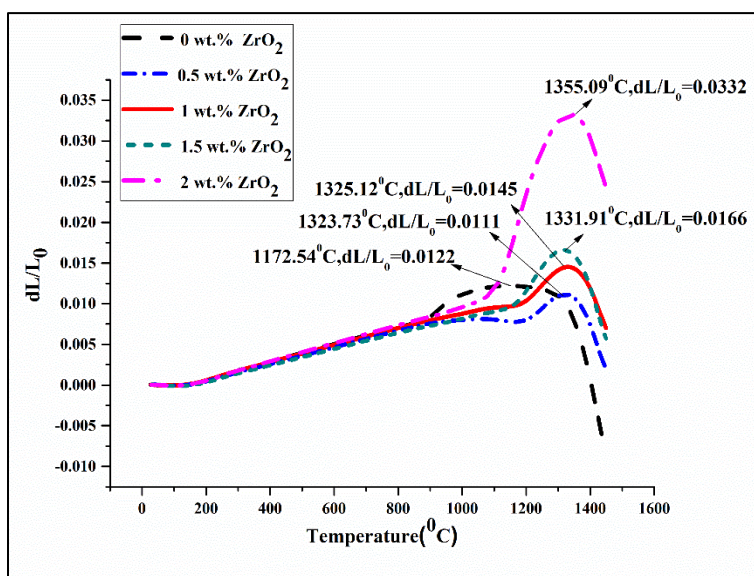


Fig 5.33 The dilatometry plot of the samples with a variation of zirconium dioxide percentage.

5.3.4 Microstructure study

Microstructure study of the fractured sample was done in a field emission scattered electron microscope in back-scattered electron mode. The micrographs of $1200^{\circ}C$ fired samples show (figure 5.34) that the samples are very porous. Uniform distribution of zirconia particles can easily be seen in the micrographs.

The $1600^{\circ}C$ sintered microstructure clearly shows the presence of ZrO_2 in the grain boundaries. The micrograph of 0.5 wt. % ZrO_2 containing sample showed (figure 5.35) very compact structure with intragranular pores. The micrographs of 0 wt. % ZrO_2 contained sample show a porous structure. The 2 wt. % ZrO_2 contained sample micrograph show grains with cracks. The cracks may be due to phase transformation of excess zirconia present in the grain boundaries.[5.8]

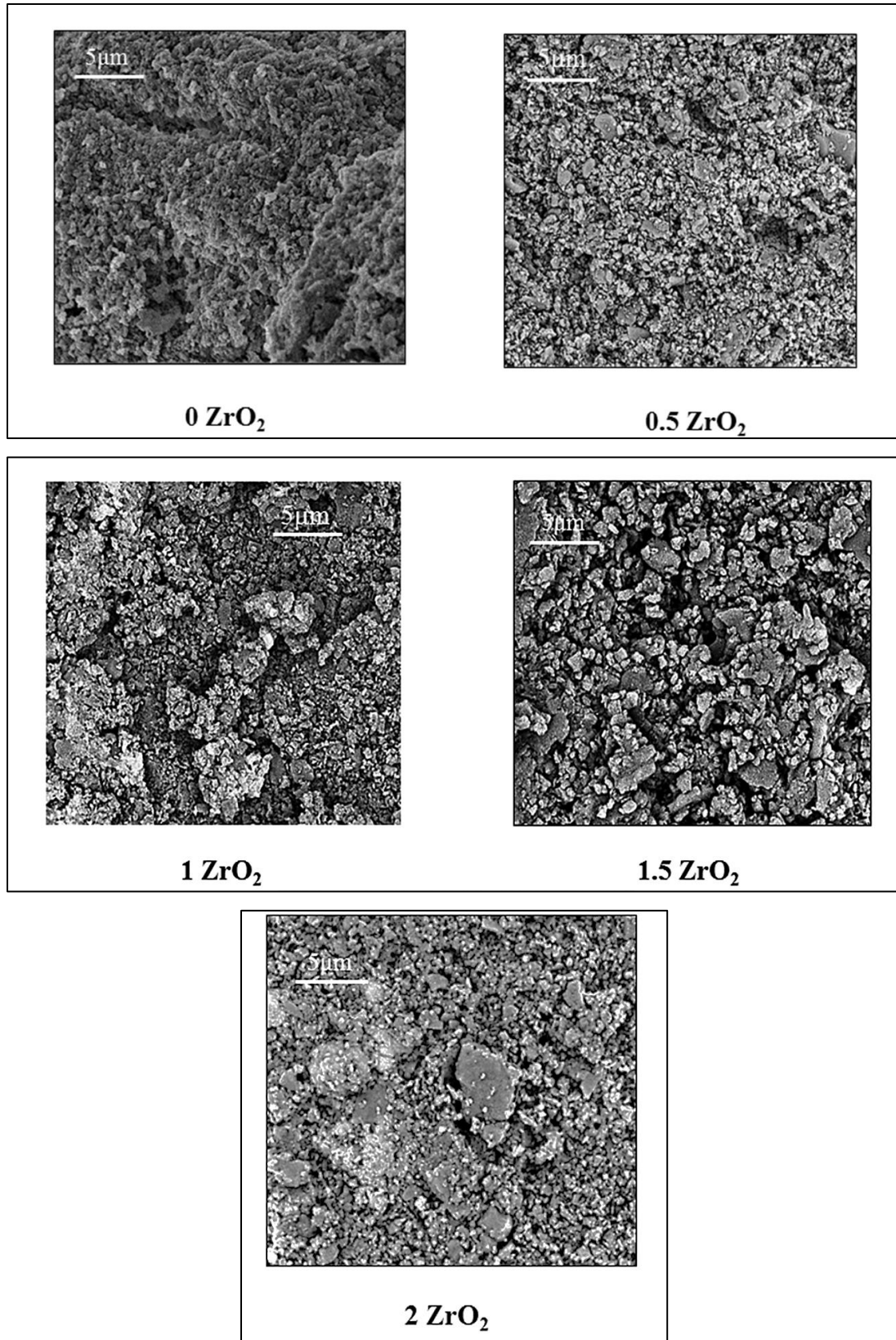


Fig.5.34 FESEM images of 1200°C sintered samples.

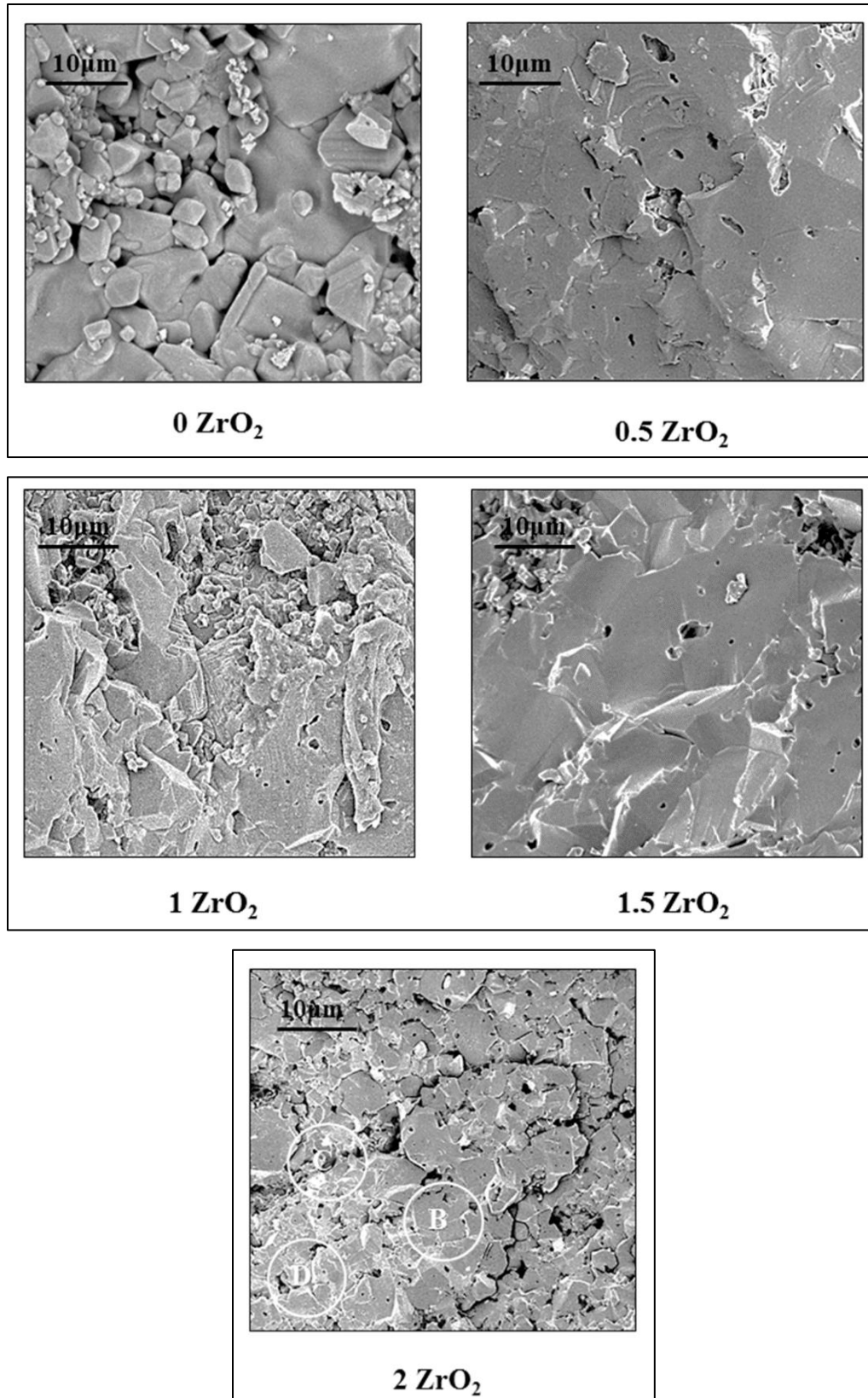


Fig.5.35 FESEM images of 1600°C sintered samples.

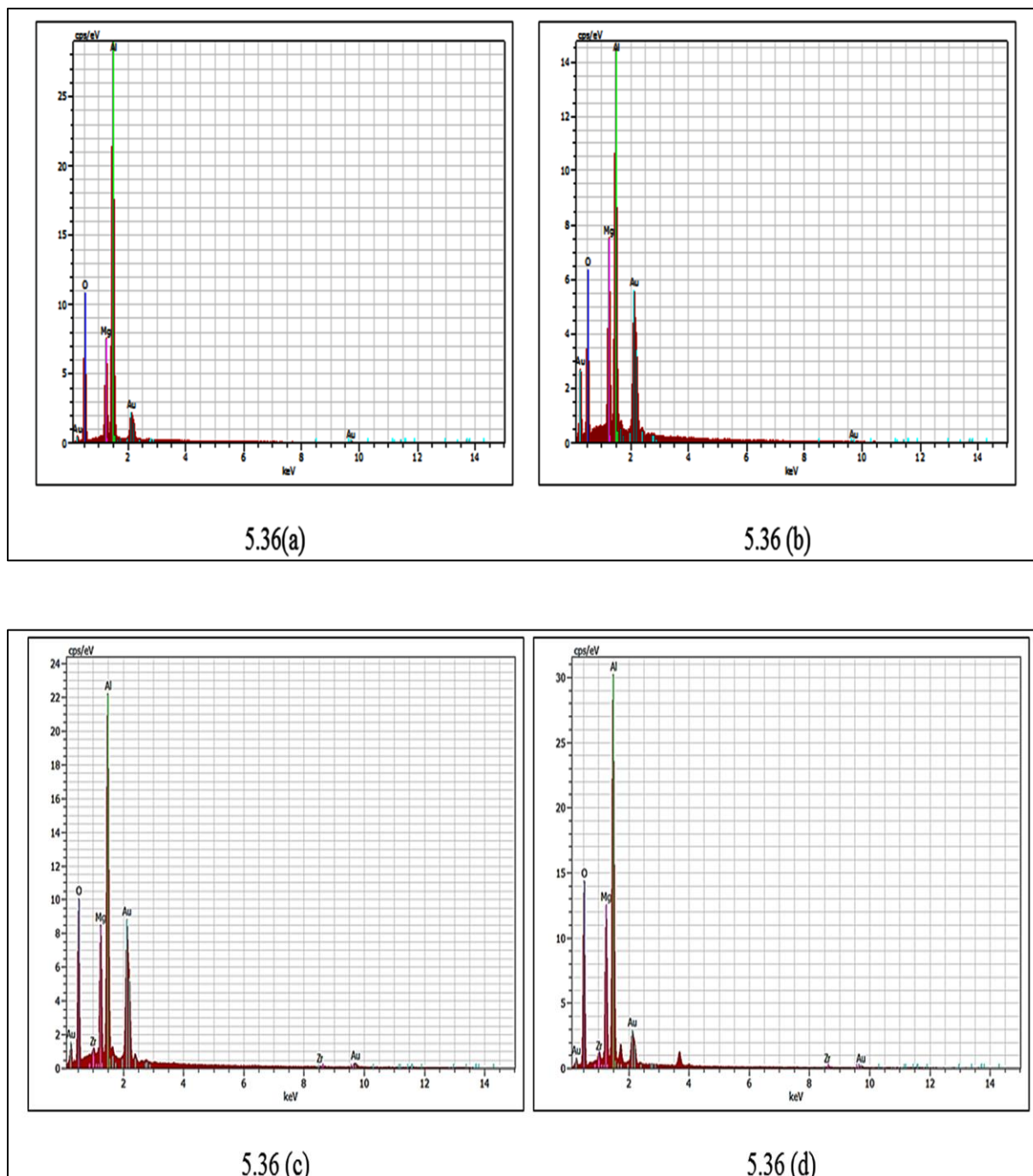


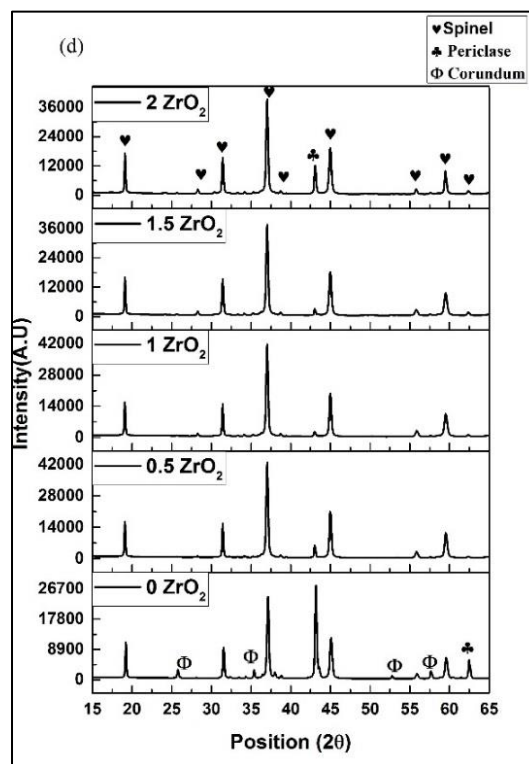
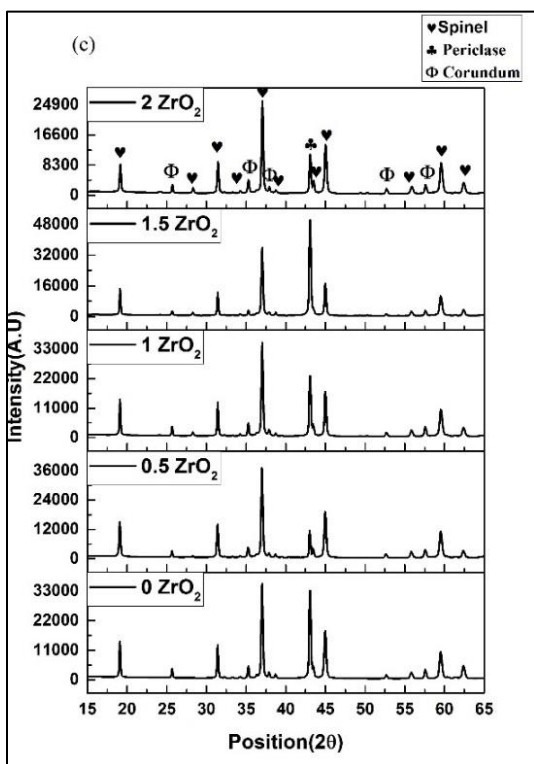
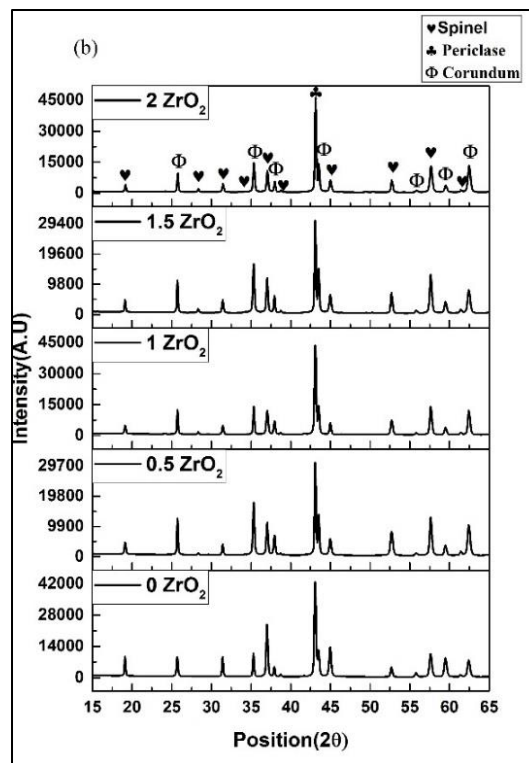
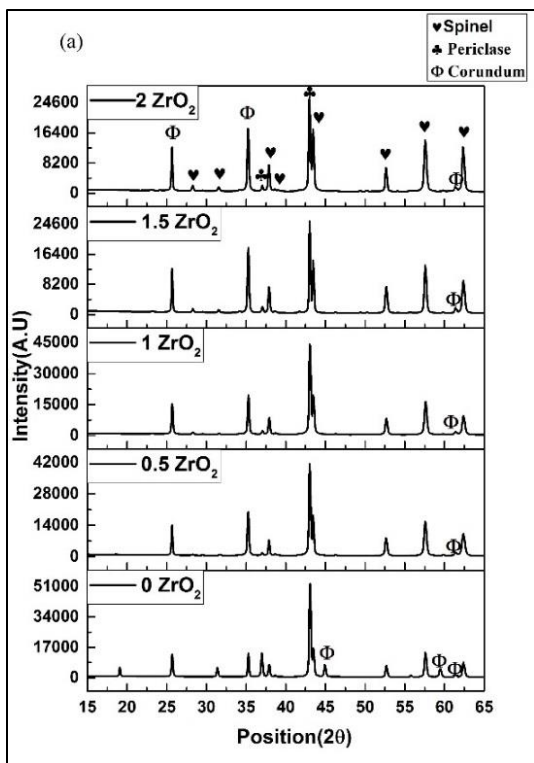
Fig.5.36 EDAX of zirconium dioxide containing samples.

EDAX frame analysis study was done on 1600⁰C sintered samples (Fig 5.35) which show that only magnesium, aluminium, and oxygen ions are present in samples without ZrO₂ (Fig.5.36(a)). But gold (Au) ions are observed in the EDAX analysis, coming from the gold coating on the samples. Again, EDAX study on 2 wt. % ZrO₂ containing sample sintered at 1600⁰C is shown in

Figure 5.36(b). Spot B, as marked in microstructural photomicrograph (Fig 5.35), which represents a spinel grain is found to contain magnesium, aluminium and oxygen ions with no presence of zirconium ion (Figure 5.36(b)). This indicates that the grains in ZrO_2 containing samples are pure spinel in composition and have nearly no zirconium ion in it. Again spots C and D, as marked in figure 5.35, which mark the different regions of the grain boundary of the ZrO_2 containing sample sintered at $1600^{\circ}C$, is found to contain Zr^{4+} ions along with magnesium, aluminium and oxygen ions [Fig.5.36(c)and 5.36(d)]. The presence of Zr^{4+} ions in the grain boundaries indicates that it acts as a barrier for grain boundary migration and grain growth which lead to uniform and dense microstructure in the case of ZrO_2 containing samples at a higher temperature.[5.8]

5.3.5 Phase analysis study

Fig 5.37(a) shows the presence of spinel phase in the $1200^{\circ}C$ fired compositions which confirm that the spinel formation has started below $1200^{\circ}C$. Reactant phase corundum and periclase are present along with spinel phase at $1200^{\circ}C$ but with increasing temperature spinel phase peak intensity has increased with a decrease in the reactant phases. Incorporation of ZrO_2 has a great influence on enhancing the spinel formation reaction. The intensity of the reactant phases was present with much-reduced intensity at $1200^{\circ}C$ for the ZrO_2 containing samples. ZrO_2 incorporation has increased the spinel formation which was also observed at 1300, 1400 even for 0.5 wt. % ZrO_2 (Figure 5.37 b and 5.37 c); whereas the high intensity of free reactant phases was observed in the batch without ZrO_2 . Complete spinellisation of the ZrO_2 incorporated sample occurred at $1600^{\circ}C$ (Fig. 5.37 (e)) whereas reactant phases were still present in the without additive batch. It can also be seen that 0.5 wt. % and 1 wt. % ZrO_2 showed the highest degree of spinel formation in all sintering temperatures. XRD of $1500^{\circ}C$ sintered samples (fig. 5.37 d) shows that ZrO_2 containing compositions had the very low intensity of the reactant phases compared to the without ZrO_2 batches. The ionic radius and ionization potential of Zr^{4+} and Mg^{2+} are similar, due to which Zr^{4+} may substitute Mg^{2+} [ionic size: $Zr^{4+} = 86$ pm, $Mg^{2+} = 86$ pm and ionization potential: $Mg^{2+}=1450.7$ kJ/mole, $Zr^{4+}= 1270$ kJ/mole], causing cation vacancy and enhancing the cation diffusion for spinel formation.



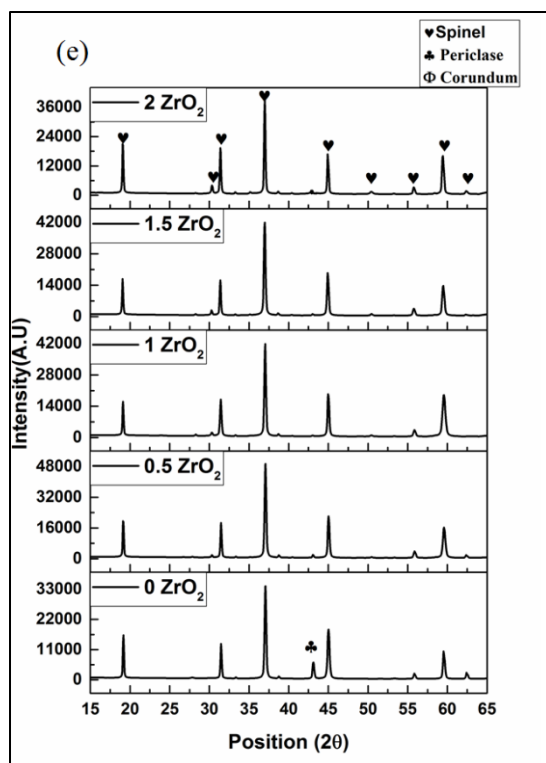
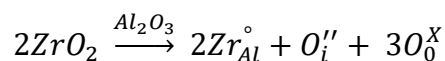
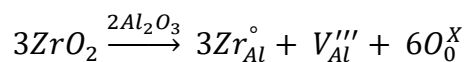
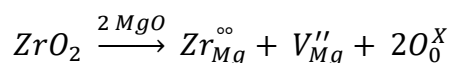
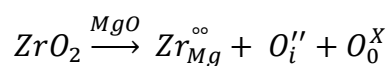


Fig.5.37 XRD plots of samples sintered at (a) 1200^oC (b) 1300^oC (c) 1400^oC (d) 1500^oC and (e) 1600^oC with variation of zirconium dioxide percentage.

The substitution of Mg²⁺ or Al³⁺ by Zr⁴⁺ may occur in accordance to following equations as suggested by Kim.[5.10]



The formation of oxygen interstitial is difficult because of the higher ionic radius of oxygen. But the cation vacancy cause by Zr⁴⁺ substitution is more possible and favorable reaction.[5.8]

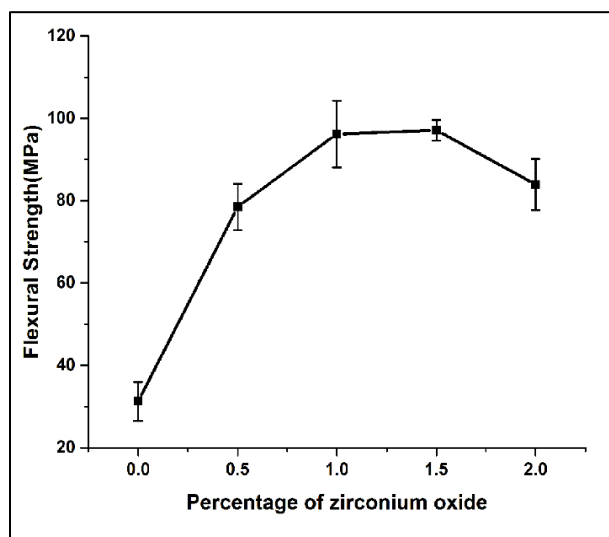


Fig.5.38 Variation of flexural strength with zirconium dioxide content for 1600°C sintered samples.

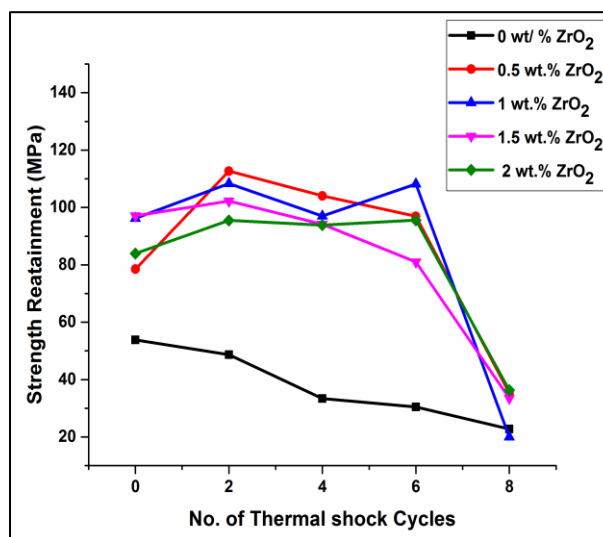


Fig.5.39 Strength retainment of the compositions after thermal shock.

5.3.6 Flexural strength study

Flexural strength values of 1600°C sintered samples improved with the addition of ZrO₂ in spinel composition (Fig. 5.38). The Flexural strength of 1.5 wt. % ZrO₂ containing sample was found to be 97 MPa whereas the sample without ZrO₂ had the strength of only 53 MPa. The incorporation ZrO₂ has improved the densification of spinel by modifying the microstructure with smaller and uniform grains and resulted in enhanced strength. The increase in strength was found to increase with the increase in zirconia content in the composition. However, the incremental effectiveness of the increase in strength with the increase in ZrO₂ content was found to be reduced by higher amounts. For 2 wt. % ZrO₂ contained composition; strength value was found to be reduced, which may be due to crack formation within the sample as observed in the microstructure.[5.8]

5.3.7 Thermal shock behaviour study

Fig.5.39 show the strength retainment capacity of the 1600°C sintered samples after thermal shocks. As the flexural strength and density values indicate that presence of ZrO₂ increased these properties significantly, the strength retainment capacity of the ZrO₂ containing samples was found to be much higher after thermal shock cycles compared to those samples without ZrO₂. This enhanced strength retainment was prominent up to 6 thermal cycles. The strength of all samples

without ZrO₂ decreased more after 4 cycles of thermal shock. But ZrO₂ containing samples showed strength retainment up to 6 cycles of thermal shock. The increase in strength of ZrO₂ contained samples compared to without ZrO₂ may be due to the presence of ZrO₂ in the grain boundaries which have helped in a micro crack generation which lead to crack deflection which resulted in increased strength retainment capacity of the samples. [5.8]

5.3.8 Conclusions

- The addition of ZrO₂ at a higher temperature resulted in higher shrinkage due to densification whereas at low temperature (1200 °C) the samples without ZrO₂ exhibits higher shrinkage value.
- The introduction of ZrO₂ resulted in only spinel phase at single stage sintering but in non-ZrO₂ samples, reactant phases were present even after firing at 1600 °C. The peak intensity of the reactant phases was low in ZrO₂ contained samples compared to without ZrO₂ batch.
- The greater extent of spinel formation and associated expansion resulted in low-density at low temperature for ZrO₂ contained samples, but at high temperature (1600 °C) ZrO₂ contained samples showed higher density due to greater sintering resulting from defects.
- The addition of ZrO₂ helped in spinel formation by creating cation vacancy as well as densification process by restricting the grain boundary movement. But the presence of ZrO₂ in higher amount i.e. more than 1% leads to micro-crack generation that affected the sintering process.
- Microstructural features show well compact and less porous structure for the ZrO₂ contained samples with traces of Zr present in EDAX of 1600 °C sintered samples.
- Flexural strength and strength retainment after thermal shock was improved with ZrO₂ addition. The ZrO₂ added samples retained high strength even after 6 cycles of thermal shocks in comparison to without ZrO₂ samples. However, the retainment drastically fall in all the samples after 8 cycles of thermal shock.

Section-IV

5.4 Effect of aluminium nitrate nonahydrate addition

5.4.1 Linear shrinkage study

The linear shrinkage behavior vs. sintering temperature plot is shown in fig.5.40. All the batches showed expansion at 1200°C due to spinel formation with no shrinkage. However, the expansion in all additive containing batches was found to be much greater than compared to that of the without additive composition at the lower sintering temperature. This higher expansion in additives containing compositions was due to a greater extent of spinel formation at the lower temperatures which may have occurred due to the presence of an additional amount of reactant phases produced via decomposition of the additives on heating. The additive containing batch showed higher shrinkage value above 1400°C indicating the greater extent of densification. It was observed that with an increase in the amount of nitrate addition the shrinkage rate was decreased. This might due to exaggerated grain growth which might have occurred due to the presence of more amount of fine alumina formed from the decomposition of the nitrate additive. [5.11, 5.12]

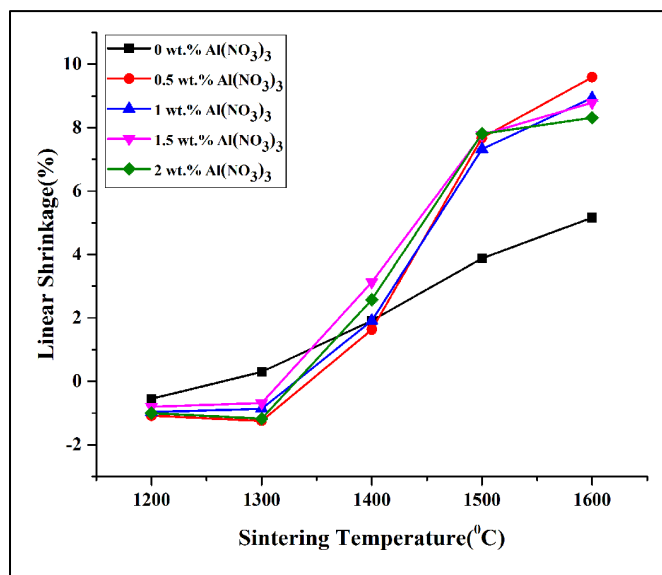


Fig.5.40 Plot of linear shrinkage vs. sintering temperature.

5.4.2 Densification study

The variation in bulk density values of all the batches against sintering temperatures and the additive percentage is represented in fig.5.41. With the increase in sintering temperature, a

common trend of increasing bulk density value was observed for all compositions due to the higher extent of sintering with increasing temperature. The addition of aluminium nitrate was found to affect the densification behavior in almost all sintering temperatures. This indicates the greater extent of spinel formation reaction (associated with volumetric expansion) in additive containing batches at a lower temperature in comparison to non-additive batch. The apparent porosity was also high for the additive containing batch at 1200°C. The apparent porosity of alumina nitrate containing batch is shown Fig.5.42. The formation of nascent alumina from nitrate additive accelerated the spinellisation reaction because of which porosity was high in low sintering temperature. When the sintering temperature was increased to 1500°C, the higher density values were observed in additive containing batch due to a greater extent of sintering in the samples. This clearly indicates that the presence of additive influenced the spinellisation process at lower temperature and also aided in the sintering of the formed $MgAl_2O_4$. The highest density value was observed for 1 wt.% additive-containing composition sintered at 1600°C. The apparent porosity results supported the bulk density values.[5.11, 5.12]

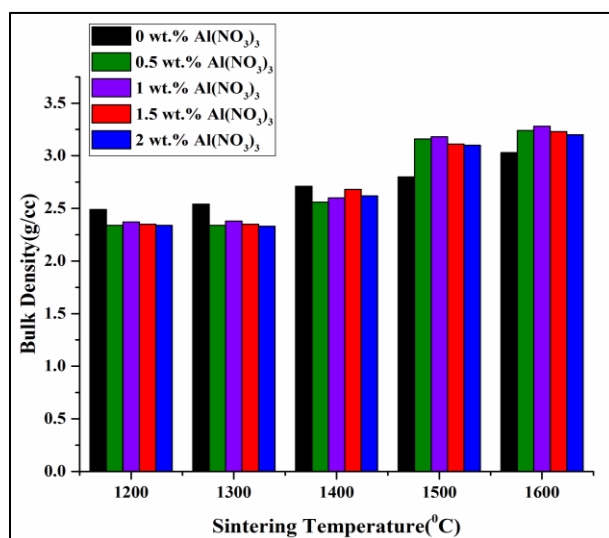


Fig.5.41 Variation of bulk density with sintering temperature and additive percentage.

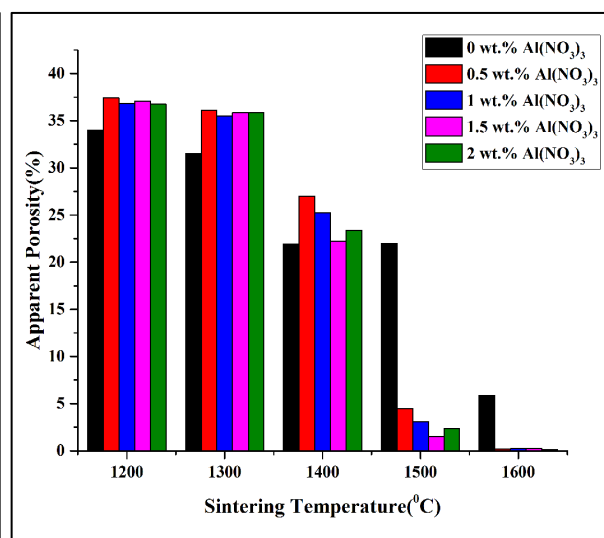


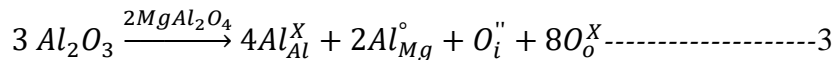
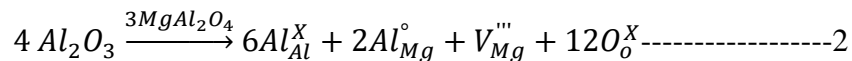
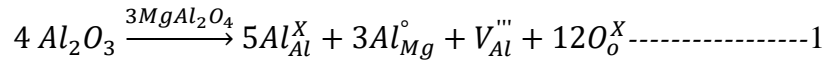
Fig.5.42 Variation of apparent porosity with sintering temperature and additive percentage.

5.4.3 Dilatometry study

Fig.5.43 represents the dilatometric plot of all the compositions. It represents both the expansion due to spinel formation and shrinkage due to sintering at higher temperatures, which run parallel.

At higher temperatures, the sintering process accelerates due to increased mass transfer and expansion behavior related with spinel formation is overtaken by shrinkage resulting from sintering. Thus, a downward turn of the dilatometric curve is observed at the high temperatures. This feature is common in all the compositions with or without the additive. Initially, there is no effect of the additive on the dilatometry plot up to $\sim 1000^{\circ}\text{C}$. However, aluminium nitrate containing batch showed much higher expansion in comparison to zero additive batch. Aluminium nitrate will decompose with an increase in temperature and yield very fine and reactive Al_2O_3 particles respectively. The presence of these fine particles will affect the stoichiometry. The effect of these particles at onset temperature is negligible. After the formation of the MgAl_2O_4 layer between MgO and Al_2O_3 , the reaction is mainly controlled by diffusion of slow moving cation over this layer. However, the process of sintering depends on the mobility of both cations and anions. As oxygen diffusion is lower than the cations due to the larger ionic size of the oxygen ion, it acts as the rate determining step in sintering. The non-stoichiometry plays an important role in this part. The reactive and fine alumina produced from decomposition of aluminium nitrate will incorporate in accordance with following reactions as suggested by Kim[5.10]-

Al_2O_3 into MgAl_2O_4 –



The creation of interstitial requires much higher structural adjustments and is less likely to occur. So, the equations 1-3 clearly indicate that the presence of fine reactive alumina into the MgAl_2O_4 will generate cation disorder and decrease oxygen vacancy concentration.

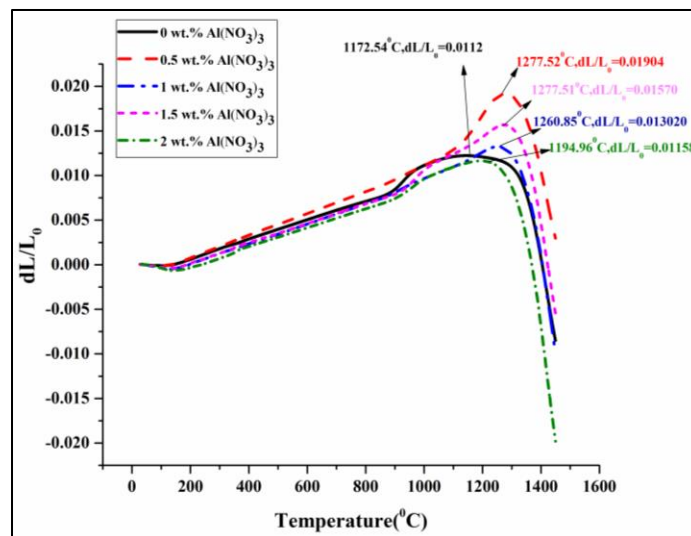


Fig.5.43 Dilatometry plots of aluminium nitrate nonahydrate containing batch.

The dilatometry plots clearly indicate higher spinellisation in alumina nitrate contain batches. This is due to increase in cation disorder which has occurred due to the incorporation of fine reactive alumina produced from insitu decomposition of alumina nitrate at a higher temperature. But we can also observe that increase in the higher amount of alumina nitrate led to higher shrinkage with an increase in temperature the presence of excess alumina which assisted in densification acting as a second phase inclusion.[5.11, 5.12]

5.4.4 Microstructure study

The FESEM micrograph of the fractured surface of without additive batch is shown in figure 5.44. The 1200°C sintered sample show a porous microstructure with fine alumina grains uniformly distributed over the coarser magnesia grains. However, the 1600°C sintered samples show a dense microstructure with little intergranular and intragranular pores.

A porous microstructure was observed in 1200°C sintered 1 wt.% aluminium nitrate nonahydrate containing a sample (Fig. 5.45). The growth of some platelet shape structure was observed on larger size grains. This may be due to the formation of nanosize spinel on coarser magnesia grains caused by diffusion of fine alumina particles. The microstructure became more porous, and the intensity of this platelet formation was found to increase with the increase in the percentage of aluminium nitrate nonahydrate addition (Fig.5.46). This might be due to increase diffusion of alumina in magnesia due to increasing cation defects as mentioned in section 5.4.3 thus

accelerating spinel formation reaction. The literature also provides some evidence of the growth of such structure. The mechanism of growth of such nano-size structure is called template mechanism.[5.13, 5.14]

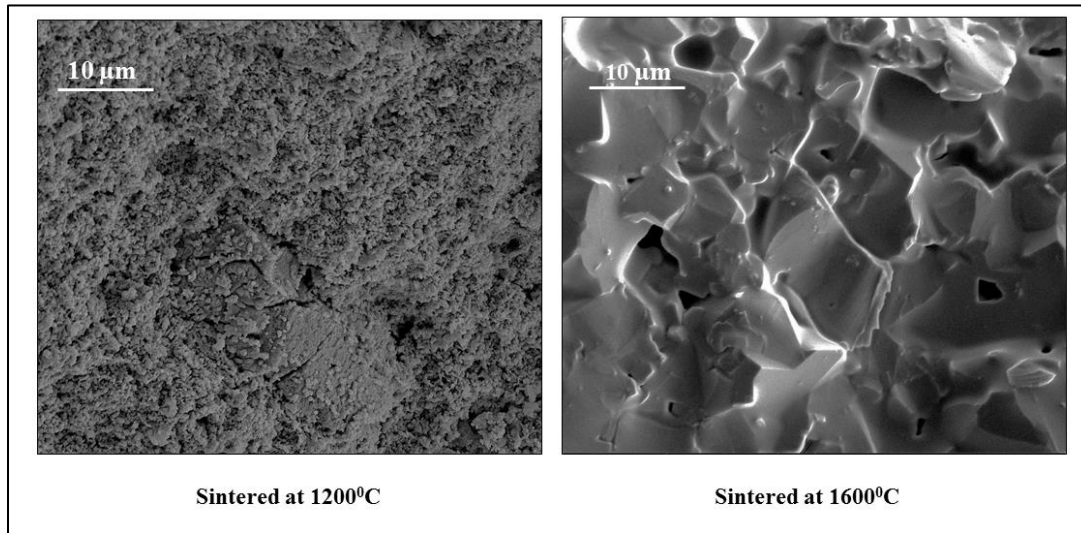


Fig.5.44 FESEM micrograph of without additive batch.

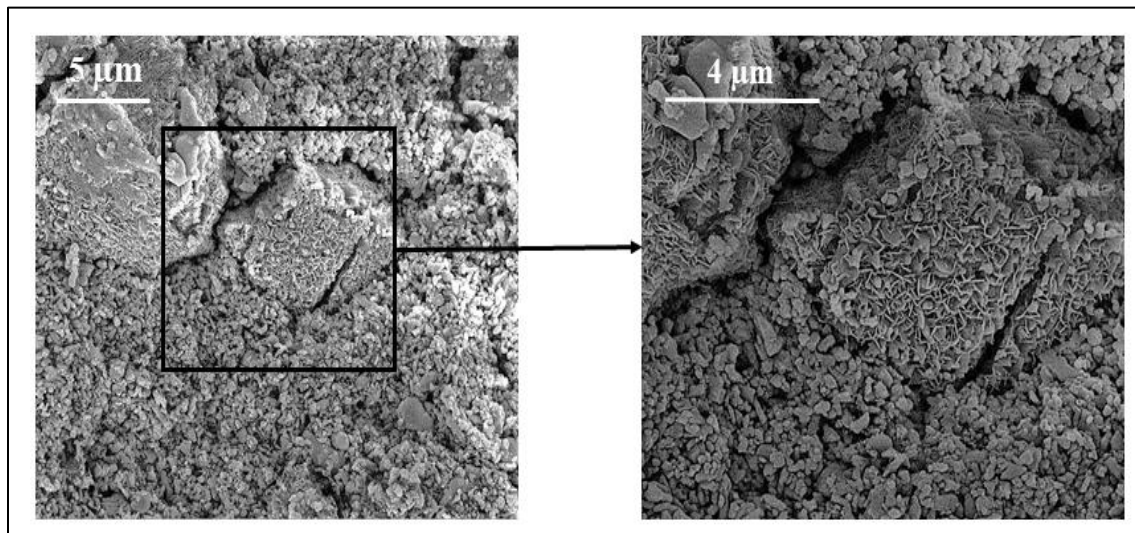


Fig.5.45 Microstructure 1200°C sintered 1wt. % aluminium nitrate nonahydrate containing sample.

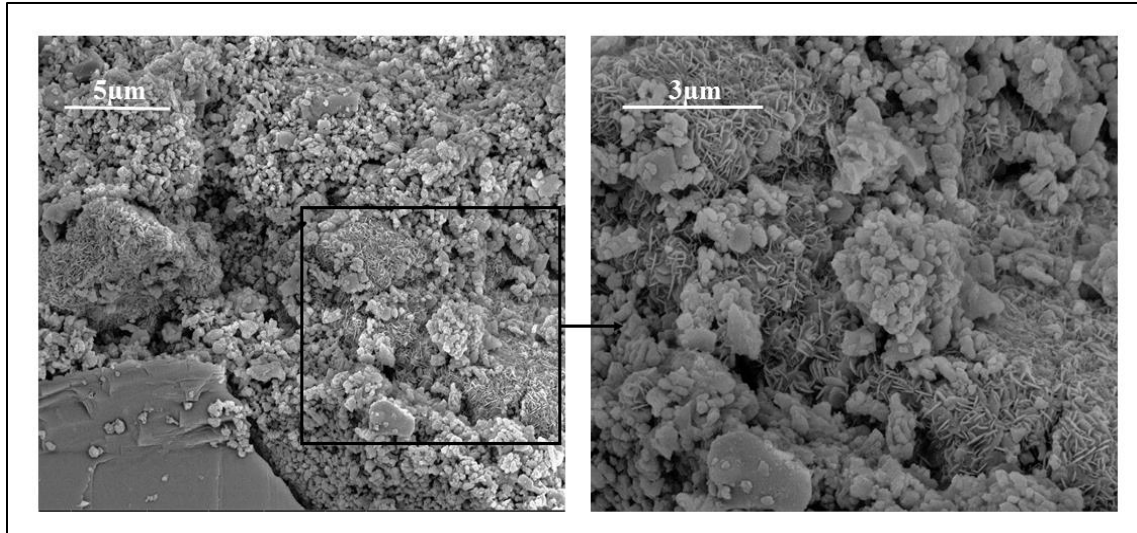


Fig.5.46 Microstructure of 1200⁰C sintered 2 wt. % aluminium nitrate nonahydrate containing sample.

The microstructure of 1600⁰C sintered 1 wt. %, and 2 wt. % aluminium nitrate nonahydrate containing batches are shown in fig.5.47. A dense microstructure with few close pores was observed. The increase in the addition of aluminium nitrate was found to aid in grain growth at higher temperature due to increase in grain boundary mobility.[5.11, 5.12]

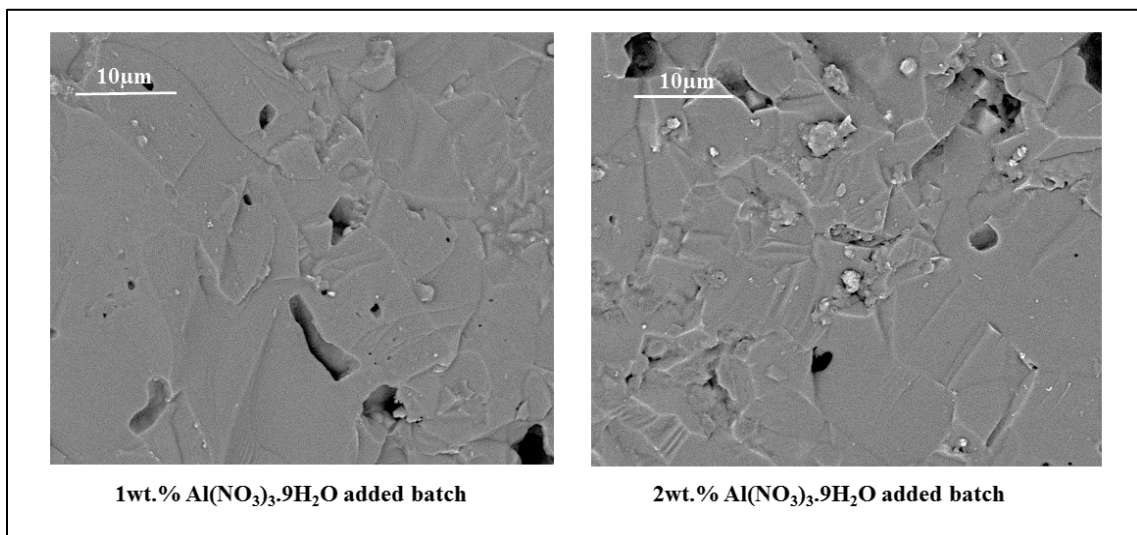


Fig.5.47 Microstructure of 1600⁰C sintered 1 and 2 wt. % aluminium nitrate nonahydrate containing batches.

5.4.5 Phase analysis study

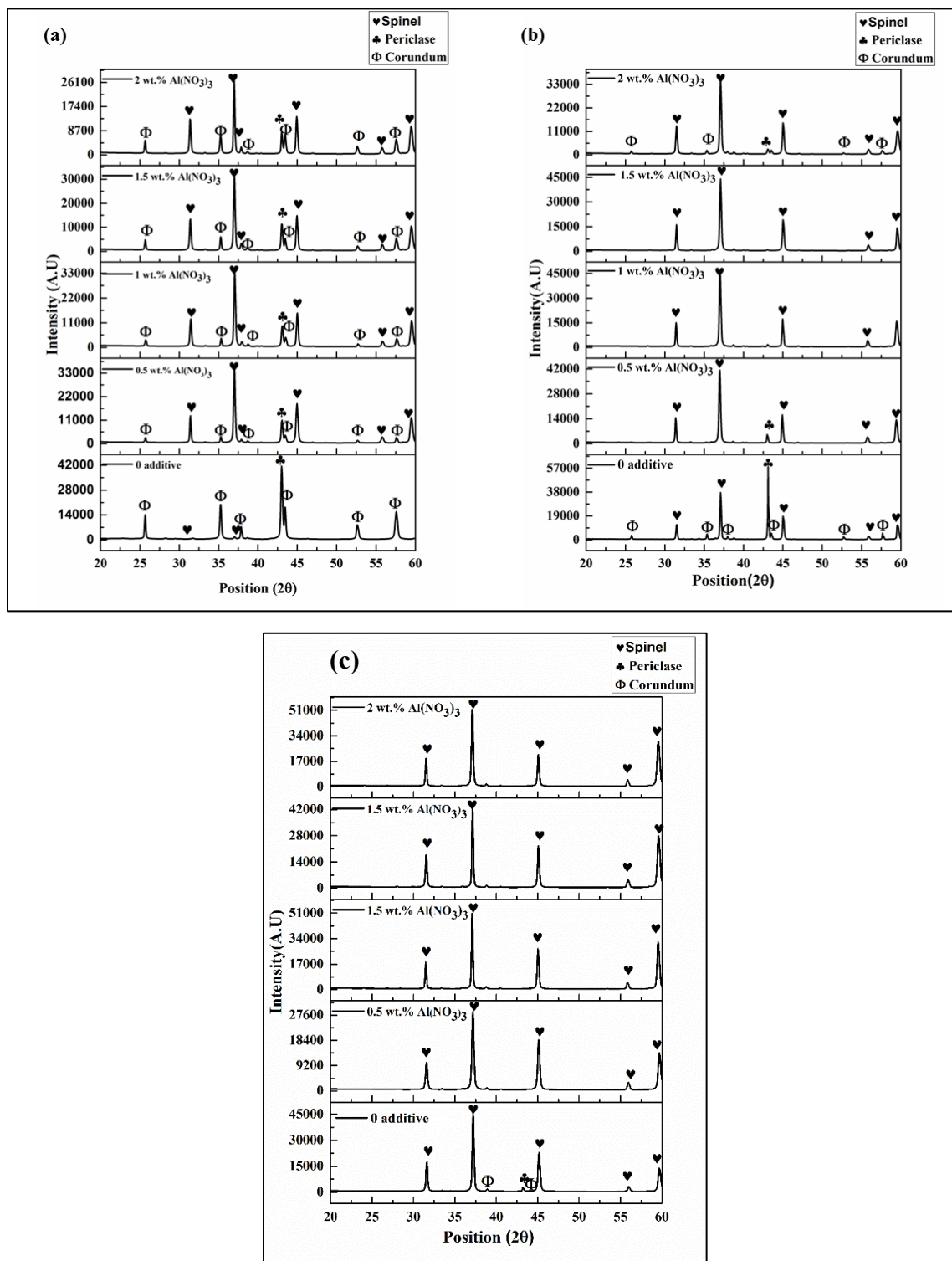


Fig.5.48 XRD of aluminium nitrate nonahydrate batch (a) 1200°C sintered (b) 1400°C sintered and (c) 1600°C sintered.

X-ray diffraction pattern of aluminium nitrate nonahydrate contained batches sintered at 1200⁰C are shown in Fig.5.48 (a). The presence of spinel peak in x-ray diffraction pattern confirms that spinel formation started below 1200⁰C in both the batches. The intensity of spinel phase was observed to be quite low in zero additive batch in comparison to the non-additive batches. The addition of aluminium nitrate was found to aid spinel formation reaction at low temperature. Effect of aluminium nitrate addition on spinel formation reaction was more compared to zero additive batch. This may be due to the generation of cation defects caused by diffusion of nascent alumina (formed from the decomposition of aluminium nitrate) into spinel which aided in spinellisation reaction.

The x-ray diffraction patterns of all 1400⁰C sintered compositions are shown in fig.5.48 (b). The increase in sintering temperature increased the amount of spinel formation in all the batches. The spinel formation was much higher in additive containing batch compared to zero additive batch where reactant phase was observed distinctly. However, in aluminium nitrate batch small reactant phase peaks were observed on addition of more than 1.5 wt. % aluminium nitrate nonahydrate which might due to exsolution of alumina. The 1600⁰C sintered samples xrd pattern were shown in fig.5.48(c). The presence of only spinel phase was observed in all the additive containing samples which confirm completion of spinel reaction. However, unreacted phases were observed in the without additive sample indicating incomplete spinellisation reaction.[5.11, 5.12]

5.4.6 Flexural strength study

Flexural strength of 1600 °C sintered samples of both the additive containing batch is shown in fig.5.49 The Flexural strength of 0.5 wt.% aluminium nitrate nonahydrate containing sample was found to be 176.98 MPa whereas the sample without additive batch merely showed the strength of only 31.25 MPa. The incorporation aluminium nitrate improved the strength of spinel by modifying the microstructure. In aluminium nitrate nonahydrate batch, strength increased rapidly with 0.5 wt.% addition of aluminium nitrate, but the addition of more amount of additive decreased the strength. This might be due to exaggerated grain growth in presence of extra alumina as observed in microstructure in section 5.4.4. This hindered the densification resulting in poor strength [5.11, 5.12]

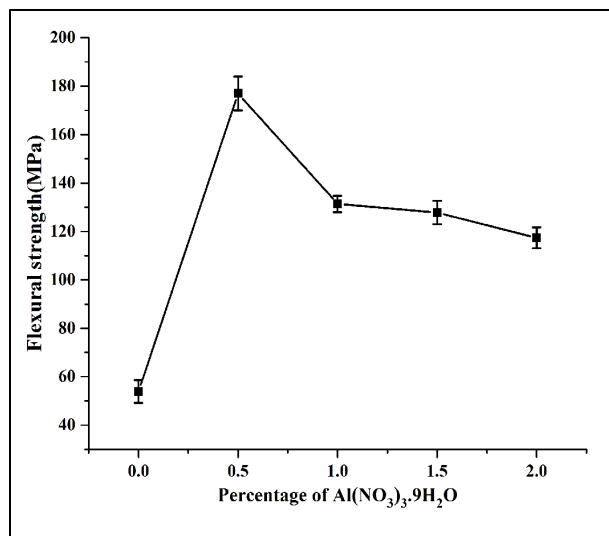


Fig.5.49 Flexural strength of 1600°C sintered sample.

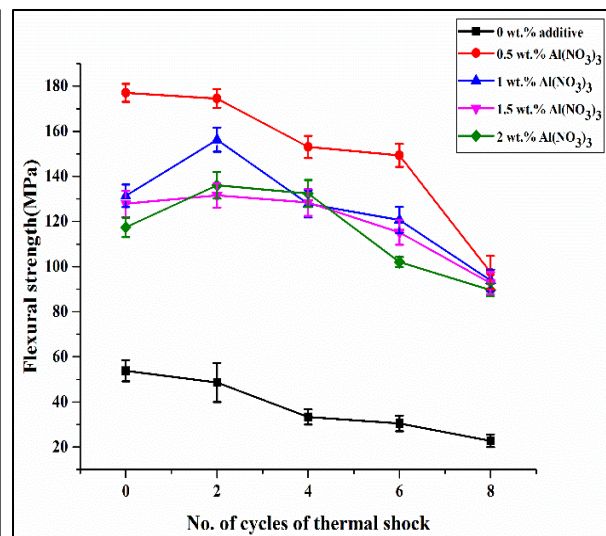


Fig.5.50 Strength retainment additive containing batch after thermal shock.

5.4.7 Thermal shock behavior study

Fig.5.50 represents the strength retainment of additive containing batch after thermal shock. The strength retainment capacity increased in both the additive containing batches in comparison to zero additive batch. In aluminium nitrate nonahydrate added batch, highest strength retainment was shown by 0.5 wt.% aluminium nitrate contained batch. The strength retainment did not vary much with a variation of additive percentage. The improvement in strength may be due to the presence of extra alumina as a secondary phase which has the ability to deflect cracks. [5.11, 5.12]

5.4.8 Conclusions

- Effect of addition of aluminum nitrate nonahydrate as a source of nascent, fine and reactive Al_2O_3 was studied on the development of solid-oxide reaction sintered stoichiometric magnesium aluminate spinel.
- Shrinkage, densification and dilatometry have shown that the additives enhance the spinel formation at low temperatures, up to 1400°C and negatively affects densification. But at higher temperatures they resulted in higher density values.
- Microstructural studies showed loose grain arrangements for all the compositions at lower temperatures but well compacted dense structure at high temperature with little inter and intragranular porosity. The presence of additive also aided in grain growth at a higher temperature.

- The strong beneficial effect was observed for the additions on flexural strength but strength fall marginally with increasing amount of the additives due to exaggerated grain growth. Phase analysis also showed the beneficial effect of the additive on spinel formation reaction.
- Retained strength after thermal shock was also found to be much higher for additive containing batches, and a slow and gradual decrease in retained strength values with increasing number of thermal shock cycles.

Section-V

5.5 Effect of magnesium nitrate hexahydrate addition

5.5.1 Linear shrinkage study

Fig. 5.51 represents linear shrinkage behavior of all the batches at different sintering temperatures. At 1200°C, all the additive containing batches showed expansion values, no shrinkage, due to spinel formation and nearly no sintering. The presence of magnesium nitrate hexahydrate was found to cause more expansion compared to that of the without additive composition. This higher expansion behavior in additive containing compositions is due to increased spinel formation at a lower temperature, which is associated with volume expansion. But after 1400°C, the shrinkage was more in additive containing batch compared to zero additive batch. This may be due to higher sintering in the additive batch. The shrinkage was found to increase upto 1 wt. % addition of magnesium nitrate hexahydrate. The addition of more than 1 wt.% led to slight fall in the shrinkage value.[5.11, 5.12]

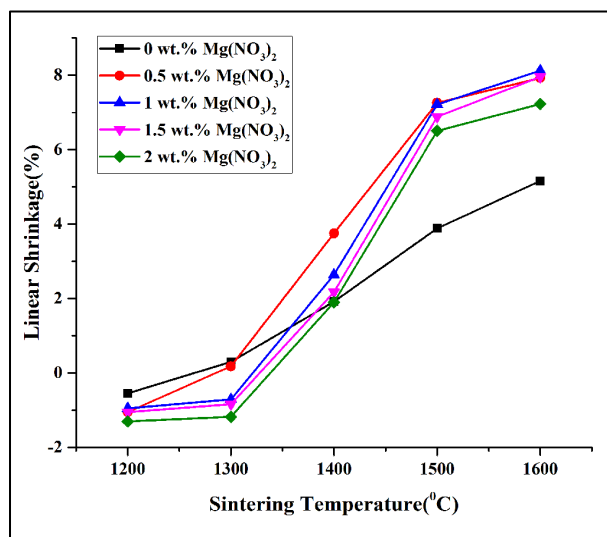


Fig.5.51 Plot of linear shrinkage vs. sintering temperature for magnesium nitrate hexahydrate batch.

5.5.2 Densification study

Fig. 5.52 represents the variation in bulk density values of all the batches against sintering temperatures. A general trend of increasing bulk density with increasing sintering temperature was common for all compositions due to greater sintering. The addition of magnesium nitrate hexahydrate was found to influence the densification behavior in almost all sintering temperatures.

At 1200^oC, additive containing batches showed lower bulk density value compared to non-additive batch. This is due to a greater extent of spinel formation reaction in additive containing compositions at a lower temperature compared to non-additive batch. The porosity values are also high for the additive containing ones at 1200^oC compared to without additive batch (Fig.5.53). With the increase in sintering temperature to 1400^oC an increase density value was observed due to greater sintering of the samples. The rate of increase of density value in additive containing samples was much higher compared to non-additive batch. When sintering temperature was further increased to 1600^oC the bulk density value of magnesium nitrate containing batch was higher than the zero additive. But the addition of more than 1 wt.% magnesium nitrate led to slight fall in density. This might be due to exaggerated grain growth occurred in the presence of extra magnesia formed from decomposition magnesium nitrate hexahydrate at a higher temperature. The apparent porosity results represented in fig 5.53 also supports the bulk density results[5.11, 5.12].

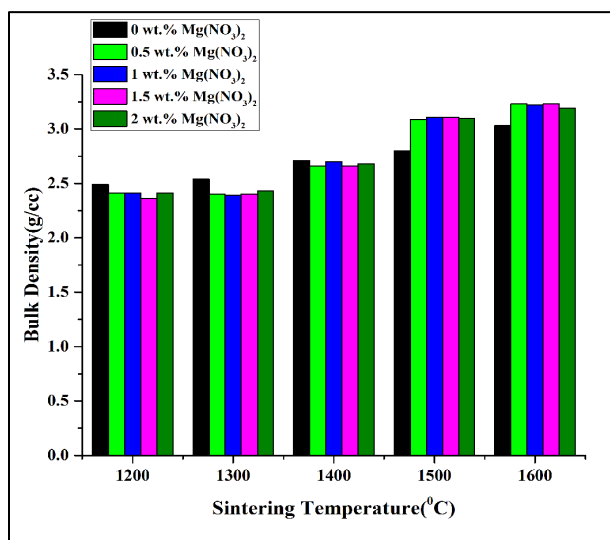


Fig.5.52 Plot of bulk density vs. sintering temperature for magnesium nitrate hexahydrate batch.

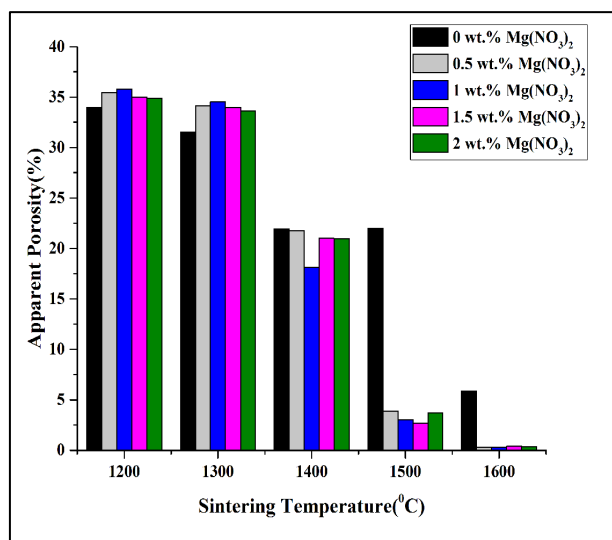


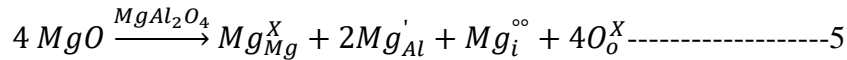
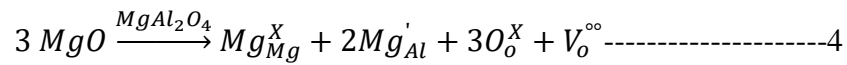
Fig.5.53 Plot of apparent porosity vs. sintering temperature for magnesium nitrate hexahydrate batch.

5.5.3 Dilatometry study

Fig.5.54 represents the dilatometry plot of all the compositions. It represents both the expansion due to spinel formation and shrinkage due to sintering at higher temperatures, which run parallel. At higher temperatures, the sintering process accelerates due to increased mass transfer and expansion behavior related with spinel formation is overtaken by shrinkage resulting from

sintering. Thus, a downward turn of the dilatometry curve is observed at the high temperatures. This feature is common in all the compositions with or without the additive. After the formation of the $MgAl_2O_4$ layer between MgO and Al_2O_3 , the spinellisation reaction depends on diffusion slow moving cations over this layer. The mobility of both cations and anions decides the sintering process. As oxygen diffusion is lower than the cations due to the larger ionic size of the oxygen ion, it acts as the rate determining step in the sintering process. The non-stoichiometry plays an important role during this step. The presence of nascent magnesium oxide from magnesium nitrate hexahydrate effects this step. The incorporation of the nascent magnesia in magnesium aluminate spinel can take place in the following way as suggested by Kim [5.10]-

MgO into $MgAl_2O_4$ –



Equations 4 and 5 indicate that the incorporation of extra MgO in $MgAl_2O_4$ will increase oxygen vacancy concentration.

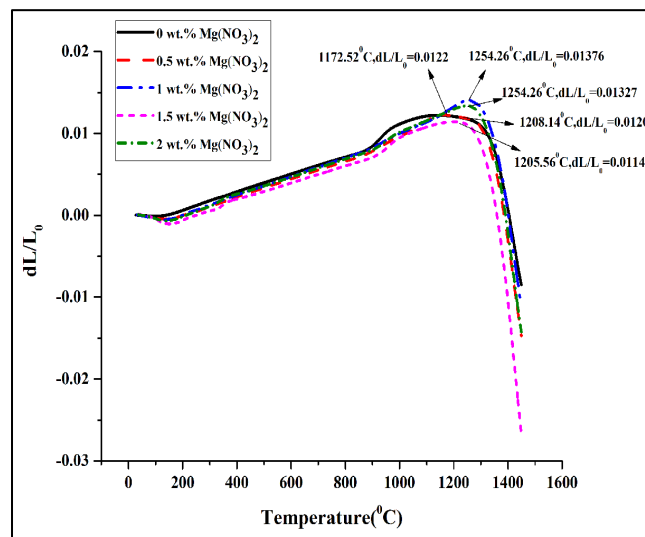


Fig.5.54 Dilatometry plots of magnesium nitrate hexahydrate containing batch.

Incorporation of fine reactive in-situ MgO produced through decomposition of magnesium nitrate at a higher temperature will increase in oxygen vacancy concentration, and so higher shrinkage due to sintering was observed in the dilatometry curve of magnesium nitrate containing batch.[5.11, 5.12]

5.5.4 Microstructure study

Microstructure study of the sintered fractured surfaces of all the batches was done using a field emission scanning electron microscope (FESEM) in back-scattered electron mode. Fig. 5.55(a) and (b) represent the microstructure of 1200°C and 1600°C sintered without additive batch respectively. A porous microstructure was observed at 1200°C, presence of spinel and reactant phases were clearly visible in the micrograph (Fig 5.55(a)). The 1600°C sintered sample showed the presence of only a single phase with a large number of intergranular pores along with small and large grains (Fig 5.55 (b)).

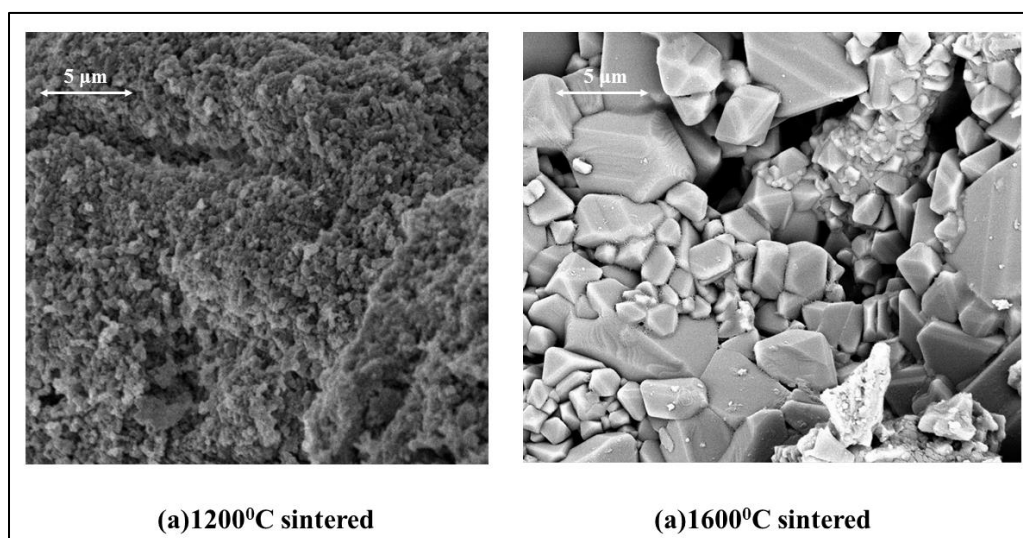


Fig.5.55 Microstructure of the without-additive batch.

The microstructure of 1200°C sintered magnesium nitrate hexahydrate containing batch shows a porous structure with a different kind of nano-size spinel template (needle-like) growing on large magnesia grains. (Fig.5.56 and 5.57) The intensity of the growth of these platelets was found to increase with an increase in the percentage of magnesium nitrate hexahydrate. The change in shape

of templates to needle-like structure might occur due to shrinkage caused by sintering of the platelets in the presence of magnesium nitrate hexahydrate[15]. As magnesium nitrate hexahydrate will produce fine nano size magnesia on decomposition, which on incorporation in these nano-sized spinel platelets increase in oxygen ion diffusion which will cause sintering of this platelets.[5.10-5.14, 5.16]

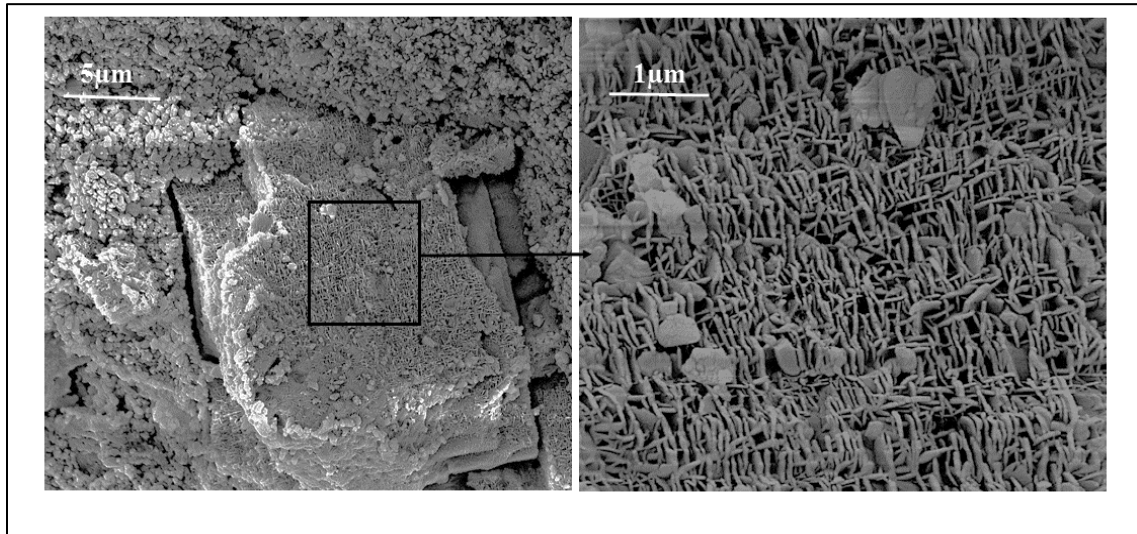


Fig.5.56 Microstructure of 1200⁰C sintered 1 wt.% magnesium nitrate hexahydrate containing sample.

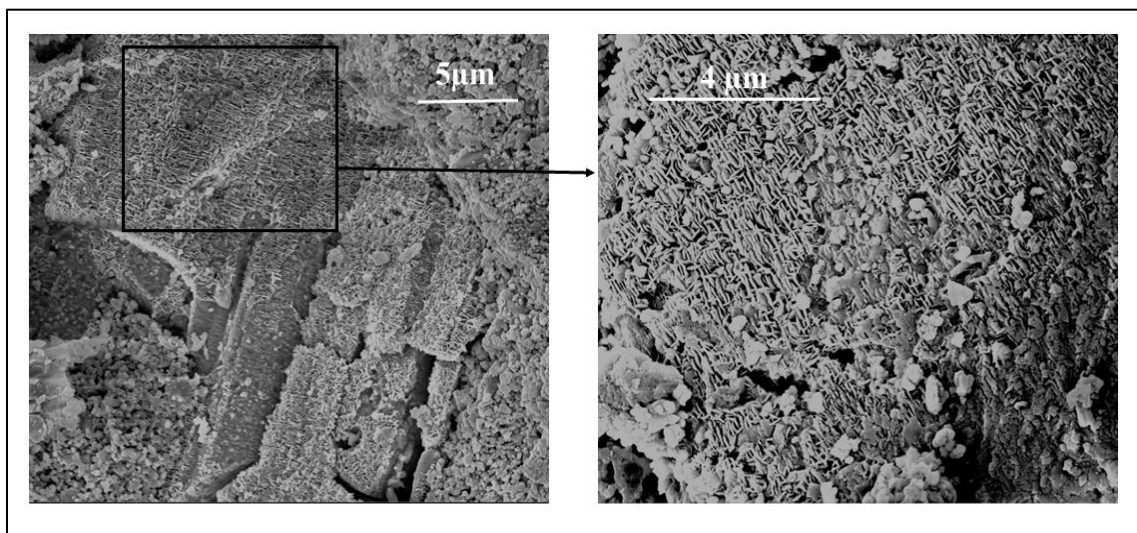


Fig.5.57 Microstructure of 1200⁰C sintered 2 wt.% magnesium nitrate hexahydrate containing sample.

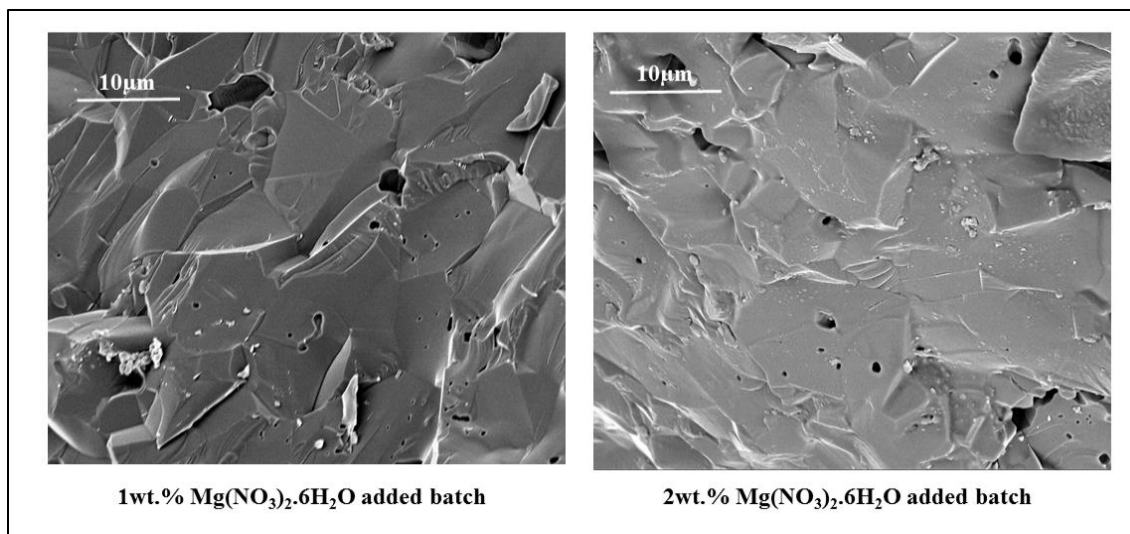


Fig.5.58 Microstructure of 1600⁰C sintered 1 and 2 wt.% magnesium nitrate hexahydrate containing batches.

The fig.5.58 represents microstructure of 1600⁰C sintered 1 wt.% and 2 wt.% magnesium nitrate hexahydrate containing batches. The addition of magnesium nitrate resulted in a dense microstructure. The increase in grain boundary mobility due to the presence of nascent magnesia lead to exaggerated grain growth. The pore size decreased with increased in magnesium nitrate addition. This might be due to a higher rate of sintering in magnesium nitrate containing batch.

5.5.5 Phase analysis study

The xrd pattern of both without additive and magnesium nitrate hexahydrate containing batches are shown in fig.5.59. The xrd patterns of 1200⁰C sintered samples are shown in fig 5.59(a). It shows spinel peaks along with reactant peak was conclude that spinel formation reaction started below 1200⁰C in both without additive and magnesium nitrate hexahydrate batch. However, the intensity of the spinel peak was quite high in magnesium nitrate hexahydrate batch in comparison to the without additive batch. This specifies that magnesium nitrate hexahydrate addition aided in spinel formation reaction. The reason for this may be due to the presence of nascent magnesia from magnesium nitrate hexahydrate which accelerated the spinellisation reaction.[5.11, 5.12]

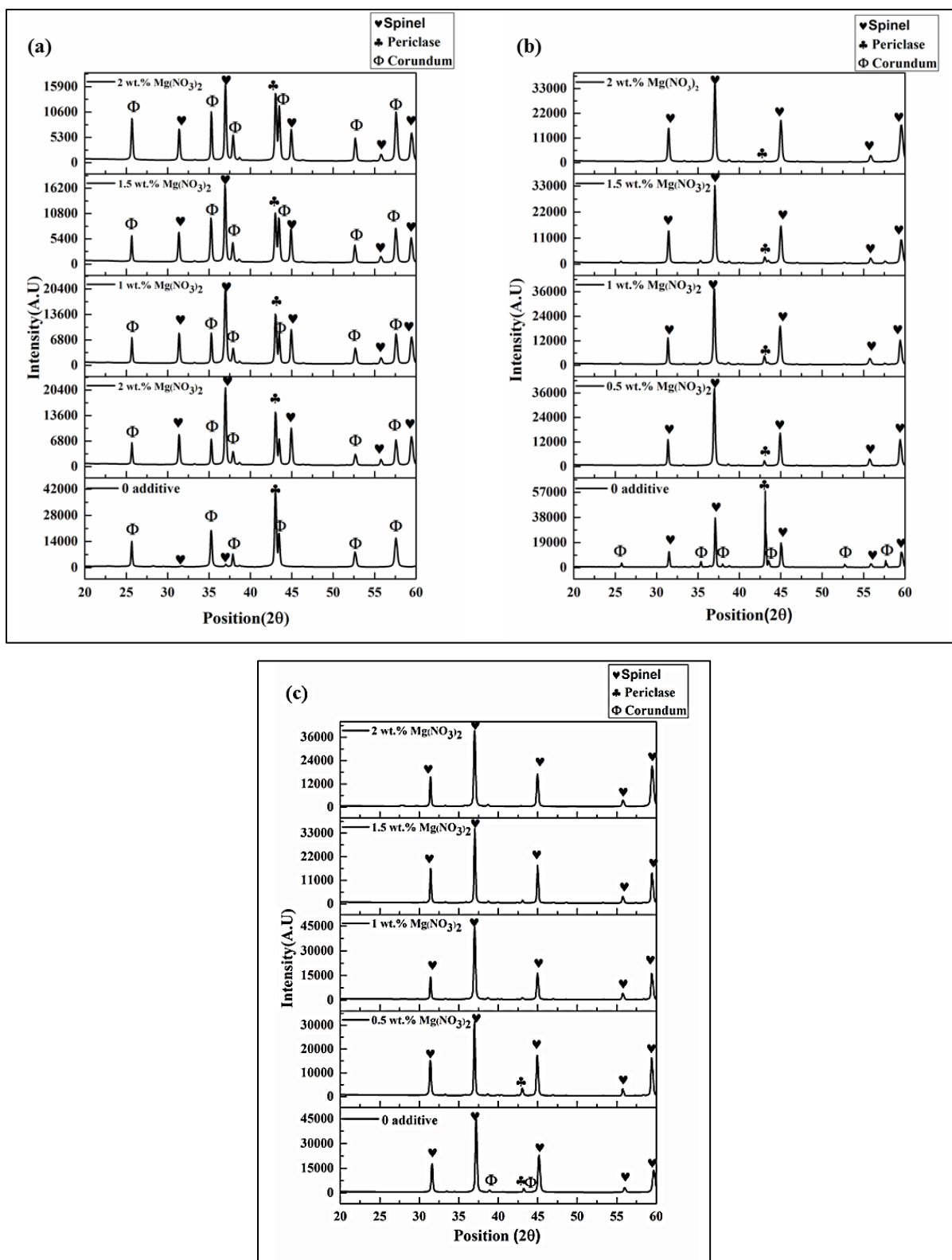


Fig.5.59 XRD of magnesium nitrate hexahydrate batch (a) 1200°C sintered (b) 1400°C sintered and (c) 1600°C sintered.

Fig 5.59(b) shows xrd pattern of 1400⁰C sintered compositions. A general trend of increase in spinel formation with an increase in sintering temperature was observed. However, the intensity of spinel peak in magnesium nitrate hexahydrate batches was high compared to zero batch. The intensity of the reactant peaks were quite small in the additive batch.

The xrd pattern of 1600⁰C sintered samples are depicted are in fig 5.59(c). Only spinel phase was observed in the additive batch which confirms the completion of spinellisation reaction. However, unreacted phases were observed in the without additive sample indicating incomplete spinellisation reaction. A small magnesia peak was observed in the 0.5 wt.% magnesia nitrate hexahydrate batch. But the addition of more amount of magnesia nitrate led to increasing in spinel amount which may be due to increasing the solubility of alumina in the presence of nascent magnesia from magnesium nitrate.[5.11, 5.12]

5.5.6 Flexural strength study

Fig 5.60 represents flexural strength plot of 1600⁰C sintered magnesium nitrate hexahydrate and zero batch. The flexural strength was found to increase drastically up to 152.06 MPa in 0.5 wt.% Mg(NO₃)₂.6H₂O addition. The increase in flexural strength in magnesium nitrate hexahydrate batch is mainly due to the occurrence of higher sintering which led to a compact microstructure with high strength. But as the amount addition of magnesium nitrate hexahydrate increased the strength started to decrease this is due to the increase in grain growth in the presence of an additional amount of nascent MgO from magnesium nitrate hexahydrate decomposition.[5.11, 5.12]

5.5.7 Thermal shock behavior study

The strength retainment of 1600⁰C sintered zero batch and magnesium nitrate hexahydrate batch after exposing to thermal shock cycle is plotted in the Fig.5.61. The strength retainment capacity of the magnesium nitrate hexahydrate batch was quite high in comparison with the zero batch. Even after 8 cycles of thermal shock the fall in strength was quite low. The increase in retainment of strength after thermal shock might be due to the presence of extra fine MgO from magnesium nitrate decomposition which might have hindered the growth of crack after thermal shock. The presence in closed pore inside the grains might be another probable cause of entrapment of crack which might have increased the strength retainment. [5.11, 5.12]

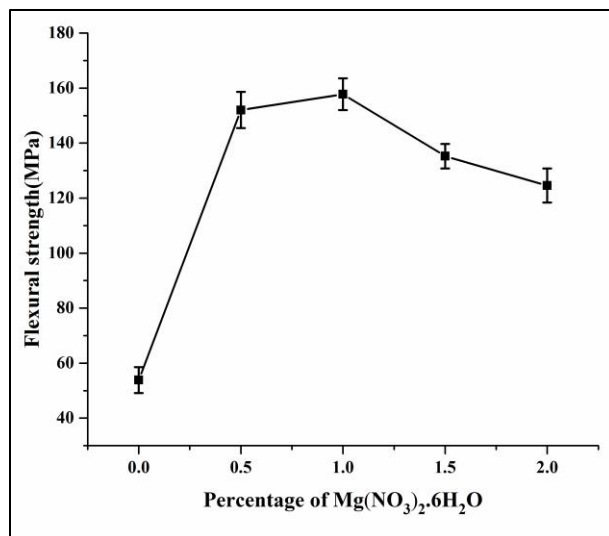


Fig 5.60 Flexural strength of 1600°C sintered magnesium nitrate hexahydrate

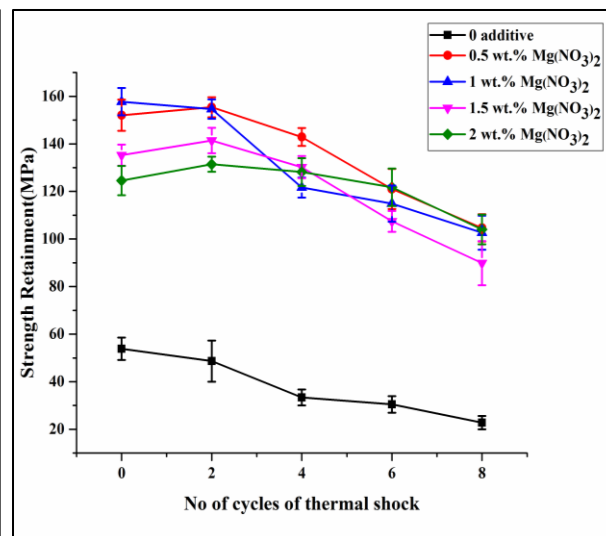


Fig.5.61 Strength retainment magnesium nitrate hexahydrate containing batch after thermal shock.

5.5.8 Conclusions

- The addition of nascent, fine and reactive MgO from magnesium nitrate hexahydrate precursor was studied on solid-oxide reaction sintered stoichiometric magnesium aluminate spinel.
- Shrinkage, densification, and dilatometry have shown enhanced spinel formation at low temperatures, up to 1400°C and negatively affected the densification. But higher density values were observed at higher temperatures.
- At lower temperatures, loose grain arrangements for all the compositions was observed in microstructure but at high-temperature microstructure became well compacted dense with minute inter and intragranular porosity. The presence of nascent MgO accelerated grain growth at a higher temperature.
- Flexural strength improved in the presence of the extra fine in-situ generated magnesia with but with increasing amount of the additives, a fall in strength was observed due to exaggerated grain growth. Phase analysis confirmed that addition of the additive had a beneficial effect on spinel formation reaction.
- Improved thermal shock was observed for additive containing batches, the retained strength decrease at a slow and gradual rate with increasing number of thermal shock cycles in additive contained batches.

Chapter 6

Summary of the work

- ❖ Dense magnesium aluminate spinel was successfully prepared from commercial grade materials using single step solid state sintering process.
- ❖ Planetary milling was found to have a profound effect on both spinel formation and densification process.
- ❖ The surface area of the starting materials was found to increase with milling
- ❖ The addition of additives like zinc oxide, zirconium dioxide was found to enhance the densification process.
- ❖ The addition of additives leads to a modified microstructure which leads to an increase in strength of the formed spinel.
- ❖ The dilatometry results showed that milling and additives addition helped in obtaining dense spinel by lowering the densification temperature.
- ❖ Phase analysis depicted that the spinel formation started below 1000⁰C in all the compositions.
- ❖ The presence of secondary phase due to additive was not detected in the additive batches.
- ❖ The thermal shock resistance improved in additive contained batch.
- ❖ The effect of in situ generated magnesia and alumina were also found to be beneficial in spinel formation and densification via solid state route.
- ❖ The presence of extra reactant phase from in situ generated magnesia and alumina from nitrate precursor additive had a beneficial effect on reaction stoichiometry.
- ❖ A significant grain growth was observed in the nitrate additives contained batches.
- ❖ The thermal shock resistance was also found to improve in the nitrate additive contained batches.

Chapter 7

Future work

- ❖ The commercial synthesis of dense magnesium aluminate spinel via single step solid state route is challenging owing to associated volume expansion due to spinel formation.
- ❖ The current work describes a reaction sintering technique to developed dense magnesium aluminate spinel by solid state reaction using milling and additives in stoichiometric composition.
- ❖ The future work may be done on the development of dense spinel using these additives in non-stoichiometric composition.
- ❖ The addition of more than one additive at a time can be studied.
- ❖ The incorporation of both milling and additive at a time can be studied.
- ❖ The development of transparent spinel from commercial grade materials using spark plasma sintering and hot isostatic pressing can be studied.
- ❖ The reaction kinetics of spinel formation and densification with milling and additive addition can also be done.

Bibliography

References (*Introduction*)

- [1.1] I. Ganesh, A review on magnesium aluminate (MgAl_2O_4) spinel: synthesis, processing and applications, *International Materials Reviews*, 58 (2013) 63-112.
- [1.2] R. Sarkar, *Refractory Applications of Magnesium Aluminate Spinel*, *Interceram Refractories*, 1 (2010) 11-15.
- [1.3] S. Zhang, W. Lee, *Spinel-containing refractories*, *Mechanical engineering-new york and basel-marcel dekker then crc press/taylor and francis*, 178 (2004) 215.
- [1.4] E. Ryshkewitch, D.W. Richerson, *Oxide ceramics*, United States: American Ceramic Society Inc., Westerville, OK. (1985).
- [1.5] C. Aksel, B. Rand, F.L. Riley, P.D. Warren, *Mechanical properties of magnesia-spinel composites*, *J Eur Ceram Soc*, 22 (2002) 745-754.
- [1.6] M. Rubat du Merac, H.J. Kleebe, M.M. Müller, I.E. Reimanis, *Fifty years of research and development coming to fruition; unraveling the complex interactions during processing of transparent magnesium aluminate (MgAl_2O_4) spinel*, *J Am Ceram Soc*, 96 (2013) 3341-3365.
- [1.7] W.H. Bragg, *The structure of the spinel group of crystals*, *Philosophical Magazine Series 6*, 30 (1915) 305-315.
- [1.8] S.H. Nishikawa, Ocirc, Ji, *Structure of Some Crystals of Spinel Group*, *Proceedings of the Tokyo Mathematico-Physical Society. 2nd Series*, 8(7) (1915) 199-209_1.
- [1.9] W.D. Kingery, H.K. Bowen, D.R. Uhlmann, *Introduction to ceramics*, John Wiley & Sons, New York (1960).
- [1.10] D.W. Budworth, *An Introduction to Ceramic Science: The Commonwealth and International Library: Materials Science and Technology (Ceramics Division)*, Elsevier, 2016.
- [1.11] G.L. Clark, A. Ally, A.E. Badger, *The lattice dimensions of spinels*, *American Journal of Science*, (1931) 539-546.
- [1.12] G.L. Clark, E.E. How, A.E. Badger, *Lattice dimensions of some solid solutions in the system MgO- Al_2O_3* , *J Am Ceram Soc*, 17 (1934) 7-8.
- [1.13] G. Hagg, G. Soderholm, *Crystal structure of Mg-Al spinels with Al_2O_3 surplus and γ - Al_2O_3* , *Zeitschrift für Physikalische Chemie*, B29 (1935) 88-94.

- [1.14] Y.M. Chiang, W.D. Kingery, Grain- Boundary Migration in Nonstoichiometric Solid Solutions of Magnesium Aluminate Spinel: I, Grain Growth Studies, *J Am Ceram Soc*, 72 (1989) 271-277.
- [1.15] T. Barth, E. Posnjak, Spinel structures: with and without variate atom equipoints, *Zeitschrift für Kristallographie-Crystalline Materials*, 82 (1932) 325-341.
- [1.16] G.A. Rankin, H.E. Merwin, The ternary system CaO-Al₂O₃-MgO, *Journal of the American Chemical Society*, 38 (1916) 568-588.
- [1.17] W.D. Callister, D.G. Rethwisch, *Materials science and engineering: an introduction*, Wiley New York (2007).
- [1.18] R. Sarkar, Phase diagrams in the MgO-Al₂O₃ system, *IIC Bulletin*, 20,Nos.(3-4) (2010) 36-37.
- [1.19] R. Sarkar, Phase diagrams in the MgO-Al₂O₃ system., *IIC Bulletin*, 20 (2010) 36-37.
- [1.20] R. Roy, E.F. Osborn, The system MgO-Al₂O₃-H₂O and influence of carbonate and nitrate ions on the phase equilibria, *American Journal of Science*, 251 (1953) 337-361.
- [1.21] A.M. Alper, R.N. McNally, P.H. Ribbe, R.C. Doman, The system MgO-MgAl₂O₄, *J Am Ceram Soc*, 45 (1962) 263-268.
- [1.22] S. Hirai, H. Murakami, H.G. Katayama, Effect of additives on the formation of MgAl₂O₄ from MgO and Al₂O₃, *J Jpn I Met*, 55 (1991) 166-171.
- [1.23] W.E. Lee, M. Rainforth, *Ceramic microstructures: property control by processing*, Springer Science & Business Media (1994).
- [1.24] C.J. Brinker, G.W. Scherer, *Sol-gel science: the physics and chemistry of sol-gel processing*, Academic press 2013.
- [1.25] K. Fujiyoshi, S. Ishida, N. Takeuchi, H. Nanri, Synthesis of whisker-like MgAl₂O₄ spinel from gibbsite and magnesium acetate, *Refractories(Tokyo)*. 53 (2001) 506-515.
- [1.26] W. Kim, F. Saito, Effect of grinding on synthesis of MgAl₂O₄ spinel from a powder mixture of Mg(OH)₂ and Al(OH)₃, *Powder technology*, 113 (2000) 109-113.
- [1.27] J. Kohl, S. Nakhil, N. Ferro, P. Bottke, M. Wilkening, T. Bredow, P. Heitjans, M. Lerch, Low-temperature synthesis, characterization, and stability of spinel-type Li₂NiF₄ and solid-solutions Li₂Ni_{1-x}CO_xF₄, *Z Anorg Allg Chem*, 639 (2013) 326-333.
- [1.28] I. Ganesh, S. Bhattacharjee, B.P. Saha, R. Johnson, Y.R. Mahajan, A new sintering aid for magnesium aluminate spinel, *Ceram Int*, 27 (2001) 773-779.

- [1.29] R. Dal Maschio, B. Fabbri, C. Fiori, Industrial applications of refractories containing magnesium aluminate spinel, *Ind. Ceram.(Italy)*, 8 (1988) 121-126.
- [1.30] P. Bartha, The Properties of Periclase Spinel Brick and its Service Stresses in Rotary Cement Kilns, *Interceram* 33,(Spec. Issue), 15, (1986).
- [1.31] S. Jörg, G. Gelbmann, R. Krischanitz, P. Fritsch, ANKRAL QF—A New Brick to Combat Tyre Stresses, *RHI Bulletin*, (2010) 8-12.
- [1.32] G. Gelbmann, R. Krischanitz, S. Jörg, Hybrid spinel technology provides performance advances for basic cement rotary kiln bricks, *Young*, 400 (2013) 200.
- [1.33] T. Fumikazu, H. Toru, Aptitude of spinel bricks for rotary kiln (cements) and results of its use, *Taikabutsu* 92 (1980) 479-486.
- [1.34] C. Parr, L. Bin, B. Valdelièvre, C. Wöhrmeyer, B. Touzo, The advantages of calcium aluminate cement containing castables for steel ladle applications, *Proceedings of ALAFAR*, 2004 (2004) 10-15.
- [1.35] R.P. Racher, R.W. McConnell, A. Buhr, Magnesium aluminate spinel raw materials for high performance refractories for steel ladles, In *Proceedings Conference of Metallurgists of Canadian Institute of Mining, Metallurgy, and Petroleum* 2004 Aug 22.
- [1.36] Y. Sadatomi, N. Enomoto, J. Hojo, Reaction behavior of slag and spinel in steel ladle castables, *J Ceram Soc Jpn*, 119 (2011) 595-600.
- [1.37] P. Kettner, G. Christof, MA-spinel brick in glass furnace regenerators, *RADEX RUNDSCH. Radex Rundsch.*(1), 3, 1986, (1986).
- [1.38] M. Olbrich, F. Rostami, Sodium sulfate attack on magnesium aluminate spinel brick, *Glastech.Ber.*, 63 (1990) 204-209.
- [1.39] M. Dunkl, D. Schlacht, G. Boymanns, F. Gebhardt, Rebonded Spinel for Use in Oxy-Fuel Superstructure Applications, *A Collection of Papers Presented at the 60th Conference on Glass Problems: Ceramic Engineering and Science Proceedings*, John Wiley & Sons, Inc.2000, pp. 221-236.
- [1.40] A.S. Sattarova, G.I. Antonov, Magnesite—Spinel refractories after service in converters for copper production, *Refractories and Industrial Ceramics*, 20 (1979) 304-307.
- [1.41] C.L. Macey, Evaluation of magnesite-spinel refractories for mineral processing kilns, *Industrial Heating*, 59 (1992) 28-29.

[1.42] C.A. Arenberg, C.W. Boquist, O.R. Magoteaux, Refractories for Uranium Reduction, American Ceramic Society Bulletin (US), 40 (1961).

[1.43] S. Angappan, L. John Berchmans, C.O. Augustin, Sintering behaviour of $MgAl_2O_4$ - A prospective anode material, Mater Lett, 58 (2004) 2283-2289.

[1.44] T. Yamamura, Y. Hamazaki, T. Kaneshige, T. Toyoda, M. Nishi, H. Kato, Alumina-spinel castable refractories for steel teeming ladle, Taikabutsu Overseas, 12 (1992) 21-27.

References (*Literature review*)

[2.1] S.K. Mohan, R. Sarkar, Study on the formation and densification of magnesium aluminate spinel using commercial grade reactants: effect of planetary milling, Journal of Australian Ceramic Society, 52 (2016) 138-147.

[2.2] S.K. Mohan, R. Sarkar, Effect of ZrO_2 addition on $MgAl_2O_4$ spinel from commercial grade oxide reactants, Ceram Int, 42 (2016) 10355–10365.

[2.3] Z. Nakagawa, N. Enomoto, Y. I-S, K. Asano, Effect of corundum/periclase sizes on expansion behaviour during synthesis of spinel, In UNITECR'95 Congress. Proc. Unified Int. Tech. Conf. on Refractories 1995 Nov (Vol. 4), 379-386.

[2.4] M.A.L. Braulio, M. Rigaud, A. Buhr, C. Parr, V.C. Pandolfelli, Spinel- containing alumina-based refractory castables, Ceram Int, 37 (2011) 1705-1724.

[2.5] M. Andrianov, Investigation of solid-phase synthesis of alumina-magnesia spinel by measuring volume changes in firing ceramics, Trudy Instituta--Moskovskii Khimiko-Tekhnologicheskii Institut imeni D. I. Mendeleeva, (1975) 126-130.

[2.6] J.M.F. Colinas, C.O. Areán, Kinetics of solid-state spinel formation: effect of cation coordination preference, Journal of Solid State Chemistry, 109 (1994) 43-46.

[2.7] N.A.L. Mansour, Effect of magnesia and alumina characteristics on the formation of spinel, Interceram, 27 (1978) 49.

[2.8] A.D. Mazzoni, M.A. Sainz, A. Caballero, E.F. Aglietti, Formation and sintering of spinels ($MgAl_2O_4$) in reducing atmospheres, Materials chemistry and physics, 78 (2003) 30-37.

[2.9] W.D. Kingery, H.K. Bowen, D.R. Uhlmann, Introduction to ceramics, John Wiley & Sons, New York (1960).

[2.10] L. Navias, Preparation and properties of spinel made by vapor transport and diffusion in the system $MgO-Al_2O_3$, J Am Ceram Soc, 44 (1961) 434-446.

- [2.11] R.E. Carter, Mechanism of solid-state reaction between magnesium oxide and aluminum oxide and between magnesium oxide and ferric oxide, *J Am Ceram Soc*, 44 (1961) 116-120.
- [2.12] R.C. Rossi, R.M. Fulrath, Epitaxial growth of spinel by reaction in the solid state, *J Am Ceram Soc*, 46 (1963) 145-149.
- [2.13] G. Yamaguchi, K. Shirasuka, M. Munekata, Some aspects of solid state reaction of spinel formation in the system MgO-Al₂O₃, *Journal of the Ceramic Association, Japan*, 79 (1971) 64-69.
- [2.14] G. Yamaguchi, M. Nakano, K. Saito, Role of oxygen in spinel formation from MgO and Al₂O₃, *Yogyo-Kyokai-Shi*, 79 (1971) 92-96.
- [2.15] W.P. Whitney, V.S. Stubican, Interdiffusion studies in the system MgO-Al₂O₃, *Journal of Physics and Chemistry of Solids*, 32 (1971) 305-312.
- [2.16] S.T. Murphy, B.P. Uberuaga, J.B. Ball, A.R. Cleave, K.E. Sickafus, R. Smith, R.W. Grimes, Cation diffusion in magnesium aluminate spinel, *Solid State Ionics*, 180 (2009) 1-8.
- [2.17] H.S. Tripathi, A. Ghosh, Spinelisation and properties of Al₂O₃-MgAl₂O₄-C refractory: Effect of MgO and Al₂O₃ reactants, *Ceram Int*, 36 (2010) 1189-1192.
- [2.18] J. Szczerba, Z. Pędzich, M. Nikiel, D. Kapuścińska, Influence of raw materials morphology on properties of magnesia-spinel refractories, *J Eur Ceram Soc*, 27 (2007) 1683-1689.
- [2.19] Z. Zhang, N. Li, Effect of polymorphism of Al₂O₃ on the synthesis of magnesium aluminate spinel, *Ceram Int*, 31 (2005) 583-589.
- [2.20] C. Ghosh, A. Ghosh, M.K. Haldar, Studies on densification, mechanical, micro-structural and structure-properties relationship of magnesium aluminate spinel refractory aggregates prepared from Indian magnesite, *Materials Characterization*, 99 (2015) 84-91.
- [2.21] R. Sarkar, S. Sahoo, Effect of raw materials on formation and densification of magnesium aluminate spinel, *Ceram Int*, 40 (2014) 16719-16725.
- [2.22] L.B. Kong, J. Ma, H. Huang, MgAl₂O₄ spinel phase derived from oxide mixture activated by a high-energy ball milling process, *Mater Lett*, 56 (2002) 238-243.
- [2.23] P. Orosco, L. Barbosa, M. del Carmen Ruiz, Synthesis of magnesium aluminate spinel by periclase and alumina chlorination, *Mater Res Bull*, 59 (2014) 337-340.
- [2.24] F. Tavangarian, G. Li, Mechanical activation assisted synthesis of nanostructure MgAl₂O₄ from gibbsite and lansfordite, *Powder Technology*, 267 (2014) 333-338.

- [2.25] H.S. Tripathi, B. Mukherjee, S. Das, M.K. Haldar, S.K. Das, A. Ghosh, Synthesis and densification of magnesium aluminate spinel: effect of MgO reactivity, *Ceram Int*, 29 (2003) 915-918.
- [2.26] C.J. Ting, H.Y. Lu, Defect reactions and the controlling mechanism in the sintering of magnesium aluminate spinel, *J Am Ceram Soc*, 82 (1999) 841-848.
- [2.27] R. Sarkar, S.K. Das, G. Banerjee, Effect of attritor milling on the densification of magnesium aluminate spinel, *Ceram Int*, 25 (1999) 485-489.
- [2.28] E. Kostić, I. Momčilović, Reaction sintered $MgAl_2O_4$ bodies from different batch compositions, *Ceramurgia International*, 3 (1977) 57-60.
- [2.29] W. Kim, F. Saito, Effect of grinding on synthesis of $MgAl_2O_4$ spinel from a powder mixture of $Mg(OH)_2$ and $Al(OH)_3$, *Powder technology*, 113 (2000) 109-113.
- [2.30] E. Mustafa, N. Khalil, A. Gamal, Sintering and microstructure of spinel–forsterite bodies, *Ceram Int*, 28 (2002) 663-667.
- [2.31] I. Ganesh, S.M. Olhero, A.H. Rebelo, J.M.F. Ferreira, Formation and densification behavior of $MgAl_2O_4$ spinel: The influence of processing parameters, *J Am Ceram Soc*, 91 (2008) 1905-1911.
- [2.32] Z. Zhihui, L.I. Nan, Influence of mechanical activation of Al_2O_3 on synthesis of magnesium aluminate spinel, *Sci Sinter*, 36 (2004) 73-79.
- [2.33] F. Tavangarian, R. Emadi, Synthesis and characterization of pure nanocrystalline magnesium aluminate spinel powder, *J Alloy Compd*, 489 (2010) 600-604.
- [2.34] P.W.D. Mitchell, Chemical Method for Preparing $MgAl_2O_4$ Spinnel, *J Am Ceram Soc*, 55 (1972) 484-484.
- [2.35] S.G. Mukherjee, B.N. Samaddar, Spinel formation from co-precipitated hydroxides of aluminium and magnesium, *T Indian Ceram Soc*, 25 (1966) 33-34.
- [2.36] R.J. Bratton, Coprecipitates yielding $MgAl_2O_4$ spinel powders, *Am Ceram Soc Bull*, 48 (1969) 759.
- [2.37] G. Gusmano, P. Nunziante, E. Traversa, G. Chiozzini, The mechanism of $MgAl_2O_4$ spinel formation from the thermal decomposition of coprecipitated hydroxides, *J Eur Ceram Soc*, 7 (1991) 31-39.
- [2.38] N. Burtan, S. Vlaicu, Spinel powders through modified coprecipitation, *Keramische Zeitschrift*, 46 (1994) 85-88.

- [2.39] J. Katanić-Popović, N. Miljević, S. Zec, Spinel formation from coprecipitated gel, *Ceram Int*, 17 (1991) 49-52.
- [2.40] M. Wang, M. Muhammed, Synthesis and characterisation of magnesium aluminate spinel ceramic precursor, *Materials Science Forum*, 235-8 (1997) 241-248.
- [2.41] D.R. Messier, G.E. Gazza, Synthesis of $MgAl_2O_4$ and $Y_3Al_5O_{12}$ by thermal-decomposition of hydrated nitrate mixtures, *Am Ceram Soc Bull*, 51 (1972) 692.
- [2.42] N.P. Tomilov, E.T. Devyatkina, Synthesis of $MgAl_2O_4$ from coprecipitated hydroxides, *Inorg. Mater.*, 26 (1990) 2200-2204.
- [2.43] T. Hattori, J.-i. Mohri, Formation Processes of Spinel ($MgAl_2O_4$) by a Thermal Decomposition of a Freeze-Dried Sulfate, *Journal of the Ceramic Association, Japan*, 89 (1981) 287-291.
- [2.44] N. Zenbee, H. Kenya, S. Mikio, Characterisation and sinterability of Mg-Al spinel by thermal decomposition of freeze dried sulfate, *Yogyo Kyokai Shi*, 89 (1982) 287-291.
- [2.45] P.H. Chae, O.K. Dong, Reaction process of the formation of Mg-Al spinel by a thermal decomposition of mixed sulfate hydrate, *Yoop Hikoechi*, 23 (1986) 71-75.
- [2.46] L.M. Healey, C.B. Ponton, P.M. Marquis, Hydrothermal processing of $MgAl_2O_4$ spinel based ceramics, *InThird ECers. Proc. 3 rd European Ceramic Society Conf. 1993*, Vol. 1, pp. 207-212.
- [2.47] M.F. Zawrah, H. Hamaad, S. Meky, Synthesis and characterization of nano $MgAl_2O_4$ spinel by the co-precipitated method, *Ceram Int*, 33 (2007) 969-978.
- [2.48] N.M. Khalil, M.B. Hassan, E.M.M. Ewais, F.A. Saleh, Sintering, mechanical and refractory properties of MA spinel prepared via co-precipitation and sol-gel techniques, *J Alloy Compd*, 496 (2010) 600-607.
- [2.49] A. Wajler, H. Tomaszewski, E. Drożdż-Cieśla, H. Węglarz, Z. Kaszukur, Study of magnesium aluminate spinel formation from carbonate precursors, *J Eur Ceram Soc*, 28 (2008) 2495-2500.
- [2.50] G. Ye, G. Oprea, T. Troczynski, Synthesis of $MgAl_2O_4$ spinel powder by combination of sol-gel and precipitation processes, *J Am Ceram Soc*, 88 (2005) 3241-3244.
- [2.51] Z. Mosayebi, M. Rezaei, N. Hadian, F.Z. Kordshuli, F. Meshkani, Low temperature synthesis of nanocrystalline magnesium aluminate with high surface area by surfactant assisted precipitation method: Effect of preparation conditions, *Mater Res Bull*, 47 (2012) 2154-2160.

- [2.52] E.N. Alvar, M. Rezaei, H.N. Alvar, Synthesis of mesoporous nanocrystalline MgAl_2O_4 spinel via surfactant assisted precipitation route, *Powder Technology*, 198 (2010) 275-278.
- [2.53] J.-G. Li, T. Ikegami, J.-H. Lee, T. Mori, Y. Yajima, A wet-chemical process yielding reactive magnesium aluminate spinel (MgAl_2O_4) powder, *Ceram Int*, 27 (2001) 481-489.
- [2.54] L.B. Carole D, C.A. Natalie, G.P. Martins, Sol-gel synthesis of MgAl_2O_4 spinel powders for optical ceramics, *Ceramics Transactions*, 1A (1988) 211-217.
- [2.55] D. Lepkova, A. Batarjav, B. Samuneva, Y. Ivanova, L. Georgieva, Preparation and properties of ceramics from magnesium spinel by sol-gel technology, *Journal of materials science*, 26 (1991) 4861-4864.
- [2.56] C.T. Wang, L.S. Lin, S.J. Yang, Preparation of MgAl_2O_4 Spinel Powders via Freeze-Drying of Alkoxide Precursors, *J Am Ceram Soc*, 75 (1992) 2240-2243.
- [2.57] O. Varnier, N. Hovnanian, A. Larbot, P. Bergez, L. Cot, J. Charpin, Sol-gel synthesis of magnesium aluminum spinel from a heterometallic alkoxide, *Mater Res Bull*, 29 (1994) 479-488.
- [2.58] Y. Kadogawa, N. Suzuki, Effect of alkali chlorides on the formation of MgAl_2O_4 by the sol-gel method, *Chemistry Express*, 5 (1990) 885-888.
- [2.59] V.K. Singh, R.K. Sinha, Low temperature synthesis of spinel (MgAl_2O_4), *Mater Lett*, 31 (1997) 281-285.
- [2.60] K.F. Waldner, R.M. Laine, S. Dhumrongvaraporn, S. Tayaniphan, R. Narayanan, Synthesis of a double alkoxide precursor to spinel (MgAl_2O_4) directly from $\text{Al}(\text{OH})_3$, MgO , and triethanolamine and its pyrolytic transformation to spinel, *Chem Mater*, 8 (1996) 2850-2857.
- [2.61] A. Saberi, F. Golestani-Fard, M. Willert-Porada, Z. Negahdari, C. Liebscher, B. Gossler, A novel approach to synthesis of nanosize MgAl_2O_4 spinel powder through sol-gel citrate technique and subsequent heat treatment, *Ceram Int*, 35 (2009) 933-937.
- [2.62] S. Sanjabi, A. Obeydavi, Synthesis and characterization of nanocrystalline MgAl_2O_4 spinel via modified sol-gel method, *J Alloy Compd*, 645 (2015) 535-540.
- [2.63] L.-Z. Pei, W.-Y. Yin, J.-F. Wang, J. Chen, C.-G. Fan, Q.-F. Zhang, Low temperature synthesis of magnesium oxide and spinel powders by a sol-gel process, *Materials Research*, 13 (2010) 339-343.
- [2.64] M.Y. Nassar, I.S. Ahmed, I. Samir, A novel synthetic route for magnesium aluminate (MgAl_2O_4) nanoparticles using sol-gel auto combustion method and their photocatalytic

properties, *Spectrochimica Acta Part A: Molecular and Biomolecular Spectroscopy*, 131 (2014) 329-334.

[2.65] Y. Suyama, A. Kato, Characterization and sintering of Mg-Al spinel prepared by spray-pyrolysis technique, *Ceram Int*, 8 (1982) 17-21.

[2.66] C.R. Bickmore, K.F. Waldner, D.R. Treadwell, R.M. Laine, Ultrafine spinel powders by flame spray pyrolysis of a magnesium aluminum double alkoxide, *J Am Ceram Soc*, 79 (1996) 1419-1423.

[2.67] Y. Chan Kang, J. Su Choi, S. Bin Park, Preparation of high surface area MgAl₂O₄ particles from colloidal solution using filter expansion aerosol generator, *J Eur Ceram Soc*, 18 (1998) 641-646.

[2.68] C. Pommier, K. Chhor, J.F. Bocquet, M. Barj, Reactions in supercritical fluids, a new route for oxide ceramic powder elaboration, synthesis of the spinel MgAl₂O₄, *Mater Res Bull*, 25 (1990) 213-221.

[2.69] U. Kanerva, T. Suhonen, J. Lagerbom, E. Levänen, Evaluation of crushing strength of spray-dried MgAl₂O₄ granule beds, *Ceram Int*, 41 (2015) 8494-8500.

[2.70] J.F. Pasquier, S. Komarneni, R. Roy, Synthesis of MgAl₂O₄ spinel: seeding effects on formation temperature, *Journal of materials science*, 26 (1991) 3797-3802.

[2.71] A. Ghosh, R. Sarkar, B. Mukherjee, S.K. Das, Effect of spinel content on the properties of magnesia-spinel composite refractory, *J Eur Ceram Soc*, 24 (2004) 2079-2085.

[2.72] T.H. Choi, B.S. Jun, Preparation and properties of MgO-Al₂O₃ spinel by SHS, *Journal of Korean Ceramic Society*, 33 (1996) 235-241.

[2.73] L. Rooi Ping, A.-M. Azad, T. Wan Dung, Magnesium aluminate (MgAl₂O₄) spinel produced via self-heat-sustained (SHS) technique, *Mater Res Bull*, 36 (2001) 1417-1430.

[2.74] Y. Tong, S. Zhao, L. Ma, W. Zhao, W. Song, H. Yang, Facile synthesis and crystal growth dynamics study of MgAl₂O₄ nanocrystals, *Mater Res Bull*, 48 (2013) 4834-4838.

[2.75] I. Gómez, M. Hernández, J. Aguilar, M. Hinojosa, Comparative study of microwave and conventional processing of MgAl₂O₄-based materials, *Ceram Int*, 30 (2004) 893-900.

[2.76] I. Ganesh, G.J. Reddy, G. Sundararajan, S.M. Olhero, P.M.C. Torres, J.M.F. Ferreira, Influence of processing route on microstructure and mechanical properties of MgAl₂O₄ spinel, *Ceram Int*, 36 (2010) 473-482.

- [2.77] S.K. Behera, P. Barpanda, S.K. Pratihari, S. Bhattacharyya, Synthesis of magnesium–aluminium spinel from autoignition of citrate–nitrate gel, *Mater Lett*, 58 (2004) 1451-1455.
- [2.78] R. Fazli, M. Fazli, Y. Safaei-Naeini, F. Golestani-fard, The effects of processing parameters on formation of nano-spinel (MgAl_2O_4) from LiCl molten salt, *Ceram Int*, 39 (2013) 6265-6270.
- [2.79] P.V.M. Kutty, S. Dasgupta, Low temperature synthesis of nanocrystalline magnesium aluminate spinel by a soft chemical method, *Ceram Int*, 39 (2013) 7891-7894.
- [2.80] J.T. Bailey, R. Russell, Sintered spinel ceramics, *Am Ceram Soc Bull*, 47 (1968) 1025.
- [2.81] M.J. Ruthner, Preparation and sintering characteristics of MgO, MgO-Cr₂O₃ and MgO-Al₂O₃, pp. 3-8.
- [2.82] O. Chisato, N. Junichi, T. Yoichi, Sintering and characterisation of spinel clinkers, *Taikabutsu*, 33 (1981) 121-127.
- [2.83] T.V. Dunaitseva, L.B. Romanovskii, E.G. Potap, Y.I. Savchenko, V.A. Perepelitsyn, N.F. Seliverstov, G.G. Galimov, Sintering of synthesized magnesia spinels and the systems based on them, *Refractories*, 31 (1990) 615-618.
- [2.84] M.A. Serry, M.A. Mandour, W. Weisweiler, Phase equilibria, microstructure and properties of some MgO-Al₂O₃ refractories, *Brit Ceram T*, 92 (1993) 227-232.
- [2.85] K. Kitagawa, I. Komaki, K. Matsukawa, K. Fueki, Surface mass transport study on Al₂O₃ and MgAl₂O₄ spinel by multiple scratch smoothening method, *Yogyo Kyokai Shi*, 88 (1980) 92-99.
- [2.86] R.J. Bratton, Initial sintering kinetics of MgAl₂O₄, *J Am Ceram Soc*, 52 (1969) 417-419.
- [2.87] R.J. Bratton, Sintering and Grain-Growth Kinetics of MgAl₂O₄, *J Am Ceram Soc*, 54 (1971) 141-143.
- [2.88] D.R. Johnson, H. Palmour, Densification kinetics of spinel sintered under rate control, *Amer ceramic soc 735 ceramic place, po box 6136, westerville, oh 43081-6136*, pp. 377.
- [2.89] J. Petkovic, E. Kostic, S. Malcic, Effect of MgO powder activity on the synthesis and sintering of MgAl₂O₄, *Ceramurgia*, 5 (1975) 175-178.
- [2.90] T. Kanai, Z. Nakagawa, Y. Ohya, M. Hasegawa, K. Hamano, Effect of composition on sintering and bending strength of spinel ceramics, *Rep. Res. Lab. Eng. Mater. Tokyo Inst. Technol. No. 13*, 75 (1988).
- [2.91] I. Teoreanu, N. Ciocea, Magnesia-alumina spinel for refractories, *Interceram*, 36 (1987) 19-21.

- [2.92] R. Sarkar, K. Das, S.K. Das, G. Banerjee, Development of magnesium aluminate spinel by solid oxide reaction, 5th Unified International Technical Conference on Refractories - a Worldwide Technology (UNITECR 97), New Orleans, LA, USA NOV 04-07, 1997.
- [2.93] P.P. Budnikov, F.Y. Kharitonov, E.I. Medvedovskaya, F.G. Kerbe, V.S. Shakhin, Sintering and recrystallization of high-purity magnesia-alumina spinel during hot pressing, *Refractories and industrial ceramics*, 11 (1970) 367-370.
- [2.94] J.G. Grabmaier, B.C. Watson, Czochralski Growth of Magnesium-Aluminum Spinel, *J Am Ceram Soc*, 51 (1968) 355-356.
- [2.95] Y.M. Chiang, W.D. Kingery, Grain-Boundary Migration in Nonstoichiometric Solid Solutions of Magnesium Aluminate Spinel: I, Grain Growth Studies, *J Am Ceram Soc*, 72 (1989) 271-277.
- [2.96] J.T. Bailey, R.J.R. Russell, Preparation and properties of dense spinel ceramics in the $MgAl_2O_4-Al_2O_3$ system, *Trans brit ceram soc*, 68 (1969) 159-164.
- [2.97] J.T. Bailey, R. Russell, Magnesia-rich $MgAl_2O_4$ spinel ceramics, *Am Ceram Soc Bull*, 50 (1971) 493.
- [2.98] E. Proverbio, M. Yasuoka, K. Hirao, S. Kanzaki, Microstructure development during sintering in polycrystalline $Mg_{0.5}Al_2O_3$ spinel, *Nippon seramikusu kyokai gakujutsu ronbunshi*, 101 (1993) 256-262.
- [2.99] L.M. Atlas, Effect of some lithium compounds on sintering of MgO, *J Am Ceram Soc*, 40 (1957) 196-199.
- [2.100] T. Noda, S. Hasegawa, Effect of addition of salt vapour on the synthesis and crystal growth of spinel, *J. Soc. Chem. Indus., Jpn*, 43 (1940) 169-172.
- [2.101] R. Helmut, Sintering characteristics of oxide ceramic materials based on $MgO-Al_2O_3$, *Keram Rundschau*, 91 (1967) 405-410.
- [2.102] E. Kostić, S. Bošković, Š. Kiš, Influence of fluorine ion on the spinel synthesis, *J Mater Sci Lett*, 1 (1982) 507-510.
- [2.103] W.T. Bakker, J.G. Lindsay, Reactive magnesia spinel, preparation and properties, *AMER CERAM SOC BULL*, NOV. 1967, 1094-1097, (1967).
- [2.104] R. Sarkar, S. Mukherjee, A. Ghosh, Effect of AlF_3 on spinel formation, *Ind Ceram*, 28 (2008) 33-36.

- [2.105] R. Sarkar, S.K. Das, G. Banerjee, Effect of additives on the densification of reaction sintered and presynthesised spinels, *Ceram Int*, 29 (2003) 55-59.
- [2.106] R. Sarkar, G. Banerjee, Single stage densification study of different magnesium aluminates in presence of additives, *Ind Ceram*, 20 (2000) 1-4.
- [2.107] R. Sarkar, G. Banerjee, Effect of oxide additions on the densification of spinels, 4th India International Refractory Congress(IREF-CON)Ranchi, 2000, pp. 111-116.
- [2.108] K. Hamano, Z. Nakagawa, T. Kanai, Y. Ohya, M. Hasegawa, Effect of Addition of Chloride on Sintering of Spinel, *Rep. Res. Lab. Eng. Mater.*, Tokyo Inst. Technol., (1986) 93-102.
- [2.109] I. Ganesh, S. Bhattacharjee, B.P. Saha, R. Johnson, Y.R. Mahajan, A new sintering aid for magnesium aluminate spinel, *Ceram Int*, 27 (2001) 773-779.
- [2.110] A. Ghosh, S.K. Das, J.R. Biswas, H.S. Tripathi, G. Banerjee, The effect of ZnO addition on the densification and properties of magnesium aluminate spinel, *Ceram Int*, 26 (2000) 605-608.
- [2.111] Y. Yu, Y.-z. Ruan, R.-p. Wu, S. Liu, H.-r. Zeng, Influence of ZnO addition on magnesium aluminate spinel synthesized by solid state reaction, *Transactions of Materials and Heat Treatment*, 4 (2008) 011.
- [2.112] R. Sarkar, T.K. Pal, G. Banerjee, Reaction sintering of magnesium aluminates: Effect of MgSO₄, *Am Ceram Soc Bull*, 82 (2003) 9601-9607.
- [2.113] R. Sarkar, S.K. Das, G. Banerjee, Effect of addition of Cr₂O₃ on the properties of reaction sintered MgO–Al₂O₃ spinels, *J Eur Ceram Soc*, 22 (2002) 1243-1250.
- [2.114] F. Mohammadi, S. Otraj, M.R. Nilforushan, Effect of MgCl₂ addition on the sintering behavior of MgAl₂O₄ spinel and formation of nano-particles, *Sci Sinter*, 46 (2014) 157-168.
- [2.115] P. Ugur, C. Aksel, The effect of SnO₂ on the improvement of mechanical properties of MgO–MgAl₂O₄ composites, *Composites Part B: Engineering*, 43 (2012) 2217-2221.
- [2.116] M. Pošarac, A. Devečerski, T. Volkov-Husović, B. Matović, D.M. Minić, The effect of Y₂O₃ addition on thermal shock behavior of magnesium aluminate spinel, *Sci Sinter*, 41 (2009) 75-81.
- [2.117] R. Sarkar, H.S. Tripathi, A. Ghosh, Reaction sintering of different spinel compositions in the presence of Y₂O₃, *Mater Lett*, 58 (2004) 2186-2191.
- [2.118] J. Aguilar, A. Arato, M. Hinojosa, U. Ortiz, Synthesis of MgAl₂O₄ at low temperature with CaCO₃ additions, *Materials Science Forum*, 442 (2003) 79-84.

- [2.119] I. Ganesh, K.A. Teja, N. Thiyagarajan, R. Johnson, B.M. Reddy, Formation and densification behavior of magnesium aluminate spinel: the influence of CaO and moisture in the precursors, *J Am Ceram Soc*, 88 (2005) 2752-2761.
- [2.120] F.J. Alvarez, D.M. Pasquevich, A.E. Bohe, Formation of magnesium spinel in the presence of LiCl, *Journal of materials science*, 40 (2005) 1193-1200.
- [2.121] K. Rozenburg, I.E. Reimanis, H.J. Kleebe, R.L. Cook, Chemical interaction between LiF and MgAl₂O₄ spinel during sintering, *J Am Ceram Soc*, 90 (2007) 2038-2042.
- [2.122] K. Rozenburg, I.E. Reimanis, H.J. Kleebe, R.L. Cook, Sintering kinetics of a MgAl₂O₄ spinel doped with LiF, *J Am Ceram Soc*, 91 (2008) 444-450.
- [2.123] A.A. Hamid, S.C. Jain, P.K. Ghosh, S. Ray, Processing, microstructure, and mechanical properties of cast in-Situ Al (Mg, Mn)-Al₂O₃ (MnO₂) composite, *Metallurgical and Materials Transactions A*, 36 (2005) 2211-2223.
- [2.124] Y.H. Baik, Sintering of MgAl₂O₄ spinel and its characteristics, *Yoop Hikoechi*, 22 (1985) 29-36.
- [2.125] J. Yu, K. Hiragushi, Sintering behavior of spinel with added TiO₂, *Taikabutsu Overseas*, 16(4) (1996),61.
- [2.126] R. Sarkar, G. Bannerjee, Effect of addition of TiO₂ on reaction sintered MgO–Al₂O₃ spinels, *J Eur Ceram Soc*, 20 (2000) 2133-2141.
- [2.127] W. Yan, X. Lin, J. Chen, N. Li, Y. Wei, B. Han, Effect of TiO₂ addition on microstructure and strength of porous spinel (MgAl₂O₄) ceramics prepared from magnesite and Al(OH)₃, *J Alloy Compd*, 618 (2015) 287-291.
- [2.128] H.S. Tripathi, S. Singla, A. Ghosh, Synthesis and densification behaviour of magnesium aluminate spinel: effect of Dy₂O₃, *Ceram Int*, 35 (2009) 2541-2544.
- [2.129] C. Zografou, P. Reynen, D. von Mallinckrodt, Non-stoichiometry and the sintering of MgO and MgAl₂O₄, *Interceram*, 32 (1983) 40-43.
- [2.130] I.S. Yi, N. Enomoto, Z. Nakagawa, Effect of SiO₂ addition on reaction sintering of MgO and MgAl₂O₄, *Rep. Res. Lab. Eng. Mater. Tokyo Inst. Technol. No. 21*, (1996) 43-47.
- [2.131] T. Kim, D. Kim, S. Kang, Effect of additives on the sintering of MgAl₂O₄, *J Alloy Compd*, 587 (2014) 594-599.

- [2.132] M. Fujita, H. Yoshimatsu, A. Osaka, Y. Miura, Preparation and properties of ZrO₂ dispersed MgO-Al₂O₃ ceramics. pt. 2. Effects of ZrO₂ content, J Ceram Soc Jpn, 103 (1995) 838-843.
- [2.133] H. Tsuboi, H. Yoshimatsu, T. Nanba, Y. Miura, Preparation and properties of ZrO₂-dispersed MgO-Al₂O₃ ceramics (Part 3), Journal-ceramic society of japan international edition, 105 (1997) 640-646.
- [2.134] I. Ganesh, J.M.F. Ferreira, Synthesis and characterization of MgAl₂O₄-ZrO₂ composites, Ceram Int, 35 (2009) 259-264.
- [2.135] O. Quénard, C. Laurent, A. Peigney, A. Rousset, Zirconia-spinel composites. Part I: synthesis of powders and dense materials, Mater Res Bull, 35 (2000) 1967-1977.
- [2.136] O. Quénard, C. Laurent, A. Peigney, A. Rousset, Zirconia-spinel composites. Part II: mechanical properties, Mater Res Bull, 35 (2000) 1979-1987.
- [2.137] B. Sahin, C. Aksel, Developments on the mechanical properties of MgO-MgAl₂O₄ composite refractories by ZrSiO₄-3mol% Y₂O₃ addition, J Eur Ceram Soc, 32 (2012) 49-57.
- [2.138] C. Aksel, T. Aksoy, Improvements on the thermal shock behaviour of MgO-spinel composite refractories by incorporation of zircon-3mol% Y₂O₃, Ceram Int, 38 (2012) 3673-3681.
- [2.139] R. Lodha, A. Ghosh, B. Mukherjee, G.N. Agrawal, Zirconia-magnesium aluminate spinel composite-Improved ZrO₂-MgAl₂O₄ composite was prepared by solid-state sintering, Am Ceram Soc Bull, 85(6) (2006) .
- [2.140] J. Kim, Effect of zirconium dioxide addition and nonstoichiometry on sintering and physical property of magnesium aluminate spinel, Case Western Reserve University, 1992.
- [2.141] B. Ma, Y. Yin, Q. Zhu, Y. Li, G. Li, J. Yu, In-situ formation and densification of MgAl₂O₄-SmAlO₃ ceramics by a single-stage reaction sintering process, Ceramics-Silikaty, 59 (2), (2015) 109-114.
- [2.142] I. Ganesh, B. Srinivas, R. Johnson, G.V.N. Rao, Y.R. Mahajan, Effect of preparation method on sinterability and properties of nanocrystalline MgAl₂O₄ and ZrO₂-MgAl₂O₄ materials, Brit Ceram T, 102 (2003) 119-128.
- [2.143] W. Zhang, G. Shi, Z.Y. Feng, Sintering performance of MgAl₂O₄ spinel with various Al₂O₃ content, Trans Tech Publ, pp. 605-609.
- [2.144] G.Li,F.Tavangarian,Sintering behavior,microstructure and mechanical properties of vaccum sintered SiC/Spinel nanocomposite, J Alloy Compd, 615 (2014) 204-210.

- [2.145] R. Sarkar, G. Banerjee, Effect of compositional variation and fineness on the densification of MgO–Al₂O₃ compacts, *J Eur Ceram Soc*, 19 (1999) 2893-2899.
- [2.146] R. Sarkar, S. Das, Auto combustion synthesis for magnesium aluminate spinel using glycine as fuel and its sintering study, *T Indian Ceram Soc*, 73 (2014) 172-176.
- [2.147] K. Sasaki, N. Emoto, N. Hagiwara, S. Tanaka, Magnesia-spinel brick containing MgO rich spinel for steel refining ladle, *Unitecr'93*, 3 (1995) 257-264.
- [2.148] I. Ganesh, A review on magnesium aluminate (MgAl₂O₄) spinel: synthesis, processing and applications, *International Materials Reviews*, 58 (2013) 63-112.
- [2.149] P. Kettner, G. Christof, MA-Spinel Brick in Glass Furnace Regenerators, *Radex Rundschau*, 1 (1986) 3-11.
- [2.150] M. Patterson, J.E. Caiazza, D.W. Roy, Transparent spinel development, *Proc. SPIE (Society of Photographic Instrumentation Engineers)* 4102, International Society for Optics and Photonics, 2000, pp. 59-68.
- [2.151] G.N. Rani, N.H. Ayachit, Low temperature synthesis of MgAl₂O₄ Spinel through sol-gel technique and its characterization, *Can J Phys*, 93 (2015) 561-564.
- [2.152] R. Sarkar, Refractory Applications of Magnesium Aluminate spinel, *Interceram Refractories*, 1 (2010) 11-14.
- [2.153] V.K. Singh, R.K. Sinha, Low temperature synthesis of spinel (MgAl₂O₄), *Mater Lett*, 31 (1997) 281-285.
- [2.154] S. Zhang, W. Lee, Spinel-containing refractories, *Mechanical engineering-new york and basel-marcel dekker then crc press/taylor and francis*, 178 (2004) 215.

References (*Experimental*)

- [4.1] Product catalogue ,Nedmag99, Nedmag industries mining & manufacturing B.V., The Netherlands.
- [4.2] Reactive aluminas for ceramic applications, Product catalogue, Almatix Inc, USA.
- [4.3] Product catalogue, Laboratory reagent and fine chemical, Loba Chemie, India, 2012–13.
- [4.4] Product catalogue, Merck millipore corporation, USA.

References (*Results and discussions*)

- [5.1] S.K. Mohan, R. Sarkar, Study on the formation and densification of magnesium aluminate spinel using commercial grade reactants: effect of planetary milling, *Journal of Australian Ceramic Society*, 52 (2016) 138-147.
- [5.2] S. Yangyuan, R.J. Brook, Preparation and strength of forsterite-zirconia ceramic composite, *Ceram Int*, 9 (1983).
- [5.3] P. Bosh, J.P. Giry, Preparation of zirconia-mullite ceramics by reaction sintering, *Sci Sinter*, 20 (1988) 141-148.
- [5.4] S.K. Mohan, R. Sarkar, Reaction sintered zinc oxide incorporated magnesium aluminate spinel from commercial grade oxide reactants, *Communicated to Advances in Applied Ceramics: Structural, Functional and Bioceramics*.
- [5.5] A. Ghosh, S.K. Das, J.R. Biswas, H.S. Tripathi, G. Banerjee, The effect of zinc oxide addition on the densification and properties of magnesium aluminate spinel, *Ceram Int*, 26 (2000) 605-608.
- [5.6] R. Lodha, A. Ghosh, B. Mukherjee, G.N. Agrawal, Zirconia-magnesium aluminate spinel composite - Improved ZrO_2 - $MgAl_2O_4$ composite was prepared by solid-state sintering, *Am Ceram Soc Bull*, 85 (2006),9201-9203.
- [5.7] R. Lodha, T. Troczynski, G. Opera, Role of oxide additives in the synthesis and sintering of magnesium aluminate spinel, *Interceram*, 57 (2008) 324-329.
- [5.8] S.K. Mohan, R. Sarkar, Effect of ZrO_2 addition on $MgAl_2O_4$ spinel from commercial grade oxide reactants, *Ceram Int*, 42 (2016) 10355–10365.
- [5.9] O. Quenard, C. Laurent, A. Peigney, A. Rousset, Zirconia-spinel composites. Part II: mechanical properties, *Mater Res Bull*, 35 (2000) 1979-1987.
- [5.10] J. Kim, Effect of zirconium dioxide addition and nonstoichiometry on sintering and physical property of magnesium aluminate spinel, *Case Western Reserve University*, 1992.
- [5.11] S.K. Mohan, R. Sarkar, Effect of insitu generated nascent magnesia and alumina from nitrate precursor on reaction sintered magnesium aluminate spinel, *Materials and Design*, DOI 10.1016/j.matdes.2016.07.095.
- [5.12] S.K. Mohan, R. Sarkar, A comparative study on the effect of different additives on the formation and densification of magnesium aluminate spinel, *Ceram Int*.42(12)(2016),13932-13943.

- [5.13] M.A.L. Braulio, L.R.M. Bittencourt, V.C. Pandolfelli, Magnesia grain size effect on in situ spinel refractory castables, *Journal of European Ceramic Society*, 28 (2008) 2845-2852.
- [5.14] M.A.L. Braulio, M. Rigaud, A. Buhr, C. Parr, V.C. Pandolfelli, Spinel- containing alumina-based refractory castables, *Ceram Int*, 37 (2011) 1705-1724.
- [5.15] D.D. Jayaseelan, S. Zhang, S. Hashimoto, W.E. Lee, Template formation of magnesium aluminate ($MgAl_2O_4$) spinel microplatelets in molten salt, *J Eur Ceram Soc*, 27 (2007) 4745-4749.
- [5.16] J. Soudier, Understanding and optimisation of MgO hydration resistance and spinel formation mechanisms for increasing performances of DVM used in crucible induction furnaces melting steel, *Proceedings of UNITECR"05"Orlando,USA, 2005*, pp. 679-683.

Publications originating from M. Tech (Research) work

Publications in SCI journals:

1. **S.K. Mohan**, R. Sarkar, *Study on the formation and densification of magnesium aluminate spinel using commercial grade reactants: effect of planetary milling*, Journal of Australian Ceramic Society 52 (1), 2016, 138-147.
2. **S.K. Mohan**, R. Sarkar, *Effect of ZrO₂ addition on MgAl₂O₄ spinel from commercial grade oxide reactants*, Ceramics International 42(8), 2016,10355–10365.
3. **S.K. Mohan**, R. Sarkar, *A comparative study on the effect of different additives on the formation and densification of magnesium aluminate spinel*, Ceramics International 42(12), 2016,13932–13943 .
4. **S.K. Mohan**, R. Sarkar, *Reaction sintered zinc oxide incorporated magnesium aluminate spinel from commercial grade oxide reactants*, submitted to Journal of Australian Ceramic Society, Under Review.
5. **S.K. Mohan**, R. Sarkar, *Effect of insitu generated nascent magnesia and alumina from nitrate precursor on reaction sintered magnesium aluminate spinel*, Materials and Design 110, 2016,145-146.

Publications in conference proceedings:

1. **S.K. Mohan**, R. Sarkar, *Formation and densification of MgAl₂O₄ spinel from commercial grade oxide reactants: effect of planetary milling*” Proceedings of 78th annual session of Indian Ceramic Society, Jamshedpur, Jharkhand, 2015.
2. **S.K. Mohan**, R. Sarkar, *Effect of ZrO₂ addition on MgAl₂O₄ from commercial grade oxides by solid oxide reaction*, Proceedings of Materials Research Society of India (MRSI) Symposium, NEIST, Jorhat, Assam, 2016.

Resume

Sanjay Krishna Mohan
House no-46, Ajanta Path, Bye lane-1,
Survey, Beltola, Guwahati-28,
Assam



Phone No: +918280471215, +918402066260

Email:sanjaykmohan11@gmail.com

Objective:

To work for an organization wherein, I can dedicate all my positive traits towards its growth & align myself with mission of the organization.

Education qualification:

Sl.no	Examination	Board /university	College /school	Year of completion	Percentage (%)
1.	M.Tech (By research)	NIT, Rourkela	National Institute of Technology, Rourkela	2016	9.06 CGPA
2.	B.E	GAUHATI UNIVERSITY	ROYAL SCHOOL OF ENGINEERING AND TECHNOLOGY	2013	72.04%
3.	AISSCE	CBSE	K.V.KHANAPARA,GUWAHATI	2009	87.2%
4.	AISSE	CBSE	K.V.KHANAPARA,GUWAHATI	2007	88.4%

Research experience:

Worked as a project assistant in project titled “*Development of nano-carbon containing magnesia carbon refractories*” funded by DST in Department of ceramic engineering under Prof.Ritwik Sarkar, NIT, Rourkela, Odisha.

Publications in journal:

1. S.K. Mohan, R. Sarkar, *Study on the formation and densification of magnesium aluminate spinel using commercial grade reactants: effect of planetary milling*, Journal of Australian ceramic society, 52 (2016) 138-147.
 2. S.K. Mohan, R. Sarkar, *Effect of ZrO₂ addition on MgAl₂O₄ spinel from commercial grade oxide reactants*, Ceramics International, 42(8) (2016) 10355–10365.
-

-
3. S.K. Mohan, R. Sarkar, *A comparative study on the effect of different additives on the formation and densification of magnesium aluminate spinel*, *Ceramics International*, 42(12) (2016), 13932–13943
 4. S.K. Mohan, R. Sarkar, *Effect of insitu generated nascent magnesia and alumina from nitrate precursor on reaction sintered magnesium aluminate spinel*, *Materials and Design*, 110 (2016),145-156.
 5. S.K. Mohan, R. Sarkar, *Reaction sintered zinc oxide incorporated magnesium aluminate spinel from commercial grade oxide reactants*, Submitted to *Journal of Australian Ceramic Society*.

Conference paper presentations:

1. S.K. Mohan, R. Sarkar, *Formation and densification of MgAl₂O₄ spinel from commercial grade oxide Reactants: effect of planetary milling*” Proceedings of 78th annual session of Indian Ceramic Society, Jamshedpur, Jharkhand, 2015.
2. S.K. Mohan, R. Sarkar, *Effect of ZrO₂ Addition on MgAl₂O₄ from Commercial Grade Oxides by Solid Oxide Reaction*, Proceedings of Materials Research Society of India (MRSI) Symposium, NEIST, Jorhat, Assam, 2016.

Projects undertaken during bachelor’s degree:

- One-year project on wind turbine construction and analysis of wind power in 7th and 8th semester of B.E course.
- One-month project on “Hydrocarbon, exploration production, separation, storage and transportation “in ONGC, Nazira, Sivasagar, Assam during 6th semester of B.E course.

Training and internships:

- 1-month summer training in 6th semester of B.E course in ONGC, Nazira, Sivasagar, Assam.
- 15 days’ summer training in 4th semester of B.E course in OIL, Duliajan, Assam.

Proficiency and Skills:

- MS-word, MS-excel, MS-PowerPoint
 - Operating system: Microsoft windows, Linux, android.
 - Language proficiency: C, C++
 - Graphics: auto-cad
 - Data analysis: Philips Xpert Highscore, Origin Pro8.
 - Other Skills: Field Emission Scattered Electron Microscopy, X-ray Diffraction, Mechanical properties of materials, Corrosion behavior, Material Synthesis Techniques, Heat Treatment, Thin film coating and membrane preparation etc.
-

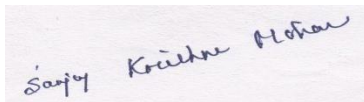
Other miscellaneous certifications:

- Certificate of participation in workshop on “Wind Disaster Problems-Challenges Ahead” organized jointly by Royal School of Engineering & Technology, Betkuchi, Guwahati-35 and Indian Society of Wind Engineering, Roorkee, India
- Completion certificate from CEC Ganeshguri Centre Guwahati on completion of 2months course on auto-cad on august 2012.
- Certificate from ONGC, Nazira, Assam Asset on completion of project entitled “Hydrocarbon exploration, production separation, storage and transportation” on July 2012.
- Certificate of participation on robotics and drama in ‘Consensio 2012’ in royal group of institutions.
- Certificate of proficiency for securing position in athletic events in school in 2007.
- Certificate of participation in young author contest conducted ITC Ltd. in 2006.
- Certificate of merit for securing 2nd position in Bharat Ko Jaano quiz competition in 2003.
- Certificate of participation in workshop on PC maintenance organized by NIIT Ganeshguri Centre, Guwahati in 2011.
- Certificate of proficiency from Regional Institute of Career Search, Tezpur for securing 20th rank in state and 9th rank in district in summer merit test in 2002.

Personal information:

- Name: Sanjay Krishna Mohan
- Date of birth: 15-12-1991
- Sex: Male
- Father’s name: Ganga Prasad Mohan
- Language Spoken: English, Hindi, Assamese, Bengali and Odiya (little).

(Sanjay Krishna Mohan)



Sanjay Krishna Mohan